MAX-PLANCK-INSTITUT FÜR QUANTENOPTIK

Proposal for a Joint German-British Interferometric Gravitational Wave Detector

M P Q 147 September 1989 GWD/137/JH(89)

Proposal for a Joint German-British Interferometric Gravitational Wave Detector

J. Hough, B.J. Meers, G.P. Newton, N.A. Robertson, H. Ward
Department of Physics and Astronomy, University of Glasgow

G. Leuchs, T.M. Niebauer, A. Rüdiger, R. Schilling, L. Schnupp, **H. Walther**, W. Winkler
Max-Planck-Institut für Quantenoptik, Garching

B.F. Schutz
Department of Physics, University of Wales, Cardiff

J. Ehlers, P. Kafka, G. Schäfer
Max-Planck-Institut für Astrophysik, Garching

M.W. Hamilton
Department of Physics and Applied Physics, University of Strathclyde, Glasgow

I. Schütz, **H. Welling**
Laser-Zentrum und Institut für Quantenoptik, Universität Hannover

J.R.J. Bennett, **I.F. Corbett**, B.W.H. Edwards, R.J.S. Greenhalgh
Rutherford Appleton Laboratory, Chilton, near Oxford

V. Kose
Physikalisch-Technische Bundesanstalt, Braunschweig

Contact persons are indicated in **bold face**.

Acknowledgements

The authors would like to acknowledge gratefully the help of the following in the preparation of this report:

Other members of the gravitational wave research group at the Department of Physics and Astronomy, University of Glasgow.

Other members of the gravitational wave research group at the Max-Planck-Institut für Quantenoptik.

J. Gea-Banacloche at the University of Madrid.

N. MacDonald at the Department of Physics and Astronomy, University of Glasgow.

The Council Works Unit of the SERC.

Staff at the Bauabteilung of the Max-Planck-Gesellschaft.

The Forestry Commission of the United Kingdom.

The Planning Department and the District Council of North-East Fife, United Kingdom.

The work at the Universities of Glasgow and Wales is supported by the Universities and by the Science and Engineering Research Council. The work at the Max-Planck-Institut für Quantenoptik is supported by the Bundesministerium für Forschung und Technologie.

Preface

For many years there has been steady progress towards the detection of gravitational radiation. It has now become clear that the next major step should be the construction of a number of long-baseline detectors around the world. An array of detectors of this type is expected to allow the observation of gravitational waves from a range of astrophysical sources, leading to improved insight in many areas including stellar collapse, binary coalescence and the expansion of the Universe.

We propose that one of these detectors be built by a collaboration formed around the gravitational wave groups in Britain and Germany. In this document we present our case for this collaborative venture and outline the design philosophy of our proposed instrument – an interferometric detector with arms of length close to 3 km.

Two detectors of the same general type are planned for the USA (LIGO project), one is planned for Italy (Italian/French VIRGO project) and another is proposed for Australia (AIGO project). It is expected that all the long baseline detectors to be built will operate as part of a coordinated worldwide network.

Contents

Chapter 1

Introduction

Gravitational waves are ripples in the curvature of space-time produced by the acceleration of mass. Because the gravitational interaction is very weak, large masses and high accelerations are needed to produce gravitational waves of significant amplitude. These are the very conditions that occur during violent astrophysical events. If the gravitational wave signals from such processes can be detected, new types of information will be gained, qualitatively different from those produced by any other observations. This is the goal of this proposal – the opening of a new window on the Universe.

Despite the prediction of the existence of gravitational waves early in this century, it was not until the early 1960's that it was appreciated by Joseph Weber that the extremely weak signals might be experimentally detectable. His pioneering searches appeared to yield positive results, which he interpreted as being due to gravitational waves of astrophysical origin. These findings caused a sensation in the astrophysical community because of the strength of the signals as well as their frequency of occurrence. However, since then, these observations have not been confirmed by other groups who have repeated searches for gravitational waves, some using improved techniques. It is only within the last few years that the researchers in the field have been able to see how to build detectors of enough sensitivity to allow the detection of gravitational waves at the levels predicted by astrophysics.

In this proposal, we outline the very significant returns to be gained from the observation of gravitational waves resulting from various types of astrophysical sources. Subsequently we describe the technology which the German/British group proposes to adopt for its detection system, and give a detailed estimate of the technological and engineering effort required.

1.1 Gravitational Wave Detection

The effect of a gravitational wave passing through a system of particles (or test bodies) is to induce a strain in space that changes the distances between the particles. The amount of this change is proportional to the amplitude of the gravitational wave and to the separation of the particles. It is this change in separation which has to be

experimentally detected against a background of perturbing influences. As is outlined in Chapter 2 the strains in space caused by predicted gravitational wave events are exceedingly small – of the order of 10^{-22} to 10^{-21} over bandwidths of several hundred Hz; the predicted frequency range of interest extends from tens of Hz to a few kHz.

Two main schemes for earth based detection of gravitational waves are being developed – sensing of the excitation of resonant bar detectors cooled to very low temperature, and laser interferometry between widely spaced test bodies.

1.1.1 Resonant bar detectors

Variants of the resonant bar detector are being developed by a number of research groups: at Stanford University, Louisiana State University, University of Maryland, University of Rome, University of Western Australia and by a collaboration in Japan. Currently Stanford, Louisiana and Rome, with bars of several tons mass cooled to below 4 K by liquid helium, have achieved strain sensitivities of close to 10^{-18} for pulses of millisecond duration. Further improvement can be expected, but it seems likely that such detectors will have great difficulty in reaching an amplitude sensitivity better than $\sim 10^{-20}$. At this level the sensitivity limitation due to the Heisenberg Uncertainty Principle in the detection of displacement begins to play a rôle. Although theoretical schemes for circumventing this limitation have been proposed, the problems in implementing them seem considerable. Furthermore, the fact that a solid bar is resonant in nature will tend to restrict its bandwidth of operation to a small fraction of its resonant frequency. This imposes a further limitation on the applicability of such detectors.

1.1.2 Detectors using laser interferometry

A totally different technique for the measurement of gravitational waves forms the basis of this proposal. The detector will use laser interferometry to sense the displacement changes between widely separated test bodies. This method offers the highest potential sensitivity and widest bandwidth for the detection of different types of sources.

The interferometric method was pioneered by Forward [1] and Weiss [2]. Prototype detectors of this type, with arm lengths ranging from 1 m to 40 m, have been constructed and operated at the Max-Planck-Institut für Quantenoptik, Garching, at the University of Glasgow, at Caltech, at MIT, and at ISAS in Japan. The best sensitivities achieved so far are comparable to those of the cooled bar detectors.

In principle the change in separation of two test bodies hung a distance apart can be measured against the wavelength of light from a very stable source, but the degree of wavelength (or frequency) stability required of the source is unreasonably high. It is much more practicable to measure the distance between test bodies along one arm with respect to the distance between similar masses along a perpendicular arm – *i.e.* to use a Michelson interferometer arrangement as in Figure 1.1. This layout is particularly appropriate since the effect of a gravitational wave is quadrupole in nature and so tends to cause the opposite sign of length change in the two arms.

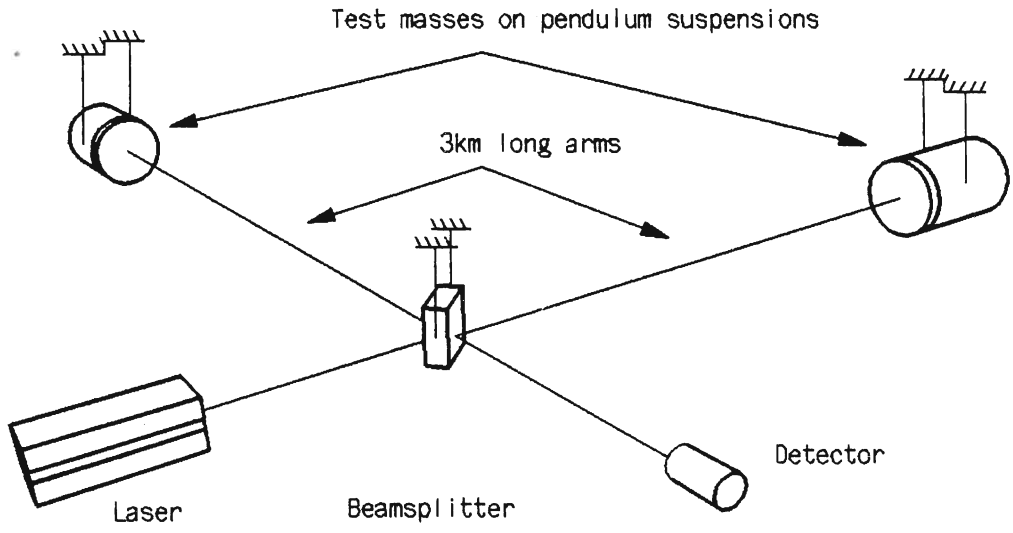

Figure 1.1: *Diagram illustrating the basic principle of a gravitational wave detector using Michelson interferometry.*

Sensitivity can be enhanced by separating the masses by a long distance (3 km in this proposal) and having multiple reflections in the arms of the detector – either by using optical delay lines or resonant Fabry-Perot cavities. These ideas form the basis of the prototype detectors at Glasgow and MPQ and of the present joint proposal from these establishments. Further details may be found in earlier proposals from Glasgow [3] and MPQ [4].

There are a number of factors which may limit the sensitivities of such detectors. For example the effects of –

- photon counting statistics (photon noise) on the precision of the measurements of displacement,
- thermal motions of the test masses,
- seismic and local mechanical noise on the movement of the test masses,
- refractive index fluctuations in the residual gas in the vacuum system enclosing the detector,
- fluctuations of the frequency, power and beam geometry of the light from the illuminating laser,

- light scattered inside the interferometer.

Again, the significance of each of these sources of noise has been assessed in the earlier proposals [4, 3], and schemes have been pointed out for reducing them to an acceptable level.

1.2 Proposed British/German Detector System

1.2.1 Scientific objectives

The overall objective of the international gravitational wave community is the observation and interpretation of gravitational wave signals from astrophysical sources such as stellar collapses, coalescing compact binary systems, pulsars, and from various processes in the early evolution of the universe. Such observations will allow new information to be obtained – for example on the mechanisms of stellar collapse, on the expansion of the universe and on the equation of state of neutron star material. The consensus of opinion is that to achieve this goal requires the construction of a worldwide network of at least four laser interferometer detectors.

The British and German research groups involved wish to construct and operate one of these detector systems. Two detectors are planned to be built in the USA (LIGO project, [5]), one is planned for Italy (Italian/French VIRGO project, [6]), and one is being proposed in Australia (AIGO project, [7]).

1.2.2 Research groups and their experience

Considerable experience in the design and operation of prototype versions of interferometric detectors has been gained by the research groups at Garching and Glasgow, both of which have been active in the gravitational wave field since the early 1970's. The experimental group at Glasgow has been greatly strengthened over the last few years by collaboration with a theoretical group interested in analysis of signals from gravitational wave detectors, led by Professor B.F. Schutz at the University of Wales. Important engineering support is being provided by the Rutherford Appleton Laboratory. Right from the start, the work of the experimental group at Garching has benefited considerably from close contact with colleagues at the Max-Planck-Institut für Astrophysik, especially with the Department of General Relativity led by Professor Jürgen Ehlers.

With our prototypes in Garching and Glasgow we have achieved some of the best sensitivities with laser interferometers. In addition we have recently demonstrated the potential for long term operation of laser interferometric detectors by carrying out a 100 hour period of coincident observation using the 30 m arm length delay line system at Garching and the 10 m arm length Fabry-Perot based system at Glasgow. More details on the prototypes and the data run are presented in Appendix A.

Well known noise sources, particularly thermally excited vibrations of the mirror substrates, but also the fundamental limit due to the Uncertainty Principle, do not allow the present prototype detectors to be upgraded to the sensitivity level required for a realistic prospect of detecting gravitational wave signals from predicted sources. These limitations can be overcome only by the use of a long baseline detector system. The British and German groups are now committed to a joint proposal for such an instrument. The prototype detectors will henceforth provide a testbed for new technologies, techniques, and concepts before they are implemented in the full-scale detectors.

1.2.3 The British/German proposal

It will become clear in the next chapter that if a high probability of making gravitational wave observations is to be achieved a sensitivity goal equivalent to 10^{-22} over a bandwidth of several hundred Hz is necessary for each detector in the network. In order to meet the high sensitivity requirements we propose a large interferometer, with arms of 3 km in length.[1]

Nevertheless the envisaged sensitivity cannot be expected to be achieved initially in the operation of a detector system, but must be approached in stages. To allow for this, and in an effort to maximise the returns from the capital investment, we believe that we must plan for two interferometer systems to be installed in our detector; one interferometer may then be developed while another is operating.

We would anticipate that the first interferometer installed should reach a sensitivity approaching 10^{-21} for millisecond pulses within about three years of the facility being commissioned and then would be operated for several years. During the operational phase some development would be carried out with the aim of improving the sensitivity to 10^{-22} for millisecond pulses. Also during this time another interferometer system would be developed to operate down to lower frequency ($\sim$ 100 Hz) with high sensitivity ($\leq 10^{-22}$). The two interferometers mentioned above would lie parallel to each other in the same vacuum housing.

The geometry envisaged is two arms with an opening angle of either 90° or 60°, both variants having their own merits. The choice depends on various boundary conditions, particularly on the choice of the site and on the plans for possible future extension. Further discussion of this question is presented in Chapter 8.

[1] It should be noted that this proposal differs from the earlier British proposal in that a longer arm length – 3 km – is being suggested at the first stage. This change has been made to allow the sensitivity goals to be approached with a higher level of confidence and to bring the detector design more into line with those being planned elsewhere.

Chapter 2

The Scientific Case

2.1 Introduction

The scientific case for building a large interferometric gravitational wave detector was fully made in the proposals submitted by the two groups in 1986 and 1987 [3, 4], and since then some extensive reviews have appeared (especially [8] and [9]). In this section we will give a brief review of the case, stressing what we have learned since the proposals were submitted. We will tie the discussion to the planned progression of the interferometer installation: a first stage reaching a sensitivity level of 10^{-21} over a 1 kHz bandwidth, followed by progress to 10^{-22} at kHz frequencies, a second detector optimised for low-frequency observing down to 100 Hz, and a final extension of sensitivity down to lower frequencies.

2.1.1 Gravitational waves

Gravitational waves are a property of any theory of gravity in which influences propagate at a finite velocity. Einstein's theory of general relativity is the only theory of gravity today that has passed the stringent experimental tests of the past two decades [10]. For our purposes one of the most important of these tests is that general relativity correctly predicts the rate of orbital decay of the Binary Pulsar PSR 1913+16 due to gravitational radiation. This is the only test so far of the predictions of the theory regarding gravitational waves, and it is an indirect one, in that the waves themselves are not detected. A direct detection of gravitational waves is still of the greatest importance for physics, and we shall see that our proposed detector can perform a range of other direct tests as well.

Within general relativity, gravitational waves travel at the speed of light, have two independent transverse polarisations, and are characterised by an amplitude that is conventionally called h, which is twice the strain induced in a system of free particles by the gravitational wave. In the optimal orientation, a laser interferometric detector measures twice this strain, so the minimum detectable h characterises the detector's sensitivity. The maximum amplitude of gravitational waves expected from sources in

our Galaxy is 10^{-18}, and that only once every decade or so. The maximum amplitude expected from extragalactic sources that might occur more than once per year is 10^{-21}, which could come from supernovae in the Virgo Cluster, where there are several thousand galaxies. Our design is aimed at providing amplitude sensitivity ten times better than this.

Although gravitational waves are difficult to detect, they carry enormous amounts of energy. The energy flux of a gravitational wave of frequency f and amplitude h is given by

$$\mathcal{F}_{\rm gw} = 3.2 \times 10^{-3} \left[\frac{f}{1\,\mathrm{kHz}}\right]^2 \left[\frac{h}{10^{-22}}\right]^2 \ \mathrm{W\ m^{-2}}. \tag{2.1}$$

In astronomers' language, a 1 kHz wave with amplitude 10^{-22} is as bright as a star of apparent magnitude -13, some 10^5 times brighter than the brightest star in the night sky. By integrating this equation over a sphere of radius r for a time τ we find the relation between the amplitude h of an isotropic wave and the energy E it carries during a time τ:

$$h = 1.4 \times 10^{-21} \left[\frac{E}{10^{-2}\,M_\odot c^2}\right]^{1/2} \left[\frac{f}{1\,\mathrm{kHz}}\right]^{-1} \left[\frac{\tau}{1\,\mathrm{ms}}\right]^{-1/2} \left[\frac{r}{15\,\mathrm{Mpc}}\right]^{-1}. \tag{2.2}$$

For convenience we normalise total energies to $10^{-2}\,M_\odot c^2$ (a fairly large burst for a conventional supernova) and distances to the distance to the Virgo Cluster.

2.1.2 Key characteristics of the detector

While many factors affect the ultimate sensitivity of a detector, they combine into relatively few key properties that determine how much science they can do. These are, in order of importance,

- **Broadband sensitivity.** The usual way of characterising the performance of a detector is to give its sensitivity to the sort of broadband bursts that are expected from supernova explosions: a typical frequency of 1 kHz and a bandwidth of 500 Hz. With various combinations of laser power, mirror reflectivity, length, and other factors, it seems possible with our proposed design to reach a photon-noise-limited strain sensitivity of 10^{-22} or even better. We shall denote the standard deviation (σ) of the broadband noise of a detector by $\sigma_{\rm bb}$. This is given in terms of the characteristics of the detector in Equation 3.6. If the arms of a detector make an angle α with each other, then $\sigma_{\rm bb}$ will contain a factor of $\sin\alpha$, the reduction in sensitivity relative to a right-angled detector. In all our equations, we shall assume that such a factor is included in $\sigma_{\rm bb}$ where appropriate. This angle does not affect any sensitivity formula in any other way.

  A detector that is capable of reaching a certain broadband sensitivity can be used for other kinds of observing, such as looking for lower-frequency coalescing binaries, pulsars, or a stochastic background. As we discuss in Chapter 3, by reconfiguring a detector's optics, it can be optimised for low-frequency sources (near

100 Hz, say), or narrow-banded to search for specific continuous wave sources. Since we are designing it to reach the photon-noise sensitivity limit over most of its useful observing spectrum, its ultimate effectiveness will depend at least in part on the sensitivity it would achieve if optimised for broadband observing. We will therefore quote sensitivity limits for various kinds of sources in terms of $\sigma_{\rm bb}$. Thus, we will make statements such as: A 10^{-22} detector, when optimised for detecting coalescing binaries, can see such binaries at 100 Mpc distance with a signal-to-noise ratio of 25.

- **Lower cutoff frequency.** Photon noise, however, may not be the dominant noise at all frequencies. Seismic noise and thermal noise in the suspension rise at low frequencies, so there is a lower cutoff frequency $f_{\rm lc}$ below which our photon-noise-limited sensitivity formulas do not apply. If the cutoff is due to seismic noise, whose spectral density rises steeply at low frequencies, then $f_{\rm lc}$ is essentially the lowest observing frequency. If the seismic cutoff can be pushed to very low frequencies, then the suspension's thermal noise will still force $f_{\rm lc}$ to stay at about 100 Hz, but some kinds of observations may yet be possible below this frequency against the more gradually rising thermal noise spectrum. In this scientific case we will emphasise mainly the observations that can be made above 100 Hz, but we will note the improvements that extending the range down to lower frequencies could bring.
- **Mirror reflectivity and arm length.** There are two other important characteristics of the detector, the length ℓ of each arm and the quality of the mirrors, which is given by the mirror losses $1 - R$, where R is the reflectivity of the mirrors in the arms. For observations of supernovae and coalescing binaries, arm length and mirror quality affect sensitivity only through the one parameter $\sigma_{\rm bb}$, so they do not need to be considered separately. For certain kinds of observing, however, such as pulsars and stochastic sources, these parameters are independent and need to be included in our sensitivity formulae. (See, for example, the formula for the narrow-band sensitivity $\sigma_{\rm nb}$, Equation 3.7.) We shall normalise the length ℓ to 3 km and the mirror losses $1 - R$ to 5×10^{-5}.

2.1.3 Observing in a worldwide network

Gravitational wave detectors cannot operate alone; detections must be confirmed by coincidences between two separated detectors. But two detectors cannot supply enough information to reconstruct the gravitational wave itself, *i.e.* to infer its amplitude, polarisation, and direction of travel. Solving this "inverse problem" is crucial to getting scientific information from the detectors, and it requires at least three detectors around the world. In order to allow for non-optimal orientation, operational down-time, special-purpose uses such as narrow-banding, and detector development, detectors at four separated sites worldwide is a sensible minimum.

We will see in Chapter 3 that it is not optimal to span the entire frequency range of interest (100 Hz to several kHz) with a single detector. Each site will need at least

two, one optimised for low frequencies, the other for high frequencies. There are further advantages from having three differently oriented (hence, differently polarised) detectors on one site. Detectors on the same site lie in the same plane, and this allows a clean measurement of polarisation, without the complications of using separated detectors of different polarisation that lie in different planes. Detectors on the same site also have no propagation time delay; this allows lower thresholds (see next paragraph) and permits simpler cross-correlation experiments. The system currently proposed has been designed to allow for an extension to three detectors.

Since detector sensitivity is limited by internal and local noise sources, presumably uncorrelated between separated sites, coincidence experiments have a lower false-alarm rate (noise-generated coincidence rate) at a given threshold than individual detectors do. For a given false-alarm rate (we adopt once per year in this proposal), the more detectors a network has, the lower will be the threshold it can operate at. Thus, each additional detector improves the performance of all the others. The performance of a network is somewhat degraded by the fact that one needs to allow coincidence "windows" for the propagation of a gravitational wave from one detector to another. All these effects are fully taken into account in the threshold levels assumed in this proposal [11].

Much coincident observing among separated detectors can be done by exchanging lists of candidate "events", where the detector output has crossed a threshold either in the time series data or in various matched filter outputs. (Matched filters for coalescing binary signals will be discussed below.) But, as we show later, some observing may involve cross-correlation of the full data sets, such as searching for unknown sources, and especially looking for a stochastic background. Moreover, even simple coincidence detections can be made with a lower threshold if the data are added coherently before filtering, rather than subjecting each data stream to individual filters that must each cross the threshold, as we have assumed above.

Recognising this, the international laser interferometric detector community has resolved to cooperate on key areas, two of which are to standardise data taking conventions and to agree on data analysis and exchange protocols. It is therefore important that all detector projects make adequate provision for analysing not only their own data but also for the joint analysis of all sites' data. We return to this in Chapter 7.

Of course, we will also watch for possible coincidences with other instruments, particularly bar gravitational wave detectors and neutrino detectors. The effectiveness of coincidence runs between laser interferometers and bars will depend on how sensitive bars eventually become; their narrow bandwidth and poorer time resolution are further complications. Neutrino detectors should prove to be very effective coincidence partners for gravitational collapse events in our Galaxy; they should allow gravitational wave detectors to operate at a threshold as low as $2\,\sigma_{\mathrm{bb}}$ for such events. But they are unlikely to be able to register neutrinos from collapses in the Virgo Cluster in the foreseeable future.

We shall now turn to an examination of the most likely gravitational wave sources, expressing the detectability of each source in terms of the key detector characteristics described earlier and those of the source. After that we will be in a position to discuss

the ultimate justification for building this detector: the science that it will do. The reader who is more interested in the scientific possibilities than in the details of source estimates and detector noise performance may go straight to that section, which is self-contained.

2.2 Detectability of Possible Sources of Gravitational Radiation

The following list of sources is by no means exhaustive, but it contains those that are the most likely to be detected, based on our present understanding of them.

2.2.1 Supernovae

Supernovae, or more generally gravitational collapses, have been the primary goal of gravitational wave detector development. We know little about the precise waveform to expect, but numerical modelling and theoretical arguments suggest that the burst will have a central frequency of about 1000 Hz and will last for one or two cycles. Provided we can model such a burst at least crudely, the signal-to-noise ratio depends on $\sigma_{\rm bb}$, on the total energy E released in the burst, and on the distance r to the source:

$$\left(\frac{S}{N}\right)_{\rm supernovae} = 10\left[\frac{\sigma_{\rm bb}}{10^{-22}}\right]^{-1}\left[\frac{E}{10^{-2}\,M_\odot c^2}\right]^{1/2}\left[\frac{r}{15\,{\rm Mpc}}\right]^{-1}. \qquad (2.3)$$

Because detector noise will generate spurious "events", a detection threshold must be set that allows, say, only one such false alarm coincidence in a network of detectors per year. A reasonable threshold on the signal-to-noise ratio is 4 for a network of 3 or 4 detectors. A first-stage high-frequency detector, with $\sigma_{\rm bb} = 10^{-21}$, could detect a large burst of $0.1\,M_\odot c^2$ energy from the Virgo Cluster, and could see a collapse in our own Galaxy that generates as little as $10^{-7}\,M_\odot c^2$ of gravitational wave energy. A supernova in Virgo could be seen by the next stage detector (operating at 10^{-22}) if it releases only $10^{-3}\,M_\odot c^2$ of energy in gravitational waves. An event that releases $10^{-2}\,M_\odot c^2$ of energy could be detected as far away as 40 Mpc, a volume of space in which there are several "starburst" galaxies and several hundreds of supernovae per year.

It is difficult to predict the strength of the radiation from a typical supernova, because perfectly spherical gravitational collapses produce no radiation at all. With a small amount of rotation a collapse becomes nonspherical but remains axisymmetric, and numerical simulations suggest that the formation of a neutron star in this way will yield between 10^{-6} and 10^{-4} solar masses of energy [12]. With more rotation, instabilities should force the collapsing stellar core into a non-axisymmetric form, with the likely emission of much larger amounts of energy. If the burst is still short-lived, then our estimates above mean that the 10^{-22} detector will have an excellent chance of seeing one from Virgo. If the energy comes out over several rotation periods, then numerical simulations will be required in order to provide a template waveform with which to filter the data; but in this case the sensitivity of the detector will be likely to be higher than for

a millisecond burst of the same energy [13]. The numerical modelling of gravitational collapse is under development in a number of research groups, including Cardiff and Garching (MPI für Astrophysik), using Cray X-MP computers. It is very likely that useful template waveforms will have been produced before the first-stage 10^{-21} detectors are operating.

The amount of rotation in a typical collapse is hard to predict, but the case for occasional events in which rotation dominates would be strong if the report of a pulsar in the remnant of SN1987a, with a pulse period of nearly 2 kHz, is confirmed [14]. Studies of neutron star models show that a star rotating that fast must either still be subject to a slowly-growing gravitational wave instability, or else it must be very close to such an instability. It would be very hard to form such a star without its having undergone nonaxisymmetric deformation, with the emission of considerable gravitational wave energy either as a burst or over a relatively few cycles of rotation.[1] Given the detection range of 60 Mpc, it would be surprising indeed if none of the thousand or so supernovae per year in that volume produced radiation of this magnitude.

2.2.2 Coalescing binaries

Since most stars begin as members of binary star systems, it is likely that a substantial fraction remain binary after the individual stars have completed their evolution and become either white dwarfs, neutron stars, or black holes. A small number of these will have been brought so close together during earlier phases of binary evolution that their orbital lifetime against the loss of energy to gravitational radiation is less than the age of the Universe. Such systems will coalesce in an astronomically short time. Systems containing white dwarfs are not of interest to us here, since they coalesce before their orbital radiation reaches a frequency we could observe. But those composed of highly compact objects – neutron stars and/or black holes – can produce observable radiation.

Coalescing binaries give off a great deal of energy before they coalesce. As the radiation from a system consisting of two $1.4\,M_\odot$ neutron stars changes from 100 to 200 Hz, the waves carry away some $5\times10^{-3}\,M_\odot c^2$ in energy, comparable to a decent supernova burst. Because this energy is spread out over many cycles, the waves' amplitude is smaller than one would expect from a supernova. Nevertheless, by matched filtering it is possible to attain a much higher signal-to-noise ratio than for a comparable supernova.

There is one well-known binary coalescence *precursor* system in our Galaxy: the famous Binary Pulsar, PSR 1913+16, which has a remaining lifetime of about 10^8 years before it will coalesce. Importantly, a second such system, PSR 2127+11C, has very recently been discovered in the globular cluster M15 [15]. Its pulse and orbital characteristics are remarkably similar to those of PSR 1913+16. The masses of the component stars will not be known until the periastron shift is measured, but if we assume a pulsar mass of $1.4\,M_\odot$, then the minimum companion mass allowed by the mass function is $0.94\,M_\odot$.

[1] The report by Pizzella and collaborators of apparent coincidences between bar detectors and neutrino detectors near the time of SN1987a has nothing to do with this scenario. Pizzella himself points out that these coincidences are inconsistent with standard general relativity.

This implies a *maximum* remaining lifetime of 10^9 years. If we take the likely companion mass to be $1.4\,M_\odot$, then the lifetime of PSR 2127+11C is half that of PSR 1913+16. Furthermore, it is possible that PSR 0021-72A, in the globular cluster 47 Tuc, is also a precursor with a short lifetime [16]. Unfortunately, this pulsar is at the limit of detectability, and exhibits a number of unexplained features, so it is too soon to draw conclusions about it.

There are two aspects of the coalescing binary signal that favour detectors with good low-frequency sensitivity. First, since most of the power in the signal is concentrated at low frequencies, the ability to detect coalescing binaries is critically dependent on the lower cutoff frequency $f_{\rm lc}$. Second, at low frequencies (100–500 Hz) the coalescing binary system is well modelled by Newtonian point masses in circular orbits; corrections due to tidal, mass-exchange, and post-Newtonian effects are significant only in the high-frequency phase of the signal. If the detector has good sensitivity at 100–200 Hz, it will not be necessary to model these extra effects in the matched filters in order to obtain good signal to noise.

Assuming that no observing is possible below the lower cutoff frequency, Krolak [17] showed that the best signal-to-noise ratio attainable for a binary at a distance r when observed with a low-frequency detector (one whose optics are optimised for finding coalescing binaries, but which would reach a sensitivity $\sigma_{\rm bb}$ if it were optimised for high frequencies) is

$$\left(\frac{S}{N}\right)_{\text{coalescing binary}} = 22\left[\frac{\sigma_{\rm bb}}{10^{-22}}\right]^{-1}\left[\frac{f_{\rm lc}}{100\,\text{Hz}}\right]^{-7/6}\left[\frac{\mathcal{M}}{M_\odot}\right]^{5/6}\left[\frac{r}{100\,\text{Mpc}}\right]^{-1}, \tag{2.4}$$

where $\mathcal{M}$ is the *mass parameter* of the binary system, defined in terms of the reduced mass μ and total mass M by

$$\mathcal{M} = \mu^{3/5}M^{2/5}.$$

This signal-to-noise ratio applies only when the detector and source are optimally oriented with respect to each other; in the general case there will be a factor smaller than unity in the equation. To attain this best signal-to-noise ratio, the data must be analysed with a family of filters matched to the signal expected from a variety of possible systems. The filter parameters are $\mathcal{M}$ and the phase of the signal on arrival. In particular, the mass parameter determines how fast the frequency of the signal increases as the orbit decays:

$$\frac{f}{\dot{f}} = 7.8\left[\frac{f}{100\ \text{Hz}}\right]^{8/3}\left[\frac{\mathcal{M}}{M_\odot}\right]^{5/6}\ \text{s}. \tag{2.5}$$

The threshold for detection with an acceptable false alarm rate must take into account the fact that there will be many filters, perhaps as many as a thousand. But this is partly compensated by the fact that there are fewer independent measurements per filter in a given time – roughly 100 per second – than for broadband bursts – 1000 per second. And in any case, at $S/N \sim 4$ we are so far out on the Gaussian tail of the noise distribution that the false alarm probability changes very rapidly with threshold, so the large number of filters makes a small change in the required threshold. This issue has been discussed in detail elsewhere [11].

We shall illustrate the possible observations by again assuming a threshold S/N of 4 for a detector in a worldwide network of 3 or 4 detectors. Our first-stage 10^{-21} detector will have a range of $\sim$ 30 Mpc if optimised for kHz bursts with a low-frequency cutoff at 100 Hz, increasing to 65 Mpc if it is optimised for low frequencies. We will see below that events at these distances are likely to be rare, but our present uncertainty about the event rate would allow perhaps two events per year in the Virgo Cluster, and up to 50 per year out to 65 Mpc, of which the worldwide network could expect to detect roughly 10% (see below).

Our 10^{-22} detector optimised for low frequencies, could see binaries composed of two $1.4\,M_\odot$ neutron stars at threshold at a distance of 650 Mpc. If the low-frequency cutoff can be lowered to 40 Hz, and if the dominant noise below 100 Hz is thermal noise from the mirrors' suspension, then detailed calculations using the shape of the thermal noise spectrum show that this range is roughly doubled to 1.3 Gpc.

Equations 2.4 and 2.5 contain an important relation: the masses of the stars enter only in the mass parameter $\mathcal{M}$. By measuring the signal amplitudes and the rate of change of the frequency, the two equations can be combined to yield a single unknown, the distance to the source. In fact there is not enough information from a single detector to make a measurement of the orientation angles needed to determine the maximum signal amplitude used in Equation 2.4, but a network of three detectors could do so. In this way, coalescing binaries become distance indicators, and this has important implications for astronomy, to which we return later.

Not all binaries will consist of neutron stars. The statistics of X-ray binaries suggest that perhaps one percent will contain a black hole of roughly $14\,M_\odot$; it is possible that a further one percent of these might consist of two such black holes. The signal-to-noise ratio of the two-black hole system would be some 6.3 times larger than that of two neutron stars at the same distance, so the range of the optimised second-stage detector for binary black holes would be more than 4 Gpc, approaching a cosmological redshift of 0.5.

The maximum range of the detector is not the whole story, since orientation-dependent effects will reduce the probability that any given coalescence will be seen. Tinto [18] has made a detailed study of these effects in a network of 4 or 5 detectors, and has concluded that it would register about 50% of all coalescences that take place within half of its maximum range, and it will see some 5–10% of all those within its maximum range. These numbers would not change greatly if the worldwide network had only 3 or 4 detectors.

An important question that we touched on above is the quality of the predicted waveform that is used to construct a filter for these signals. It assumes a point-mass Newtonian binary with a circular orbit. The circular assumption is a good one for binaries this close, since eccentricity decreases faster than orbital radius under the action of gravitational radiation reaction. The influence of tidal, mass-exchange, and post-Newtonian effects have been considered in detail by Krolak [17], who found that they begin to be important above 500 Hz or so. The estimates we have used here for signal-to-noise ratios are dominated by the power in the signal between 100 and 200 Hz, so they will be insensitive

to any such corrections. On the other hand, if such effects can be modelled reliably then they can be used to improve the signal-to-noise ratios we have quoted here, and to extract further astrophysical information from the observations.

The event rate out to any distance is very uncertain, however, since our estimates rely on the two firmly identified precursor systems, PSR 1913+16 and PSR 2127+11C. The most likely value for the rate is probably 3 events per year out to 100 Mpc [19], which would give an event rate in a network of 3 or 4 optimised 10^{-22} detectors of 40-80 per year. We had elsewhere estimated [11] that this rate may be uncertain by a factor of 100 either way, allowing a detection rate that could range from one every two years up to several thousand per year. But the recent discovery of the second coalescence precursor PSR2127+11C [15] considerably reduces the small-number-statistics uncertainty in this estimate, placing the likely event rate between 3 and several thousand per year. Further pulsar searches currently underway by the same group may well raise this yet again by overcoming some of the selection effects that inhibit the discovery of pulsars in highly eccentric binaries.

2.2.3 Pulsars and other continuous-wave sources

There are many possible long-lived or continuous sources of gravitational radiation in the frequency range accessible to our proposed detector. These include pulsars with "lumps" in their crust; unstable pulsars spinning down after having been formed with too large an angular velocity; and unstable accreting neutron stars where the instability is being driven by the accretion of angular momentum ("Wagoner stars"). Little is known about how many such sources in our Galaxy emit significant amounts of radiation, but the proposed detector would be able to set very stringent limits on this.

In Chapter 3 we discuss various ways to configure the optics of a detector in order to make it narrow-band, with enhanced sensitivity near the expected frequency of a particular source [20, 21, 22]. Equation 3.7 gives the narrow-band sensitivity $\sigma_{\rm nb}$ of a photon-noise limited detector; it can be seen to depend not only on $\sigma_{\rm bb}$ but also on the quality $1 - R$ of the recycling mirrors used and the length ℓ of the detector's arms. Equation 3.8 gives the minimum bandwidth of such a detector; it is typically about 2 Hz. However, as Figure 3.4 shows, thermal noise from mirror vibrations is likely to dominate the photon noise, by a factor of perhaps up to 5.

The sensitivity achievable on a continuous source increases with the square root of the observation time $\tau_{\rm int}$. One might contemplate narrow-banding a detector for a period of up to a few months in order to make an important observation; a significantly longer observation might not be desirable, given the importance of searching for bursts and for continuous sources at other frequencies. For a continuous wave of amplitude h, the expected signal-to-noise ratio of such an observation would be (if it is photon-noise limited)

$$\left(\frac{S}{N}\right)_{\substack{\text{pulsar}\\ \text{photon noise}}} = 6\left[\frac{h}{10^{-27}}\right]\left[\frac{\sigma_{\rm bb}}{10^{-22}}\right]^{-1}\left[\frac{\tau_{\rm int}}{10^{7}\,\text{s}}\right]^{1/2}\left[\frac{1-R}{5\times 10^{-5}}\right]^{-1/2}\left[\frac{\ell}{3\,\text{km}}\right]^{1/2}. \qquad (2.6)$$

If thermal noise does dominate, as seems likely, this becomes something like

$$\left(\frac{S}{N}\right)_{\substack{\text{pulsar}\\ \text{thermal noise}}} = 1.2\left[\frac{h}{10^{-27}}\right]\left[\frac{\tau_{\text{int}}}{10^7\,\text{s}}\right]^{1/2}. \tag{2.7}$$

In these equations, we have allowed a factor of $1/\sqrt{5}$ reduction in signal-to-noise to take account of the fact that the typical source will not be optimally oriented with respect to the detector. For waves from a pulsar whose frequency is known, the threshold does not need to be set very high: 2 would be enough to make one interested in extending the observation, and 4 would be convincing. Analysing the data from such an observation will be easy: the heterodyning technique described by Schutz [23] reduces even four months' worth of data to a manageable size.

We find that a source with a gravitational wave frequency of 4 kHz at a distance of 50 kpc (such as the reported pulsar in SN1987a) would need to radiate only 2×10^{32} W to be detectable above thermal noise. This is well below the upper limit of 7×10^{35} W inferred from the reported observations of the pulsar [14]. The achievement of better thermal noise (see Figure 3.4) would improve on this gravitational wave luminosity limit by a factor of 10.

Even if the detector is not optimised for a particular frequency, it would be possible to use data from a broadband recycling detector to search for a known source. In this case, photon noise would be expected to dominate thermal noise, as in Figure 3.3. The signal-to-noise ratio is then independent of the length or mirror quality of the detector except as they influence σ_{bb}. For frequencies below the optimum frequency of the detector (say, 1 kHz), a 10^{-22} detector can reach $h \sim 2 \times 10^{-27}$ in $\tau_{\text{int}} \sim 10^7$ s (again allowing a factor of $1/\sqrt{5}$ for antenna-pattern effects). This is still a very interesting level for several pulsars. For frequencies above 1 kHz, the signal-to-noise ratio falls off from the above value inversely with the pulsar frequency. This would give a 2σ sensitivity of about 2×10^{-26} for the pulsar in SN1987a, at which level it would be radiating about 6×10^{34} W. This would still be an interesting observation.

Another interesting class of sources are Wagoner stars, where accretion drives a non-axisymmetric Chandrasekhar-Friedman-Schutz (CFS) instability of the neutron star, causing it to radiate gravitational wave energy at a rate proportional to the accretion rate and hence to the X-ray luminosity. This leads to the relation, for a narrow-banded detector dominated by thermal noise, and allowing for typical antenna-pattern effects,

$$\left(\frac{S}{N}\right)_{\text{Wagoner star}} = 3\left[\frac{f}{300\,\text{Hz}}\right]^{-1/2}\left[\frac{F_X}{10^{-11}\,\text{W m}^{-2}}\right]^{1/2}\left[\frac{\tau_{\text{int}}}{10^7\,\text{s}}\right]^{1/2} \tag{2.8}$$

where F_X is the X-ray flux from the system. Several X-ray sources exceed the reference flux of $10^{-11}\,\text{Wm}^{-2}$. For a narrow-band observation to be possible, the gravitational wave frequency must be known in advance, at least to within the bandwidth of the detector. It may be possible to infer this frequency from low-amplitude modulations of the X-ray flux. In order to keep the bandwidth as large as possible, a thermal-noise-dominated detector would probably be operated with less-than-maximum narrow-banding, with the bandwidth adjusted to set the photon noise (which falls with the square root of the

bandwidth) just below the thermal noise. For the noise levels indicated in Figure 3.4, the bandwidth could be as large as 50 Hz.

There may be pulsars in the solar neighbourhood that are not visible electromagnetically (because they are beamed elsewhere or because they are old and radio-quiet), but which could still be radiating gravitational waves. But the problem of conducting an all-sky search for such signals is formidable: the Earth's motion produces Doppler effects that need to be removed from any observations lasting longer than about 30 minutes, and these corrections are different for each different location on the sky. The longer an observation lasts, the better will be its directional resolution, and therefore the greater will be the number of possible locations that have to be looked at. Simply performing the data analysis on 4 months' worth of data over a 2 Hz bandwidth is beyond the capacity of present computers [23].

One would normally expect to have to analyse a data set in a time no longer than the time it took to take the data in the first place. Given a computer capable of performing fast Fourier transforms (FFTs) at a computation speed of 300 Mflops, the longest duration of a narrow-bandwidth (2 Hz) observation on which one could perform an all-sky search is about 5 days at 100 Hz. This would give a signal-to-noise ratio in our proposed 10^{-22} detector (when thermal-noise-dominated, and allowing for antenna-pattern effects) of

$$\left(\frac{S}{N}\right)_{\text{FFT}} = 2\left[\frac{h}{10^{-26}}\right]\left[\frac{\mathcal{S}}{300\,\text{Mflops}}\right]^{1/8}, \tag{2.9}$$

where $\mathcal{S}$ is the speed of floating point operations in an FFT on the computer. A pulsar could thus be reliably identified even for $h \sim 10^{-26}$; this is quite an interesting sensitivity level for pulsars.

Another possible way of looking for unknown pulsars is by cross-correlating the output of two or more detectors. Cross-correlation requires much less computing but has a sensitivity that is lower than the optimum achievable in a single detector in the same observation time τ_{int}:

$$\left(\frac{S}{N}\right)_{\text{correlation}} = \left(\frac{S}{N}\right)_{\text{optimum}} \times (\tfrac{1}{2}B\tau_{\text{int}})^{-1/4}, \tag{2.10}$$

where B is the bandwidth of data being correlated. Since the optimum signal-to-noise ratio increases as $\tau_{\text{int}}^{1/2}$, it follows from this that a correlation experiment lasting a time τ_{c} and a single-detector observation lasting τ_{s} will have the same sensitivity over a bandwidth B if

$$\tau_{\text{c}} = \tfrac{1}{2}B\tau_{\text{s}}^2.$$

The single-detector observation lasting 5 days could only be matched over a 2 Hz bandwidth by a correlation experiment lasting 6,000 years! So cross-correlation is not a serious alternative to direct analysis of a single detector's data for a *narrow-band* all-sky pulsar search.

In order to conduct an all-frequency (up to 2 kHz), all-sky search in a fixed time of, say, 10^7 s, analysing the data with a 300 Mflops computer, the best strategy would be to

make a series of observations restricted to successive bandwidths of about 13 Hz, each lasting 18 hours. The sensitivity of such a search would be a few times 10^{-26} for h in the thermal-noise-dominated case. If further information suggested that a particular frequency band was interesting – for example a newly formed pulsar was spinning down at a significant rate that wasn't well determined by electromagnetic observations, or a frequency was indicated by X-ray data in a Wagoner star but not well determined – then a narrow-band search could further improve the sensitivity.

2.2.4 Stochastic background radiation

There have been many predictions of a measurable background of gravitational radiation, usually as a by-product of theories to explain other things in cosmology, such as phase transitions or galaxy formation. One of the most interesting, since it makes definite predictions, is the cosmic string scenario for galaxy formation. If strings did actually provide the seeds around which galaxies condensed, then their decay must have produced a gravitational wave background that is detectable by cross-correlation between two detectors.

The signal-to-noise ratio of a cross-correlation to find the stochastic background can be found from our cross-correlation formula for searches for continuous sources, Equation 2.10, provided we interpret $(S/N)_{\text{optimum}}$ correctly. It is given by the ratio of the typical amplitude of the stochastic field *within the bandwidth B of the correlation experiment* to the narrow-band noise σ_{nb} in the detector in the same bandwidth. The radiation's amplitude within a bandwidth B can be expressed in terms of the energy density in the radiation per unit logarithmic interval of frequency, Ω_{gw}:

$$\Omega_{\text{gw}}(f) = \frac{1}{\rho_{\text{c}}} \cdot \frac{dE_{\text{gw}}}{d^3x d\ln f}\,, \tag{2.11}$$

where ρ_{c} is the critical closure density of the Universe – about $1.75 \times 10^{-9}\,\text{J m}^{-3}$ if Hubble's constant H_0 is 100 km/s/Mpc – and where dE_{gw}/d^3x is the energy density of stochastic gravitational radiation. Then the radiation in a bandwidth B about frequency f has an effective amplitude given by

$$h = 1.8 \times 10^{-25} \left[\frac{f}{100\,\text{Hz}}\right]^{-3/2} \left[\frac{B}{2\,\text{Hz}}\right]^{1/2} \left[\frac{\Omega_{\text{gw}}}{10^{-8}}\right]^{1/2} \left[\frac{H_0}{100\,\text{km s}^{-1}\,\text{Mpc}^{-1}}\right]. \tag{2.12}$$

In order to optimise the experiment, the bandwidth should be chosen to make photon noise, thermal noise from the suspension, and thermal noise from mirror vibrations roughly equal. The exact details will depend on the performance of the real detector, but a typical bandwidth might be 10 Hz. Using the photon noise σ_{nb} multiplied by $\sqrt{3}$ to allow for the three noise sources, and allowing the usual factor of $\sqrt{5}$ for orientation, we find that one can achieve a signal-to-noise ratio of

$$\left(\frac{S}{N}\right)_{\text{stochastic}} = 3 \left[\frac{f}{100\,\text{Hz}}\right]^{-5/2} \left[\frac{\sigma_{\text{bb}}}{10^{-22}}\right]^{-1} \left[\frac{\Omega_{\text{gw}}}{10^{-8}}\right]^{1/2} \left[\frac{H_0}{100\,\text{km s}^{-1}\,\text{Mpc}^{-1}}\right] \tag{2.13}$$

over an observation lasting 10^7 s in our proposed 10^{-22} detector. This detector should be able to reach $\Omega_{\rm gw} \sim 10^{-8}$, considerably below the predictions of cosmic string theory and well below the sensitivity one could expect from pulsar timing.

Correlation experiments require, of course, two independent detectors. When we have only one detector operating, we will do such experiments with our international collaborators. An important consideration is that sensitivity falls off if the separation between detectors is larger than $\lambda_{\rm gw}/2\pi$. Baselines within Europe are therefore preferable, but even on the shortest conceivable one – between Munich and Pisa – the sensitivity begins to fall off significantly above 100 Hz. (There is still a solid angle in which the sensitivity is high, but this does not help a stochastic search, since the effective wave amplitude will decrease with decreasing solid angle of acceptance for such an experiment. In fact, this argument can be elaborated to show that the sensitivity will fall off with separation d roughly as $d^{-1/2}$.) On a baseline between Scotland and Pisa we should be able to reach $\Omega_{\rm gw} \sim 2 \times 10^{-8}$, and even in a transatlantic correlation experiment we could get to $\sim 2 \times 10^{-7}$, which is still interesting in terms of the predictions of cosmic string theory.

2.2.5 Unpredicted sources

As with the opening of any other window in astronomy, one can be confident that there will be unexpected sources of gravitational waves at some level. If they are strong enough to stand out above the broadband noise, then they will be readily detected and studied. If they are weaker but have some structure, such as the coalescing binary signal, then they may still be detectable using cross-correlation between detectors. The signal-to-noise ratio is less than the optimum obtainable by matched filtering using prior knowledge of the waveform by the same factor as in Equation 2.10 above, $(\frac{1}{2}B\tau_{\rm int})^{1/4}$, where B is the bandwidth and $\tau_{\rm int}$ the correlation time.

For example, suppose two 10^{-22} recycling detectors optimised for broadband bursts observe a weak signal lasting 1 s with a typical frequency of 200 Hz, not very different from the parameters of a coalescing binary. In this case, photon noise dominates. Allowing for antenna-pattern effects, and using a 200 Hz bandwidth gives

$$\left(\frac{S}{N}\right)_{\rm hypothetical} = 11 \left[\frac{E}{10^{-2}\, M_\odot c^2}\right]^{1/2} \left[\frac{r}{15\,{\rm Mpc}}\right]^{-1}.$$

So a source radiating the same energy as a coalescing binary could be seen in the Virgo cluster. Whether such sources exist and are frequent enough to give a reasonable event rate is a question that will only be answered by observation. Certainly such correlations should be done after supernova events, for example, in order to look for neutron star spindown or any unpredicted aftermath radiation.

2.3 Scientific Output of an Interferometric Detector

Having reviewed various sources of gravitational waves in the previous section, we shall organise the present section according to the scientific questions that gravitational wave observations are likely to answer. In many cases such answers will come from combining observations of several different kinds of sources. We will begin our list with three new tests of relativistic gravity that observations of gravitational waves can perform.

- **Test of gravitational wave polarisation.** Simply seeing gravitational waves would, of course, be a milestone for relativistic gravity. But many theories predict gravitational waves, and a network of detectors can distinguish among them. With four or more detectors, one has redundant information in the observations. Using general relativity one attempts to deduce the amplitude, polarisation, and direction of the wave. If the resulting data are self-consistent, then general relativity provides a good model of the wave, particularly of its polarisation properties. If they are not self-consistent, then a different theory of gravity may be necessary.
- **Speed of propagation of gravitational waves.** If a supernova at 15 Mpc were seen optically and detected by the gravitational wave network, there should be less than a day's delay between the gravitational wave and the optical detections, provided the gravitational wave travels at the same speed as the light from the supernova. Over a travel time of some 45 million years, the coincident arrival of the waves within a day would establish that their speeds were equal to within one part in 10^{10}.
- **Test of strong-field gravity.** A further test can be made if black hole coalescing binaries are detected. Computer simulation should soon be accurate enough to make detailed predictions of the dynamics of the merger of the holes, and of the radiation they emit, with only a few parameters (such as the masses, spins, total angular momentum, and impact parameter of the collision). Given a reasonable signal-to-noise ratio, matching the observations to the predictions could provide a stringent test of strong-field gravity.
- **Morphology of the supernova core.** Observations of bursts from gravitational collapses tell us a number of things about supernovae themselves. We could learn how many collapses do not produce visible supernovae; how often rotation plays an important role in the collapse; whether the collapse has formed a neutron star or a black hole; and what the mass and angular momentum of the compact object are.
- **Neutron star equation of state.** This is one of the most important areas where gravitational wave astronomy can provide information that is crucial to nuclear physics: the interactions of neutrons in these conditions are poorly understood and inaccessible to laboratory experiments. Supernova gravitational wave observations constrain the equation of state by telling us what the timescale of collapse and rebound is, what the mass and angular velocity of any neutron star formed in the

collapse might be, and what the upper mass limit of neutron stars is. Coalescing binaries similarly offer information on neutron star masses (through the mass parameter $\mathcal{M}$) and on mass exchange once the initial point-mass approximation breaks down. Observations of pulsars radiating from frozen-in mass deformations constrains the solid crust equations of state. Observations of the frequencies of CFS instability modes either in new neutron stars spinning down or in Wagoner stars provide a very sensitive constraint on the equation of state, and also give information about neutron matter viscosity, another poorly understood subject.

- **Compact-object statistics.** It is very hard to devise unbiased indicators of the numbers and distribution of pulsars, old neutron stars, and black holes. Observations of gravitational waves from supernovae and coalescing binaries can give a new measure of the mass functions of these populations and of their formation rate. Searches for unknown pulsars, if successful, could give a relatively unbiased indication of their distribution in the solar neighbourhood.
- **Hubble's constant.** If the event rate of coalescing binaries is sufficient to give a few per year from within 100 Mpc, then the fact (noted above) that coalescing binaries are reliable distance indicators allows one to measure Hubble's constant to within a few percent in a year or two of observations [24]. This in turn will determine the age of the Universe and the distance scale to external galaxies.
- **Cosmological mass distribution.** Given a reasonable event rate, coalescing binaries are good tracers of the stellar distribution out to 500 Mpc or (for black holes) a few Gpc. Their distribution would indicate structure out to 500 Mpc with a resolution of 10–100 Mpc, a length scale on which we have little information at present. Such observations could provide a stringent test of the homogeneity and isotropy of the Universe.
- **The early Universe.** By confirming or ruling out a stochastic background of gravitational radiation as predicted by cosmic string theory, gravitational wave observations can be crucial to the cosmic string theory of galaxy formation. If other backgrounds are detected, they will have to be explained by some physics in the early Universe. If the explanation has to do with phase transitions, for example, then this would have implications for particle physics; if an early generation of very massive objects is the cause, then this has implications for galaxy formation as well.

Chapter 3

Interferometric Gravitational Wave Detectors – an Outline

A gravitational wave curves the spacetime through which it passes. This results in a change in the time it takes for light to travel between two free masses or, equivalently, in a change of apparent separation. The phase shift on the light may be detected if it is converted to an intensity change by interfering two beams of light which have been differently affected by the gravitational wave, such as in a Michelson interferometer.

For optical path lengths small compared with the wavelength of the gravitational wave (300 km for a 1 kHz signal) the phase shift is proportional to the length of each arm. Thus, one can gain in sensitivity both by increasing the physical arm-length of the interferometer, and by bouncing the light back and forth many times in each arm before interference takes place at the beamsplitter (see Figure 3.1).

3.1 Interferometer Types

Two different techniques for achieving the required long optical path length in the arms of an interferometer have been proposed. These are the optical delay line (originally invented by Herriot, Kogelnik and Kompfner [25]) developed at MIT and the Max-Planck-Institut, and the Fabry-Perot scheme investigated at Glasgow and Caltech. A major difference between these approaches is that in the delay line the multiple traverses of the light within an arm are spatially separated, whereas with the Fabry-Perot they are coincident.

At first sight the Fabry-Perot system would appear to offer considerable advantages since it requires much smaller mirrors and the light beams occupy a much smaller volume in the interferometer arms. It should thus be possible to fit more receivers into a given vacuum pipe diameter. Additionally it is possible to achieve a very large number of effective traverses in the arm with a Fabry-Perot, while delay lines with 3 km long arms are limited to 50 to 100 beams even with the largest mirrors that can reasonably be used.

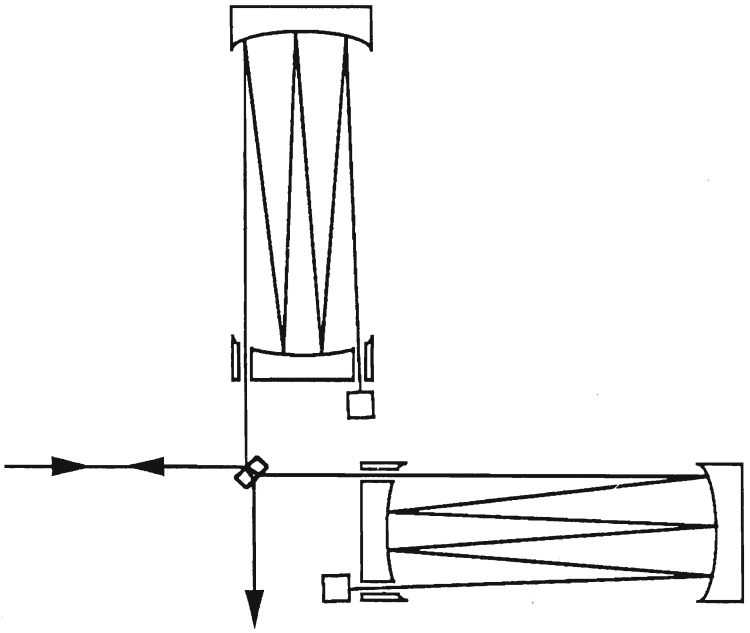

Figure 3.1: *Schematic diagram of the proposed multi-pass Michelson interferometer.*

Set against these advantages, however, are potential practical complications. These include possible thermal lensing effects on the focussing of the light transmitted through mirror substrates, the requirement for very high stability of mirror alignment, and in particular the fact that Fabry-Perot receivers are somewhat more complex to operate. An insight into this complexity can be gained by noting that for a Fabry-Perot receiver to operate at all it is required that each of the two arms independently stays closely in resonance with the input laser light. The ultra narrow optical linewidth of very long high finesse cavities, together with the typical levels of laser frequency noise, means that extremely precise control of laser frequency and/or arm length are needed to maintain the resonance condition. In addition, one must control the relative phase of the beams returning from the two arms. The delay line need only provide this relative phase control – a significant simplification. Despite these factors the Fabry-Perot prototypes have proved very successful and have achieved sensitivities similar to that obtained with the delay line prototype.

3.2 Sensitivity and Noise Sources

The magnitude $\delta\phi$ of the phase shift out of a delay line in which the light is stored for a time τ_s is

$$\delta\phi = h\frac{\nu}{f}\sin(\pi f \tau_s)\,, \tag{3.1}$$

where h is the amplitude of a continuous gravitational wave of frequency f and ν is the frequency of the sensing light. It can be seen that maximum signal is obtained if the storage time τ_s is half the period of the gravitational wave. (The sign of the gravitational

wave reverses every half period, tending to cancel the induced signal.) So if we have a detector of length ℓ and wish to observe a gravitational wave of frequency f, maximum phase shift is obtained if a delay line has a number of reflections N of

$$N = \frac{c}{2\ell f} = 50 \left[\frac{\ell}{3\,\mathrm{km}}\right]^{-1} \left[\frac{f}{1\,\mathrm{kHz}}\right]^{-1}, \tag{3.2}$$

where c is the speed of light.

3.2.1 Shot noise in a simple interferometer

The induced phase shift produces a power change at the output of the interferometer. If this is to be detectable, it must be larger than the $\sqrt{n}$ uncertainty associated with an average count of n photons (unless squeezed light techniques are used). This photon shot noise will limit the detectable gravitational wave amplitude in a simple delay line to

$$h_{\mathrm{DL}} \geq \left(\frac{\pi\hbar\lambda\,\Delta f}{\epsilon I_0 c}\right)^{1/2} \frac{f}{\sin(\pi f \tau_{\mathrm{s}})}, \tag{3.3}$$

where $\hbar$ is Planck's (reduced) constant, λ is the light wavelength, Δf is the measuring bandwidth, ϵ is the photodetector quantum efficiency and I_0 is the light power in the interferometer. Operating in the storage time limited regime ($f\tau_{\mathrm{s}} = \frac{1}{2}$), the pulse sensitivity of such a simple interferometer is therefore limited to

$$h_{\mathrm{DL}} \sim 2.4 \times 10^{-21} \left[\frac{\epsilon I_0}{50\,\mathrm{W}}\right]^{-1/2} \left[\frac{f}{1\,\mathrm{kHz}}\right]^{3/2}, \tag{3.4}$$

where it is assumed that a bandwidth $\Delta f = f/2$ is chosen and that light of wavelength $\lambda = 532\,\mathrm{nm}$ is used.

In Chapter 2 we have seen that our eventual goal must be a sensitivity for kHz bursts of $\sim 10^{-22}$. The shot noise limit of Equation 3.4 must therefore be considerably improved.

3.2.2 Shot noise in recycled interferometers

A method for increasing the effective light power and so reducing the photon noise was suggested in 1981 independently by Drever [26] and Schilling. The interferometer normally operates with its output on a dark fringe, so virtually all of the light coming back from the arms of the interferometer travels back towards the laser (see Figure 3.1). By suitable placement of the recycling mirror $\mathrm{M_0}$, this light may be coherently added to the incoming light. Since the number N of reflections in the arms of the interferometer is quite low (cf. Equation 3.2) and mirrors of loss $1 - R \leq 10^{-4}$ are available, little light is lost on a single round trip and the power enhancement from this recycling may be high.

In order to match the storage time to the gravitational wave frequency, optimising a detector for lower frequencies ($\leq 500\,\mathrm{Hz}$) requires a number of reflections, and thus a

mirror diameter, that becomes impracticably large with a delay line system, though there is no problem if optical cavities are used. The signal storage time may, however, still be matched to the gravitational wave period by placing a partially reflecting mirror M_3 in the output port of the interferometer (see Figure 3.2). This technique, which

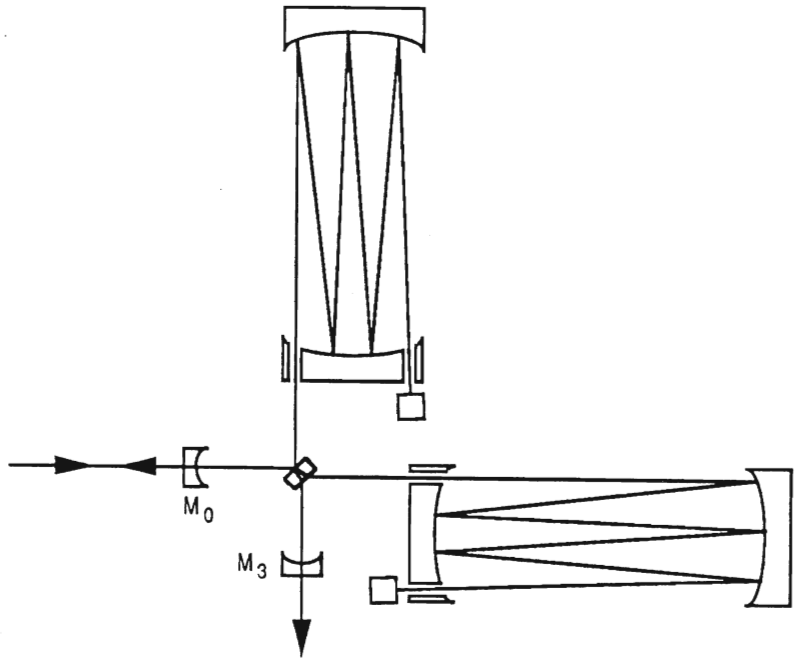

Figure 3.2: *Schematic diagram of a multi-pass Michelson interferometer showing the two recycling mirrors.*

ensures that both the laser light and at least one gravitational-wave-induced sideband are resonant within the optical system, is known as dual recycling [22]. A signal storage time τ_s', determined by the reflectivity of M_3 together with that of the delay line (or cavity), gives a detector bandwidth of $\Delta f \approx 1/\tau_s'$ while the frequency of optimum sensitivity is determined by the positioning of M_3. This allows good broadband sensitivity to be achieved at low frequency.

If the losses in the delay line mirrors dominate the losses due to imperfect fringe contrast, the photon noise limited sensitivity for an optimised detector becomes

$$h_{\rm DL} \approx \sqrt{\frac{\lambda\hbar f\,\Delta f(1-R)}{\epsilon I_0 \ell}}\,. \tag{3.5}$$

For pulses, a choice of $\Delta f = f/2$ gives a sensitivity

$$h_{\rm DL} = \sigma_{\rm bb} \approx 10^{-22}\left[\frac{f}{1\,{\rm kHz}}\right]\left[\frac{\epsilon I_0}{50\,{\rm W}}\right]^{-1/2}\left[\frac{1-R}{5\times10^{-5}}\right]^{1/2}\left[\frac{\ell}{3\,{\rm km}}\right]^{-1/2}. \tag{3.6}$$

So a 10^{-22} detector should be possible as long as it is feasible to obtain and use high laser power, in combination with good quality mirrors.

To allow maximum recycling gain, power must not be allowed to escape via the output port of the interferometer; this places a stringent requirement on the fringe contrast that has to be achieved. For example an effective contrast ratio of $\sim 10^{-4}$ will be required to avoid degrading the sensitivity of a detector optimised for 1 kHz signals.

It is also possible to enhance the sensitivity within a narrow bandwidth and so improve the detectability of continuous gravitational wave signals. This is achieved by dual recycling with long signal storage times. The best shot noise limit for narrowband signals, again assuming the mirror losses are dominant, now becomes

$$h_{\mathrm{DL}} = \sigma_{\mathrm{nb}} \approx \left(\frac{\lambda\hbar c}{\pi\epsilon I_0 \tau_{\mathrm{int}}}\right)^{\frac{1}{2}} \frac{(1-R)}{\ell} = 10^{-28}\left[\frac{\epsilon I_0}{15\,\mathrm{W}}\right]^{-\frac{1}{2}}\left[\frac{1-R}{5\times10^{-5}}\right]\left[\frac{\ell}{3\,\mathrm{km}}\right]^{-1}\left[\frac{\tau_{\mathrm{int}}}{10^7\,\mathrm{s}}\right]^{-\frac{1}{2}}, \tag{3.7}$$

where τ_{int} is the integration time. The detector bandwidth in this optimised case is

$$\Delta f \approx \frac{c(1-R)}{\pi\ell} = 2\left[\frac{\ell}{3\,\mathrm{km}}\right]^{-1}\left[\frac{1-R}{5\times10^{-5}}\right]\mathrm{Hz}\,. \tag{3.8}$$

Other narrowbanding arrangements have been proposed: resonant recycling [20] and detuned recycling [21]. However, dual recycling has better tuning properties and can be added naturally to a broadband high-frequency system; it therefore seems the best choice.

In the long run when tens of watts of laser power will be used, heating of optical components due to absorption may produce significant distortion of the beam shape. In the case of a reflecting mirror the deformation of the wavefront is due to the expansion of the heated material, and in the case of a mirror used in transmission is also due to a change in the index of refraction. Wavefront distortion degrades the coupling into cavities for mode cleaning and recycling and into the interferometer arms in a Fabry-Perot based system. In addition it degrades the fringe contrast inside the interferometer and thus reduces the recycling gain. To control these effects, materials of low absorption and carefully chosen thermal properties will be used, and the interferometer will be made as symmetrical as possible.

As will be seen shortly, the power level required to attain a given photon noise limited sensitivity may be reduced if it is possible to use the noise reducing properties of squeezed light.

3.2.3 Other noise sources

There are, of course, noise sources other than photon counting fluctuations. The most important of these are:

- **Optical noise:** Fluctuations in the frequency, power and geometry of the light, possibly coupled via scattered light, may produce spurious phase fluctuations. Careful design of the interferometer optical system together with active control of laser beam quality are required. Further consideration of these topics appears in Chapter 4.
- **Seismic noise:** Ground vibrations may induce motion of the test masses. Isolation measures are discussed in Chapter 6.
- **Thermal noise:** Each normal mode of the test masses will have thermal motion associated with it. The normal modes must be arranged to lie outside of the frequency region of interest, so that the noise observed is only from the tails of the resonances. A high mechanical Q reduces this noise. The relevant modes include both the internal acoustic modes of the test masses and the pendulum modes of their suspensions. The Q of the latter may be higher than that of the materials involved since only a small fraction of the energy of motion is stored in the flexures.
- **Refractive index fluctuations in the vacuum:** these fluctuations determine the maximum allowable gas pressure for a given strain sensitivity.

  Fluctuations of the number of molecules in the light path lead to small changes in the refractive index. The resulting apparent path length variations depend on the magnitude of these index fluctuations and on the degree to which they can coherently affect the multiple traverses of the light within an interferometer arm. The largest coherent effect occurs when Fabry-Perot cavities are used; some small correlation is also inevitable with delay line systems.

  The "vacuum noise" lines on the sensitivity graphs (Figures 3.3 and 3.4) indicate an upper bound for the noise due to index fluctuations in thermodynamic equilibrium, assuming the vacuum specifications laid down in the beginning of Section 5.2, *i.e.* $< 10^{8}$ mbar for hydrogen and $< 10^{-9}$ mbar for heavier molecules, such as water and nitrogen.
- **Quantum limit:** Heisenberg's Uncertainty Principle limits the accuracy of the displacement measurement.

The significance of the most fundamental noise sources in the proposed interferometer is shown in Figures 3.3 and 3.4.

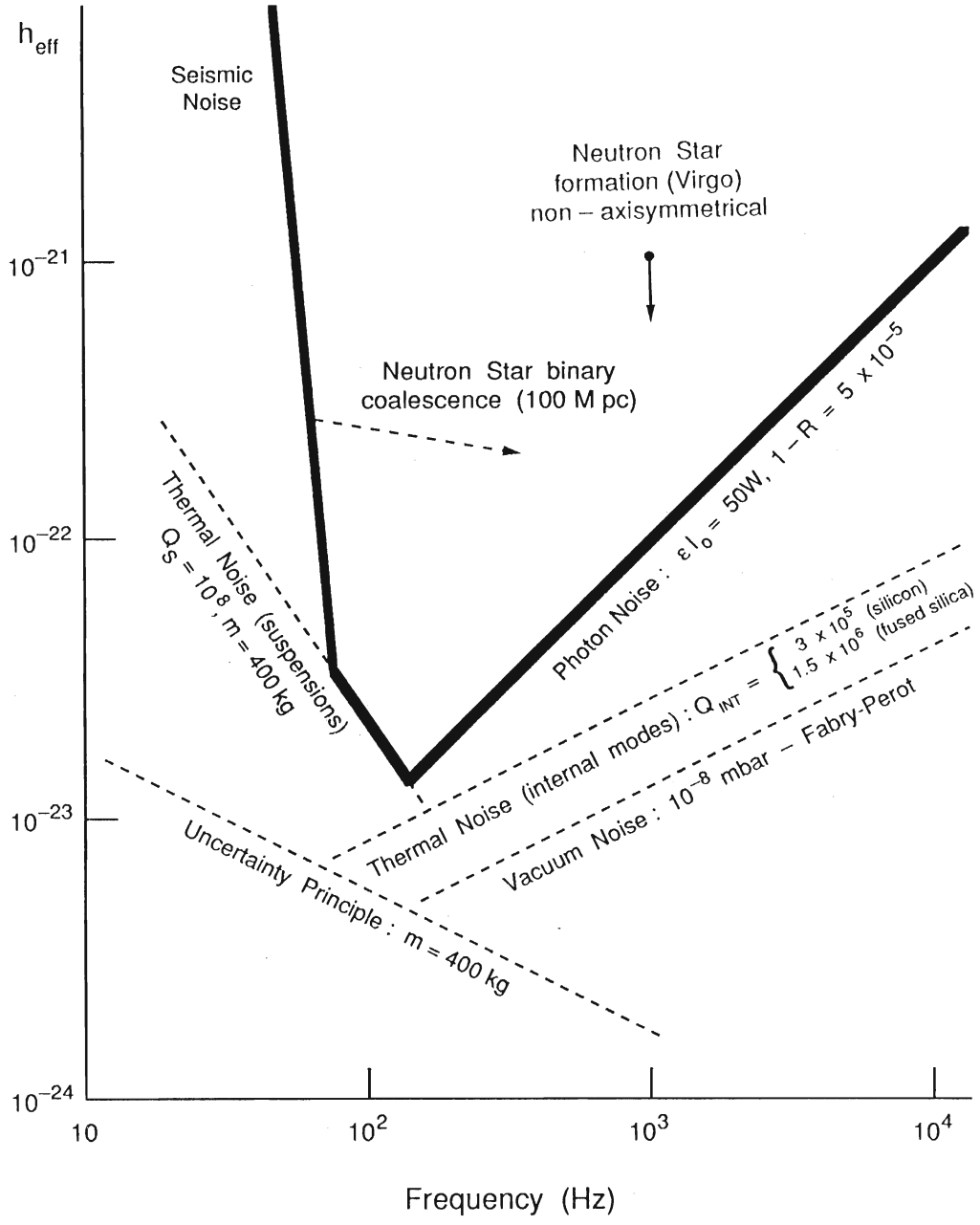

Figure 3.3: *Some burst sources and relevant noise levels. The ordinate is the effective amplitude* $h_{\rm eff}$*, which is defined as* $(S/N)\,\sigma_{\rm bb}(f)$*, where* S/N *is the signal-to-noise ratio given for different sources in the text and* $\sigma_{\rm bb}(f)$ *is the value of the photon noise at the burst's central frequency* f*, as shown in the figure. For sources that have to be picked out by filtering, the effective amplitude is approximately* $h\sqrt{n/2}$*, where* h *is the true amplitude and* n *is the number of cycles of the waveform over which the signal can be integrated.*

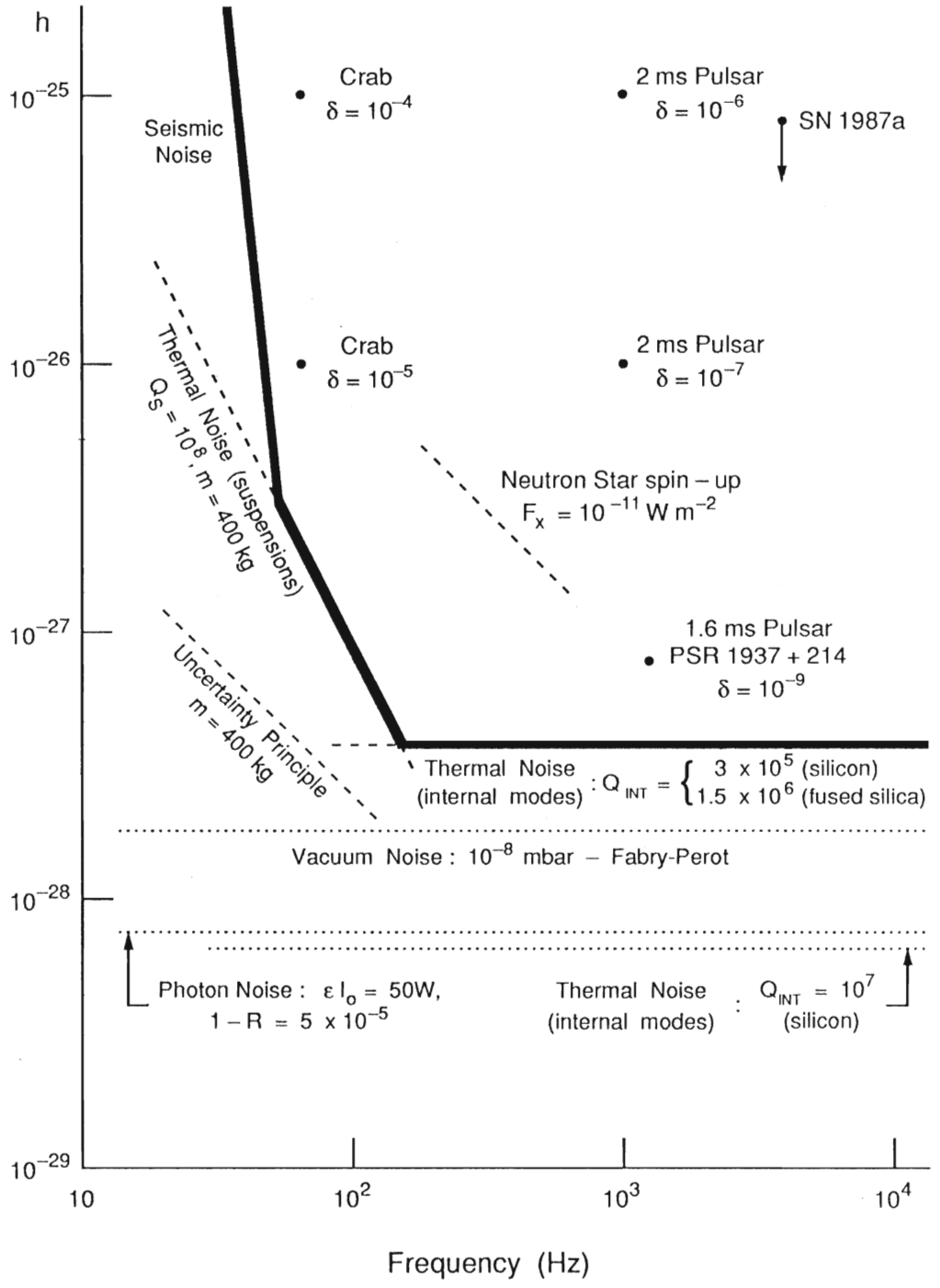

Figure 3.4: *Signals from possible sources of continuous radiation. An integration time of 10^7 s is assumed. Note that due to possible non-optimum relative orientation of source and detector, signal strengths may need to be reduced by a factor of up to $\sqrt{5}$. Thermal noise for Q_{INT} ranging from 3×10^5 to 10^7 is shown, representing estimated lower and upper limits to the internal Q of suspended masses.*

3.2.4 Some basic noise formulae

Two of the main noise limits shown in Figures 3.3 and 3.4, photon noise and seismic noise, are discussed in detail in Chapters 3 and 6 respectively. The other noise limits are calculated from the following formulae, further details of which can be found in our previous proposals [3, 4].

For:

- **test masses** – mass m, density ρ, speed of sound in material v_s, internal quality factor $Q_{\rm INT}$,
- **pendulum suspensions** – angular frequency ω_0, quality factor Q_S,
- **vacuum system** – residual pressure p of gas of refractive index n_0 (measured at standard pressure p_0) and thermal molecular speed v_0,
- **optical parameters** – arm length ℓ, mean beam width $2\bar{w}$,

and detector operating frequency $f = \omega/2\pi$, the squared spectral density of the resulting apparent gravitational wave amplitude is given by –

Thermal noise due to internal modes:

$$\tilde{h}^2 \approx \alpha \cdot \frac{16\,k\,T}{\pi^3\,\rho\,{v_s}^3\,Q_{\rm INT}\,\ell^2}\,, \tag{3.9}$$

(where $\alpha \sim 2.5$ allows for the summation of the effects of a number of resonant modes);

Thermal noise due to pendulum suspension:

$$\tilde{h}^2 \approx \frac{16\,k\,T\,\omega_0}{m\,Q_S\,\omega^4\,\ell^2}\,; \tag{3.10}$$

Heisenberg Uncertainty Principle:

$$\tilde{h}^2 \approx \frac{8\hbar}{m\,\omega^2\,\ell^2}\,; \tag{3.11}$$

Refractive index fluctuations:

$$\tilde{h}^2 \approx \frac{2\sqrt{2}\,(n_0-1)^2}{N_0\,v_0\cdot\ell\,\bar{w}}\left(\frac{p}{p_0}\right), \tag{3.12}$$

where N_0 is the number of molecules per unit volume (2.7×10^{25}molecules/m^3), and the other symbols have their standard meanings.

3.3 Squeezed Light Techniques

The use of "squeezed light" was originally proposed as a means of reducing the shot-noise level in laser interferometer gravitational wave detectors [27, 28]. Its use could allow our design goals to be achieved with less laser power and consequently reduced demands on the thermal properties of the optical components. Squeezed light has since been produced experimentally [29] and used to enhance the sensitivity of conventional, relatively small, interferometers [30]. The extension to interferometers such as those considered in this proposal is in principle straightforward.

For the squeezed-light method to be useful, it is necessary that the interferometer sensitivity be limited by "shot noise" (also called "photon noise"). This limit may be understood as follows. If n photons enter the interferometer during the sampling time interval, then the smallest detectable change in the relative phase of the light from the two arms is $1/\sqrt{n}$. Operation at this quantum limit is desirable and has been achieved in several of the prototype interferometers discussed in this proposal. (Photon pressure fluctuations, which are another kind of "quantum noise," would limit the sensitivity only at light power levels much higher than envisaged for the planned large interferometer [27]). The shot noise limitation of a Michelson interferometer with two equal arms is caused by quantum noise introduced by the stochastic nature of the beamsplitter. The $1/\sqrt{n}$ limit holds only if the noise imposed by the beamsplitter is not correlated with the phase of the laser beam illuminating the interferometer.

Caves [31] realised that the impact of the stochastic nature of the beamsplitter on the field fluctuations of the transmitted and reflected beam may be manipulated by coupling light with special properties into the second, normally unused, input port to the beamsplitter. This injection may be carried out, when the output beam spatially overlaps the input beam (as is the case for the Fabry-Perot interferometer, and most likely for the 3 km delay lines), by using a Faraday isolator and a polarisation-sensitive beamsplitter. This is illustrated in Figure 3.5, which shows the squeezed light being coupled into the system along the same path followed by the return, signal beam.

The properties of this light necessary for achieving a reduction of the shot noise level cannot be described in the framework of a classical field theory. The fluctuations in the light are then in a regime where they are dominated by Heisenberg's uncertainty relation. In order to achieve the noise reduction in one quadrature of the field the uncertainty relation has to be fulfilled asymmetrically, hence the name squeezed light. The best experimentally observed reduction of the noise power is 70% and more than 90% is expected to be reached in the near future [29].

When handling squeezed light one immediately finds it to be extremely fragile. Any dissipation such as absorption and non-unity detector quantum efficiency introduces fluctuations and the initially squeezed light changes its properties in the direction towards the regular shot noise level. As a result the shot noise reduction achievable in an interferometer will always be limited. In a real interferometer the limitation will arise mostly from wavefront aberrations that affect the fringe visibility $V = (I_{\max} - I_{\min})/(I_{\max} + I_{\min})$ and from the efficiency η of the detection system [32]. With these practical limitations

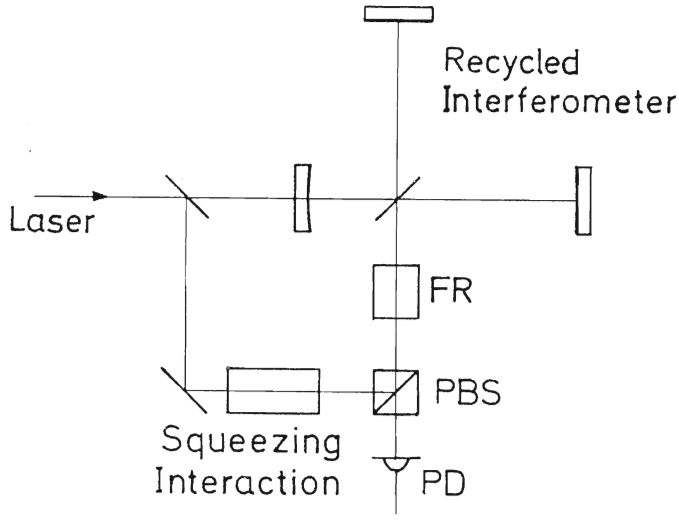

Figure 3.5: *Schematic diagram showing a possible application of squeezed light techniques to a recycled interferometer. Squeezed light is injected via a polarising beamsplitter (PBS) using the directional properties of a Faraday rotator (FR) arranged to rotate the plane of polarisation by 45°. The same Faraday rotator and polarising beamsplitter direct the interferometer output light to the photodetector (PD).*

in mind, Equation 3.3 has to be multiplied by the following factor:

$$\frac{1}{\sqrt{\eta}}\left[\sqrt{2}(1-V)^{1/2}+1-\eta+\eta\,\epsilon\right]^{1/2},$$

where $\epsilon \leq 1$ is a factor describing reduction of noise power at the interferometer output due to squeezing. For perfect squeezing ($\epsilon \to 0$), perfect interference fringe visibility ($V \to 1$) and perfect detection efficiency ($\eta \to 1$) the factor goes to zero. Such complete noise reduction will of course never be reached, since infinitely large squeezing requires an infinite amount of energy in the light field. With numbers already demonstrated experimentally ($\eta = 0.9$, $\epsilon = 0.2$ and $V_{\text{prototype}} = 0.98$) the noise reduction factor would be 0.7. It is sensible to expect some improvement in these numbers which would have a noticeable effect on the noise reduction: *e.g.*, $\eta = 0.95$, $\epsilon = 0.05$ and $V = 0.999$, leading to a noise reduction factor of 0.35. Such a reduction factor, corresponding to a ten-fold increase in light power, would have a significant impact since the threefold increase in strain sensitivity means that the gravitational-wave detector will look three times further out into space.

Alternatively, and perhaps more importantly, the use of squeezed light may make it possible to reach the target sensitivity for much lower laser power. In the example just given, 5 W of power with $\epsilon = 0.05$ would be the equivalent of 50 W with $\epsilon = 1$, and would avoid potential mirror heating problems altogether.

It is important to note that the squeezing technique is compatible with conventional (or "broadband") light recycling [14]. Thus both methods can be combined to give an even

further increase in sensitivity. On the other hand, squeezing would be less useful with the narrowband recycling schemes (such as resonant recycling and dual recycling [22]), if these are pushed to the limit, *i.e.*, if they are used to increase the effective interaction time of the gravitational wave with the light all the way up to the limit determined by the absorption losses. Such large total losses (resulting from the very long interaction time) would destroy any initial amount of squeezing. In practice, however, one would probably not envisage operation at quite the loss-limited bandwidth, and for any broader bandwidth (*i.e.*, shorter signal recycling time) the use of squeezed light would still bring about an increase in sensitivity (or make possible a reduction in laser power).

Finally, one should note that the option to use squeezed light at some stage places no restriction on the design of the detector; in particular, one may obtain squeezing at any desired wavelength. In the method of subharmonic generation in a nonlinear crystal (optical parametric oscillator) one can double the frequency of the laser light and then down-convert it again, via the parametric process, into squeezed light at the frequency of the laser and coherent with it. (This is symbolised in Figure 3.5 by the box labeled "squeezing interaction.")

Chapter 4

Proposed Detector System

Both to allow maximum flexibility in the short term and also to provide for possible long term developments, we believe the detector should be designed so that either the delay line or Fabry-Perot optical system can be accommodated.

Further, to ensure the fastest route to possible scientific results, it is proposed to construct first a delay line system optimised for millisecond pulses. For this type of signal the optical path in the interferometer arms achievable with delay lines is close to optimal; and the relative simplicity of control and operation should allow the most rapid development to useful gravitational wave sensitivity.

Following successful development of this receiver it is planned that a second interferometer optimised for lower frequency performance will be constructed. For this rôle the long optical path lengths available using Fabry-Perot cavities may prove to be an important practical advantage.

Each of the proposed receivers will incorporate appropriate recycling techniques to improve shot noise limited performance; such schemes have been discussed in the preceding chapter. Further improvements in the shot noise limit, or alternatively the achievement of a given sensitivity with lower laser power, should be possible in the longer term by employing squeezed light techniques.

A description of a receiver using delay lines will next be given, since such a system forms the first goal of this proposal. Following this is a brief outline of a possible Fabry-Perot system – a candidate for the second interferometer.

4.1 The Proposed Delay Line System

It is important that the form of delay line system adopted is compatible with the eventual addition of a second receiver. Furthermore it would be a desirable feature if the interferometer could also operate with light of 1 μm wavelength, though it should be stressed that the plan and expectation is that 0.5 μm light will be used. (Refer to the section on lasers for further discussion of this point.) Both of these considerations make it important to use an arrangement of the multiple beams in the delay lines that is as

compact as possible. Such an arrangement will increase the potential for noise coupling to the interferometer output via scattered light effects, but estimates show that suitable (and achievable) control of arm length and laser frequency can eliminate this problem.

Two possible delay line schemes have been devised which give reasonably compact layouts – the modified Herriot delay line (Figure 4.1), and the modified White cell (Figure 4.2). Both of these techniques share the important feature that the light beam is returned along its path by an extra mirror, after half the number of traverses have been accomplished. This gives two significant advantages: twice the optical path length is obtained with a given number of spots on the mirrors; and the outgoing light beam from an arm is coincident with the ingoing beam, making the implementation of the recycling optics particularly straightforward.

The conventional Herriot scheme used in the prototype interferometer at the Max-Planck-Institut employs two large concave mirrors, with a hole in the near end mirror through which the laser beam enters and exits. Repeated traverses of the laser beam within the delay line cause a circular or ellipsoidal pattern of spots to appear on each mirror. The number of traverses before the beam exits is controlled by the ratio of the mirror separation to their radius of curvature, while the ellipticity of the spot pattern on the mirrors is controlled by the direction of the input laser beam. The outgoing beam behaves to first order as if it is reflected at the input hole and hence is not collinear with the input beam. In the proposed modified Herriot system an extra hole is used in the mirror at the near end of the arm. The laser beam exits the delay line through this hole and is reflected back along its original path by an additional mirror – the 'retro' mirror.

The modified White cell uses a different arrangement of mirrors. The main feature is that at the remote end of each arm are two medium sized concave mirrors, while at the near end there is one large segment of a concave mirror, together with a small retro-mirror used to return the beam. The mirrors are oriented so that the laser beam is repeatedly reflected from one of the remote mirrors to the large segment at the near end and then back to the other remote mirror. As the traverses take place, two columns of spots are formed on the large mirror segment, until one spot misses the mirror and is caught and redirected back by the separate retro-mirror. The multiple spots on each of the two far mirrors are closely coincident. An additional feature is that with suitable choice of mirror radii it is possible to arrange that the (separated) spots on the near mirror are all significantly smaller than those (coincident) on the remote mirrors. It is thus possible in principle to use smaller mirrors than in the Herriot case. Practical tolerance limits on the mirror curvatures may, however, reduce the benefit that can be obtained using this idea.

It is planned to use mirrors of diameter up to 0.45 m, allowing an optical path length per arm of $\sim 30 \times 3$ km to be achieved using either of the proposed optical systems.

Each main mirror will be suspended directly as the lower mass in a double pendulum system; if necessary the small retro-mirrors may be attached to larger suspended masses. Reaction masses will be provided for the mirrors that require axial feedback control.

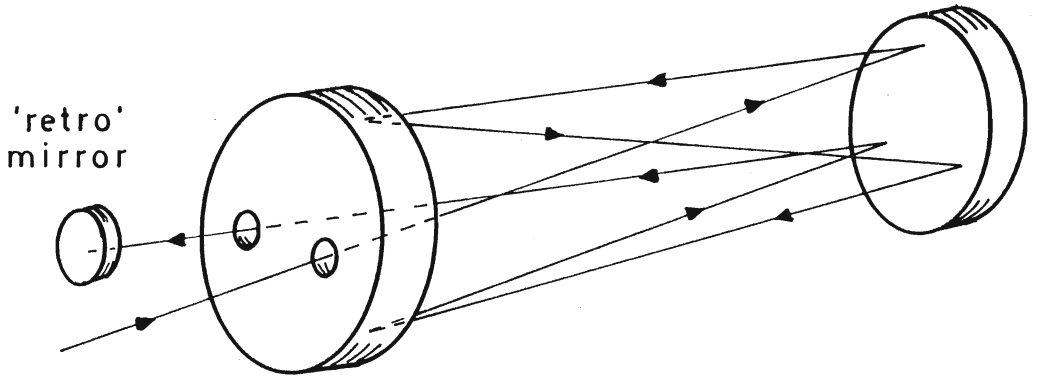

Figure 4.1: *Schematic diagram of a modified Herriot multiple reflection system. Arrows show the path followed by the light beam up to the reflection from the retro-mirror; the return path is coincident.*

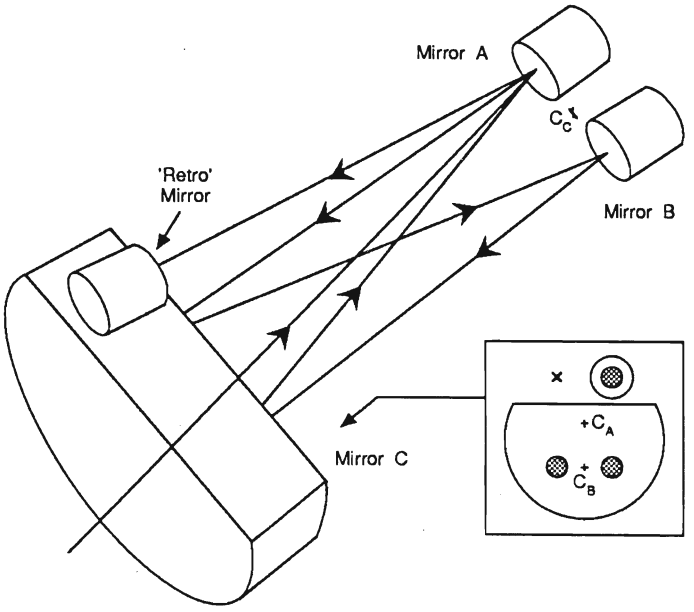

Figure 4.2: *Schematic diagram of a modified White cell multiple reflection system. The positions of the centres of curvature of the main mirrors are indicated by* C_A, C_B, C_C.

4.2 Commissioning of the Delay Line Interferometer

It is planned that the interferometer will be commissioned in a number of stages of gradually improving gravitational wave sensitivity requiring increasing complexity. Initially the system will be operated as a standard Michelson interferometer, the signal from the interfered output being used to hold the system locked on a dark fringe. This requires some modulation technique.

The simplest modulation scheme, both conceptually and operationally, utilises Pockels cells inside the interferometer arms to modulate the optical path length difference. A simplified diagram of this internal modulation technique is given in Figure 4.3. The Pockels cells also serve as fast control elements to keep the interferometer locked to a dark fringe. Although the internal modulation technique has been quite successful on the prototypes, this simple approach contains a significant flaw which will limit the sensitivity in our proposed delay line. Existing Pockels cells are known to cause irregular wavefront distortions and to absorb power. These effects would seriously reduce the efficiency of recycling.

A more general consideration arising whenever the control element affects the incoming and outgoing beams, is that there is both an immediate and a delayed (echo) effect. Their combination renders the phase control feedback loop ineffective at a frequency of half the free spectral range of the delay line (and at odd multiples of this frequency).[1]

Several schemes have been studied to modulate the light externally, which avoids having the Pockels cells inside the interferometer arms. For example, one can frequency modulate the input laser beam which together with a static path length difference in the two arms yields a modulated output signal.[2]

Another possibility is to combine the output of the interferometer with a modulated external beam derived from the main beam (first suggested in this context by Drever). In this case it is necessary to maintain the optimum phase relationship between these two beams. This modulation scheme has been experimentally verified by the Orsay group.

Figure 4.4 outlines one possible candidate scheme for external modulation which is consistent with high power operation and recycling, both of which are necessary for high sensitivity operation. The extra (external) coherent light beam is obtained by reflecting a small fraction of the light from one arm at the rear surface of the beamsplitter. This light is *rf* phase modulated and then interfered at an auxiliary beamsplitter with the signal light coming from the main output port of the interferometer. The resulting *rf* intensity fluctuations are detected (with opposite polarities) by the photodiodes at the two outputs of the beamsplitter. Demodulation of the *rf* difference signal then yields the

[1] The free spectral range of the delay line is defined as the reciprocal of the light storage time in one arm.

[2] This scheme was proposed by L. Schnupp at a European Collaboration Meeting on Interferometric Detection of Gravitational Waves, Sorrento, 1988.

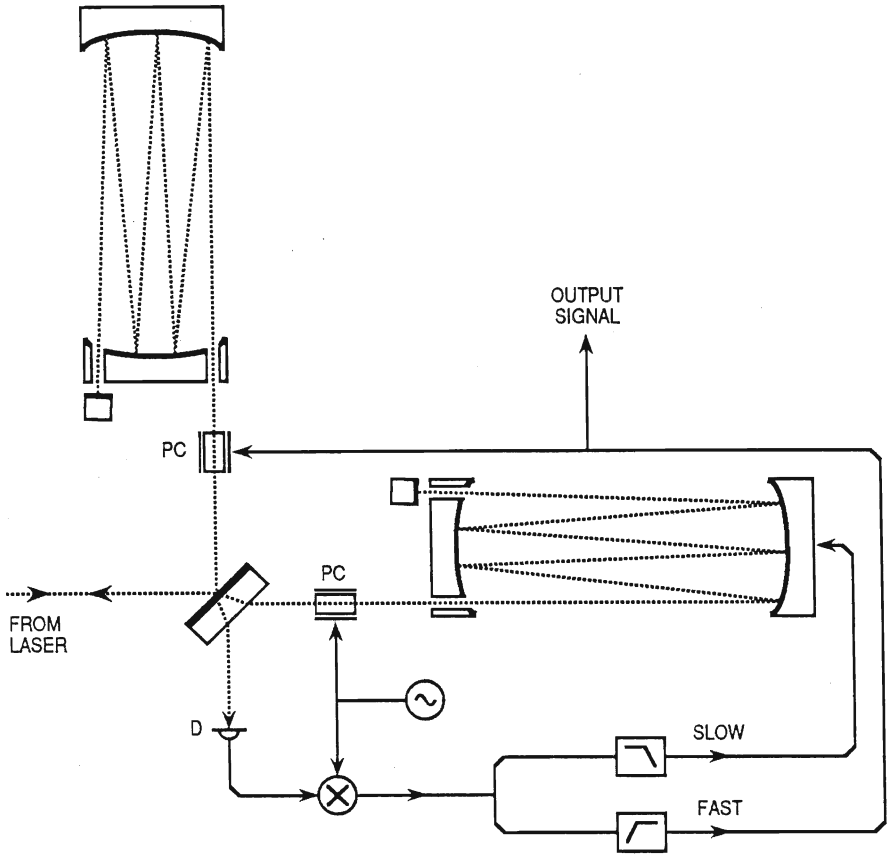

Figure 4.3: *A simplified internal modulation scheme. One Pockels cell is modulated producing a signal at the photodiode proportional to small deviations from a dark fringe. The correction voltage is then derived by mixing this signal with the reference oscillator. The path difference is servoed to a null using two phase adjusting elements: the large low frequency contributions are compensated by shifting one mirror and the high frequency corrections are made with the other Pockels cell. This correction voltage provides the output signal of the interferometer. (In practice both Pockels cells are modulated and used as fast correction elements.)*

signal for arm length difference control (the gravitational wave output signal). The low frequency component is used to move the main mirrors in the detector arms, while the high frequency corrections are achieved by moving the main beamsplitter. The echo, caused by moving the beamsplitter, is cancelled by applying the same signal, delayed by half the storage time, to the retro-mirror.

Frequency pre-stabilisation of the laser will be provided by a small stable reference cavity using the standard *rf* reflection locking technique [34]. Geometry stabilisation of the laser beam (mode cleaning) will in the first stage of development be provided by passing the input light through a single mode optical fibre – a technique currently successfully used on the prototype instruments at Garching and Glasgow.

A second stage of frequency stabilisation together with control of absolute arm length will then be added; the signal from this will be derived by mixing a small amount of input light with the bright fringe output from the beamsplitter. Again this is a technique that has been very successfully developed on the Garching prototype.

As part of the progression to the use of higher laser power, the fibre will then be replaced by a long mode-cleaning resonator, with the cavity length actively controlled so that it remains on resonance with the laser light. (This mode cleaning provision is described in greater detail in a subsequent section.)

In preparation for the eventual addition of recycling, another stage of frequency stabilisation will be added using the mode cleaner as a frequency reference. This will be followed by the installation of a second mode cleaner (placed in front of the one used as the frequency reference), the length of which will be actively controlled to maintain it on resonance.

Broadband recycling will then be implemented by installing a recycling mirror in the input beam line before the beamsplitter. The overall cavity formed by the recycling mirror and the interferometer arms will be kept on resonance by a servo system controlling the axial position of the mirrors in the arms, the correction signal being obtained using the standard *rf* reflection locking technique for cavities. Fast phase correction, which may be required during the acquisition of lock of the recycling cavity, and which can also be used for further frequency stabilisation, will be obtained using an electro-optic modulator following the mode cleaning cavities.

As a final stage dual recycling will be implemented. To achieve this the position of the mirror which is added to increase the signal storage time will be adjusted so that the desired gravitational wave frequency is resonant. This will be achieved by taking a small fraction of the incident light, frequency shifting it by a free spectral range of the recycling cavity plus the gravitational wave frequency, and using this to *rf* reflection lock the signal cavity.

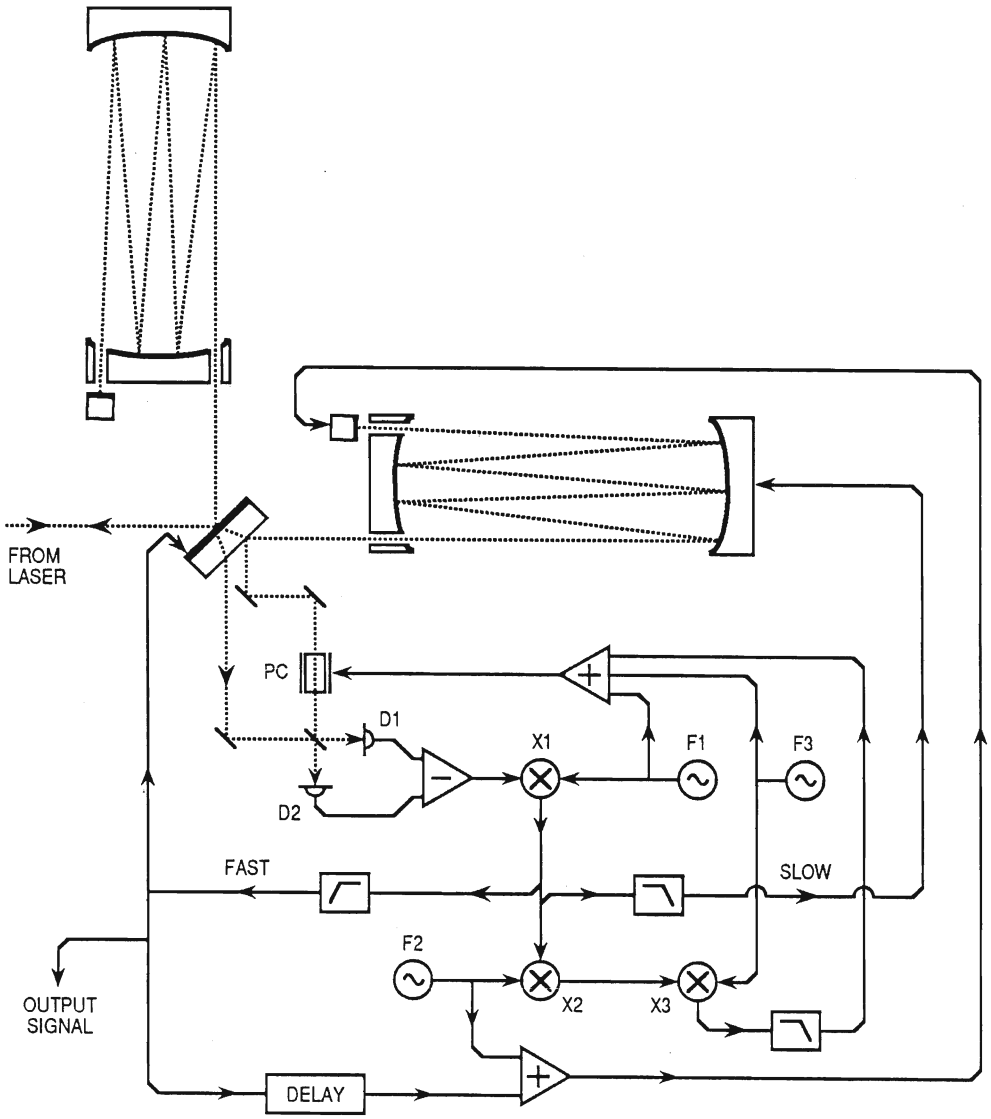

Figure 4.4: *A possible locking system to maintain the interferometer output on a dark fringe. F1 is the* rf *source used for the main phase modulation discussed in the text; the gravitational wave signal will appear in the output of demodulator X1 (The fast correction is applied to the beamsplitter and, in order to cancel the echo, is time delayed and applied to the retro-mirror.) For this main modulation technique to work, the phase of the externally modulated beam needs to be controlled so that the gravitational wave signal has maximum size and well-defined sign. A small differential arm length modulation, simulating a gravitational wave signal, is imposed by modulating one of the retro-mirrors at frequency F2 ($\sim$ 10 kHz). The amplitude (for the particular value of the phase of the external beam) of the resulting modulation signal in the main interferometer output appears at the output of demodulator X2. The optimum phase of the external beam may then be found by dithering this phase at frequency F3 ($\sim$ 10 Hz) and feeding back a phase correction signal from the output of demodulator X3.*

4.3 Proposed Second Detector with Fabry-Perot Cavities

This interferometer based on Fabry-Perot cavities will use two 400 kg test masses in each arm and is mainly intended for operation at lower frequencies between 100 Hz and a few hundred Hz. The mirrors may be an integral part of the test masses, achieved by either fusing or optically contacting the optically ground mirror substrates to larger test masses. The cavities will be of the flat/curve arrangement with flats at the near end and curves of 4.5 km radius at the far end. Reaction masses will be provided for each test mass to allow control of cavity lengths. A possible arrangement for controlling the interferometer is shown in Figure 4.5.

Recycling and dual recycling will be added as for the delay line case. Note that care must be taken that the phase modulation for the main cavity locking signals is able to pass into the overall cavity formed by the recycling mirror and the arms; this can be achieved by using a frequency at a free spectral range of this overall cavity.

To ease acquisition of lock of the whole system one possibility is to use a separate optical interferometer to damp and lock the inner interferometer formed by the beamsplitter and the near end test masses. This would be illuminated by a stabilised Helium Neon laser. It would be expected that this auxiliary interferometer would be turned off when the system is fully locked with the main illuminating laser.

4.4 Interferometer Control Systems

4.4.1 Axial control of main interferometer components

For the delay line based interferometer there are four control systems associated with the axial control of the main interferometer components – to control differential arm length to keep the interferometer on a null fringe and provide the main signal output for searching for gravitational waves; to control absolute arm lengths to minimise light scattering problems; to maintain the overall cavity formed when recycling is used on resonance; and to maintain the correct resonance conditions for the dual recycling system.

For the possible Fabry-Perot based system for the second interferometer an extra control system to allow independent locking of the two Fabry-Perot cavities is required, and it would be advantageous to have two further auxiliary systems to help with acquisition of lock.

4.4.2 Alignment control of the interferometer and associated optical components

There are many places in any design of interferometric receiver where it is vital that relative alignment of interfering light beams be optimised and actively controlled. Examples

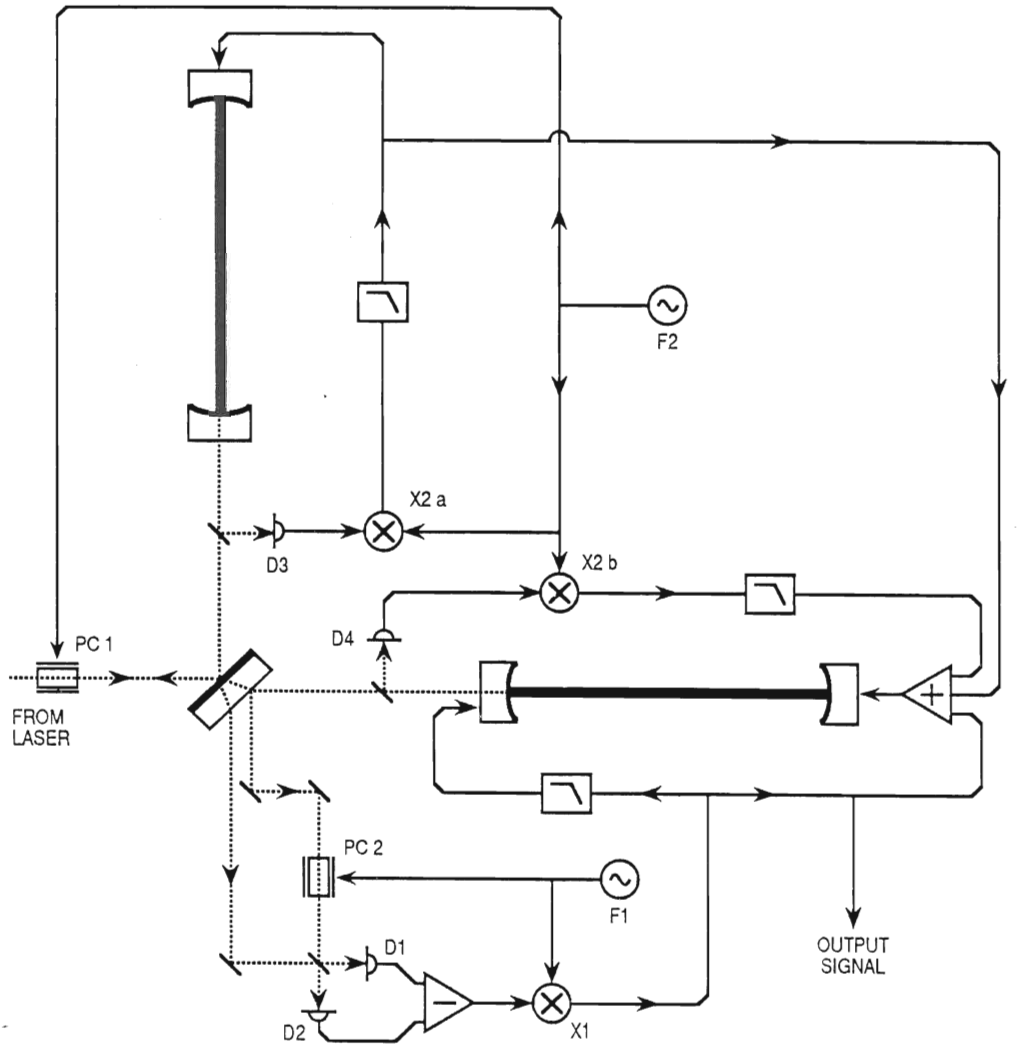

Figure 4.5: *A possible locking scheme for a Fabry-Perot based interferometer. Phase modulation of the light sent to the two cavities is applied by PC1 – a Pockels cell electro-optic modulator. A small fraction of the light reflected from one cavity is detected by photodiode D3 and after demodulation the resulting low-pass filtered signal is used to control the cavity length. An external modulation scheme is indicated for detecting the main differential displacement signal which is used to maintain the correct operating point of the Michelson interferometer formed by the two cavities and the main beamsplitter. This is shown in more detail in Figure 4.4. The second cavity is kept at its correct resonance condition by a slow feedback signal derived from the small amount of light diverted to photodiode D4. Standard recycling involves placing a mirror between PC1 and the main beamsplitter. In this situation the phase modulation frequency will be chosen to correspond to a resonance frequency of the overall recycling cavity. A further reflection locking system, using an additional (and different* rf *frequency) phase modulation by PC1, will be used to derive the signal to control the laser frequency and common mode length of the two arms so that the recycling cavity remains on resonance.*

include the alignment of the mode cleaning cavities for maximum power throughput, the adjustment of the beams returning from the two interferometer arms to optimise fringe visibility, and the alignment of the mirrors used for standard and dual recycling.

For precision of adjustment, the signals used to maintain alignment of two interfering beams will have to be derived from a direct measurement of the phase gradient between the beams. The proposed method of achieving this is to employ an extension of the standard differential phase modulation technique used to obtain the signal to lock the relative average phase of two beams. The addition is that a two axis photodetector (such as a quadrant device) is also used to monitor the interference pattern. Decoding the signals from this detector gives a measure of the differential phase gradient in two orthogonal directions. Information on all four degrees of freedom is obtained by making such a measurement at two spatially separated locations along the beam path. This technique has been successfully applied to the case of cavity alignment on the 40 m prototype at Caltech.

Valid signals for this type of alignment scheme are only available when the relative phase of the interfering beams is stably locked. It is therefore necessary that there are other coarser controls which are sufficiently accurate for initial alignment. Optical levers and other motion sensitive optical sensors will be used for this, and will also provide the method of maintaining alignment during short losses of lock of the interference. They will also provide signals to allow damping of some of the mechanical degrees of freedom of the optical components involved. Two optical levers will be used for each mass to be controlled; one will act locally to the mass, while the other will operate with higher precision by acting over the characteristic length of the relevant optical cell – up to 300 m for the mode cleaners, and 3 km for the main arms of the interferometer. These systems will use either He-Ne light or possibly light from a solid state laser. Automatic systems will handle the transfer of feedback control signals from the three alignment monitors.

Systems of the type described above will be used for –

- alignment of each of the two mode cleaner cavities,
- alignment of each of the two interferometer arms (either delay lines or Fabry-Perots, and
- alignment of each of the two recycling systems.

The systems will also allow damping of some mechanical movements of the optical components involved.

Simpler systems using optical levers and other motion sensitive optical sensors will be used to align and stabilise the positions of other suspended optical components such as modulators, mode matching lenses and beam steering mirrors.

There will be six control systems for alignment of the cavities and arms, each operating in two dimensions, and approximately thirty systems for control of orientation and movement of components, each operating in up to four degrees of freedom.

4.5 Laser Stabilisation Requirements

4.5.1 Mode cleaning and frequency stabilisation

Experience with the prototypes have shown that fluctuations in shape, orientation, and position, of the input laser beam are important noise sources. These geometry fluctuations can be considered to be variations in the mode content of the beam. They can be attenuated by transmitting the light through "mode cleaning devices", such as single mode glass fibers (as suggested by Weiss), or resonant cavities [35].

To reduce geometry fluctuations of the laser beam to an acceptable level, it is considered essential that mode cleaning is incorporated in the design of both delay line and Fabry-Perot systems. To achieve our desired sensitivity goal the mode cleaning has to provide a reduction in the major fluctuations in the geometry of the beam by a factor of $\sim 10^3$ in the hundred Hz region and somewhat less at higher frequencies [3]. Resonant cavities should be able to handle much higher optical power than the currently used single mode fibres, and will also provide the important additional benefit of passive filtering action for fast fluctuations of laser amplitude and frequency.

High efficiency of optical throughput is of prime importance both for good sensitivity in the interferometer, and also to avoid possible problems due to heating of the mode cleaner mirrors when many tens of watts are being transmitted. Following a conservative approach, knowing from experiment that $\sim 0.25\,\mathrm{W}$ loss per mirror can be tolerated, and making the reasonable assumption that mirror losses will be $\sim 100\,\mathrm{ppm}$, it seems appropriate to choose a finesse for the cavity of ~ 100. Such a cavity will use equal reflectivity mirrors of $R \sim 97\%$, and with curvatures suitably chosen for optimum mode cleaning action [35], giving good power transmission.

In order to achieve the required mode cleaning performance two similar cavities will therefore be used in cascade. One mode cleaner cavity will also be used as the fast reference for the second stage of frequency stabilisation of the laser. It is therefore important that it is long enough for sufficient (shot noise limited) stability to be obtained.

A reduction of laser frequency noise down to $\sim 3 \times 10^{-8}\,\mathrm{Hz}/\sqrt{\mathrm{Hz}}$ should be sufficient to keep direct coupling by scattered light to the interferometer output to an equivalent level of $h \sim 10^{-24}/\sqrt{\mathrm{Hz}}$ – our eventual sensitivity goal at $\sim 100\,\mathrm{Hz}$ as limited by photon noise. Somewhat better stability would be useful with a Fabry-Perot system, though in this case balancing of the responses of the cavities in the two arms also helps reject any residual frequency fluctuations. With recycling the overall cavity formed in the interferometer system will have a linewidth of $\sim 3\,\mathrm{Hz}$ and will therefore provide passive filtering of laser frequency fluctuations by a factor of ~ 60 at 100 Hz and more at higher frequencies.

It seems appropriate to opt for a relatively long mode cleaning cavity – 100 m. This will give a shot noise frequency stability of the transmitted light of $\sim 1.7 \times 10^{-6}\,\mathrm{Hz}/\sqrt{\mathrm{Hz}}$ with 10 W of light, which seems a satisfactory level of performance.

To achieve this level of stability will require adequate mode cleaning of the light prior to the cavity used as the frequency reference. This will come partly from the first 100 m

cavity, with any extra geometry stabilisation necessary being provided by an active beam pointing system, or by an additional short resonant cavity. Very high servo gain will be required to reach the frequency stability goal. As mentioned earlier, pre-stabilisation of the laser to a small stable reference cavity (and possibly to an atomic line) will be performed, both for good long term stability, and also to ease the achievement of the necessary high gain. Two stage frequency stabilisation systems have been developed for both the Garching and Glasgow prototypes. At Glasgow, using a small rigid cavity together with a 10 m higher finesse cavity, loop gains of $\sim 10^8$ at 1 kHz have been achieved without any intracavity device in the laser. Already this performance would be satisfactory if Nd:YAG or argon lasers are used.

It should be noted that the design of the vacuum system is such that it would be straightforward to increase the length of the mode cleaning cavities should extra passive filtering of fast fluctuations of laser frequency and amplitude be required.

4.5.2 Power stabilisation

Stabilisation of the low frequency power fluctuations of the illuminating laser is required primarily to avoid the coupling of this noise to the interferometer output due to unavoidable slight offsets of the fringe locking point. Another potential route for coupling is via unbalanced radiation pressure effects in the two arms.

A satisfactory technique developed for high gain stabilisation of power fluctuations is to compare the photocurrent produced by a sample of the light with a reference value, and use the resulting signal to feedback to the laser power supply. This has been demonstrated at Orsay (VIRGO) and at MPQ to provide performance which should be adequate for our proposed system. If more gain-bandwidth is required the feedback signal can be used to adjust an electro-optic attenuator placed in the optical path before the pickoff point. A suitable attenuator for plane polarised light can be constructed using multiple Pockels cells, together with an analysing polariser, and such a system has been studied in detail at Glasgow [36].

4.6 Laser Systems

Currently there are two types of lasers suitable as light sources for interferometric gravitational wave detectors: argon ion lasers and Nd:YAG lasers. The principle advantage of the argon ion laser is that the technology already exists. At present all major prototype experiments are using argon ion lasers operating at 514 nm. Nd:YAG lasers suitable for our purposes, on the other hand, are just now being developed and the state of the art is progressing rapidly. The chief advantage is that they are more efficient and have higher output power. Another consideration is that the Nd:YAG high power line is at 1064 nm which then must be frequency doubled in order to obtain light with a wavelength close to that of the argon laser. This wavelength is preferred because shorter wavelength allow smaller beam diameters leading to smaller optical components. Another practical advantage is that visible light is easier to work with than infrared. Thus, on the

whole, the doubled Nd:YAG laser approach is the favoured scheme when the technology becomes available.

4.6.1 Argon ion laser

At present the argon ion laser is still the best choice if one considers power to wavelength ratio, mode purity of the beam, stability, and reliability. The most powerful argon ion lasers commercially available offer a multi line power of 25 W. For single mode operation this corresponds to about 6 W, perhaps up to 8 W under optimum conditions. To arrive at higher light powers it has been proposed to add the output of several lasers coherently. For this purpose these lasers could be seeded with the light from a stabilised master laser, in this way forcing all lasers to oscillate locked in phase. The feasibilities of this technique and of other schemes for coherent addition have already been verified experimentally in Orsay and in Glasgow [37, 38]. The major disadvantage of this type of laser is its rather poor efficiency. For the required single line, single mode operation only a few times 10^{-4} of the input power is converted into light. This means that 1 MW of continuous power would be necessary to sustain laser light powers of around 100 W.

4.6.2 Nd:YAG laser

Over the last few years a very promising alternative to the argon ion laser has been under development: the Nd:YAG laser. Although mainly used as a pulsed laser in the past, there are now commercially available models offering up to 1 kW of continuous wave light power, although in multi line mode. These types are pumped by discharge lamps, giving an efficiency of about 1%.

Frequency doubling techniques are under active development and already 2 W single mode of continuous frequency doubled light have been observed from a flash lamp pumped laser at MPQ and 6.5 W *cw* have been obtained from a similar laser by a research group in the Research Institute of Synthetic Crystals, Beijing, China.

Semiconductor laser diodes can pump Nd:YAG much more efficiently than flash lamps ($\sim$ 10% has been achieved). So far only low power versions of this type are commercially available, the main reason for this being the fact that the price for laser diodes is still rather high. But the evolution in this field is rather spectacular, and the price is expected to drop to an economical level in the relatively near future. Development of diode-pumped Nd:YAG lasers is progressing worldwide. The Laser-Zentrum at the Universität Hannover is working on such systems and on the provision of frequency doubled light in support of this proposal. Similar laser development is being pursued at Stanford and Orsay in support of the LIGO and VIRGO projects respectively.

For Nd:YAG lasers to be used for gravitational wave interferometers they must, like the argon ion lasers, be operated, single line, single mode, and also need to be frequency stabilised. First experiments is this field with light at 1064 nm [39] showed (for an output power of 100 mW) that the Nd:YAG laser can definitely compete with the argon

ion laser in terms of noise performance. Very recent results from Orsay suggest this is also true for much higher laser powers (up to 18 W).

Our intention is to use frequency doubled Nd:YAG light for the interferometers. In the unlikely circumstance of suitable Nd:YAG laser systems not being ready for initial operation of the interferometers, we still have the possibility of starting using argon ion lasers.

Chapter 5

The Vacuum System

5.1 Introduction

In order to accommodate two interferometer systems with reasonable ease of access, separate vacuum tanks are provided for the test masses of the delay line and for the test masses of the Fabry-Perot based system. Thus two tanks are required at each end of both arms. These tanks are chosen to be of 3 m diameter with access horizontally from the side, the size being determined by the need to accommodate a double pendulum suspension and five layer isolation stack for each test mass, and also to accommodate reaction masses for the test masses whose axial positions have to be controlled. The pipe diameter has to allow free passage of the beams for the two interferometers, and design indicates that a free internal diameter of 1.26 m is adequate. The basic diameter of the pipe has to be some 12 cm larger to allow for baffles to be installed to reduce the effects of scattered light on the operation of the interferometers. A central tank to accommodate the beamsplitters and other optical components is required and this should be 4 m diameter. One input and one output tank is also required for each interferometer to hold beam conditioning and recycling optics. The proposed vacuum system is shown in outline in Figure 5.1 .

A further design feature of the interferometers is the use of long mode cleaning cavities for the input light, as discussed in Chapter 4 . The two mode cleaners for a single interferometer would be housed in a pipe of 0.4 m diameter running parallel to one of the arms; the mode cleaners for the second receiver would be housed in a similar pipe lying along the other arm.

5.2 Detailed Description

As discussed widely in earlier proposals a high vacuum is required for the system. To achieve the goals of this proposal the average pressure should be no greater than $\sim 10^{-8}$ mbar (hydrogen) with a partial pressure of heavier molecules, such as water and nitrogen, not exceeding $\sim 10^{-9}$ mbar in total.

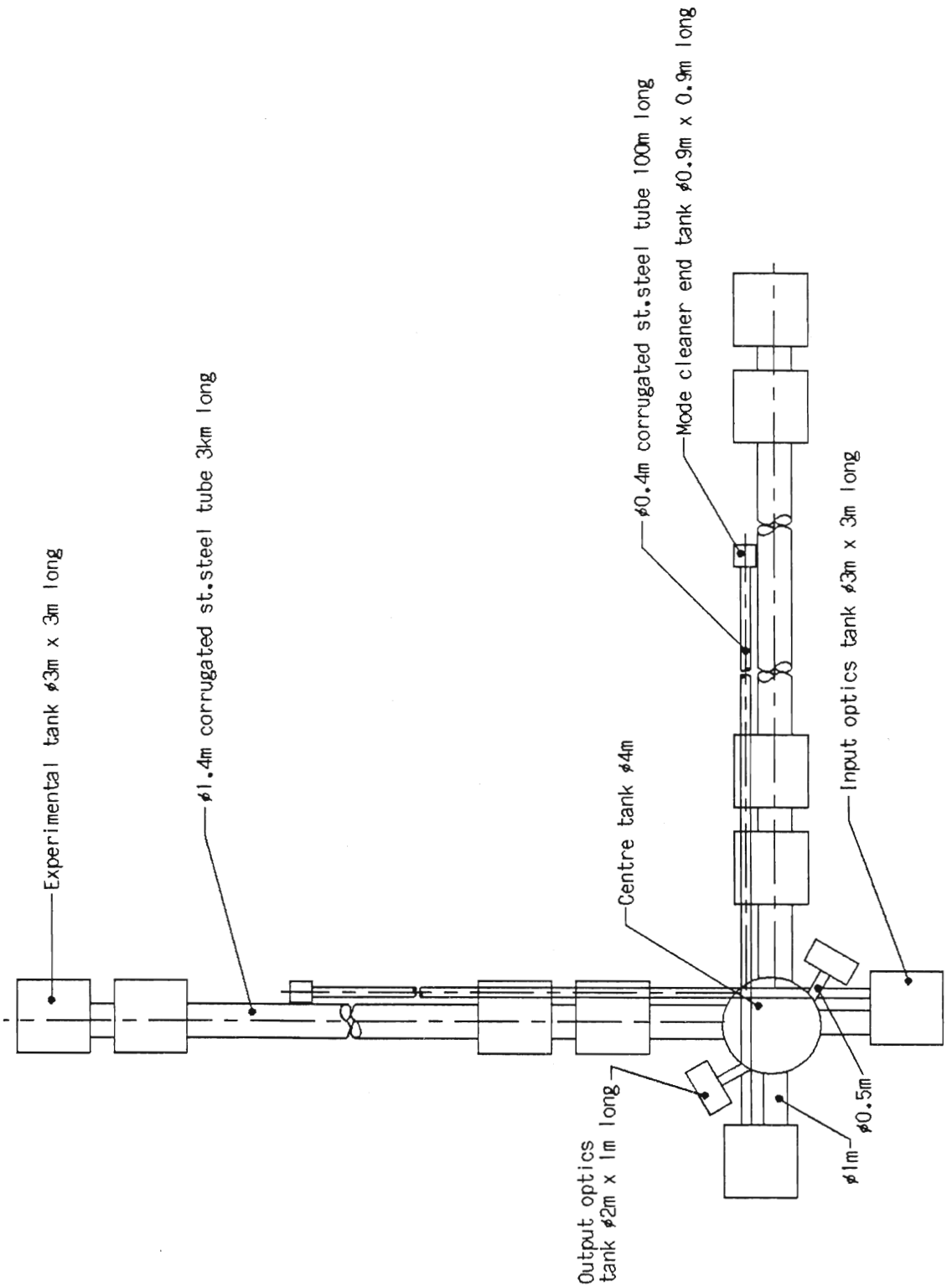

Figure 5.1: *Schematic diagram of the vacuum tubes and tanks*

5.2.1 The tube

The tube is constructed from welded stainless steel sheet, 0.56 mm thick, corrugated as shown in Figure 5.2 to give the required strength when under vacuum. The mean diameter is 140.5 cm, with a clear bore of 138 cm. Approximately 70 circular stainless steel baffles, with an aperture of 126 cm, are uniformly spaced inside the tube.

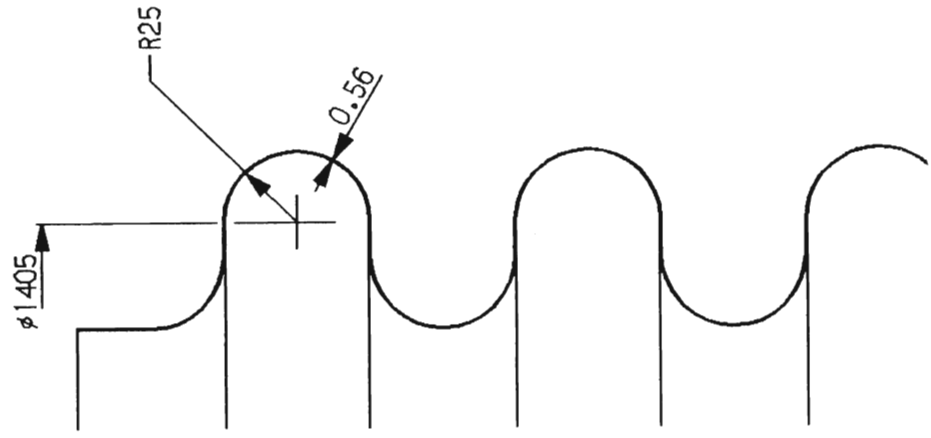

Figure 5.2: *Cross section of proposed corrugated tube wall. (All dimensions in mm)*

The tube is supported on lightweight electrically insulating legs at approximately 4 m intervals to limit the sag of the tube to less than about 5 mm. This leaves a clear bore of about 125.5 cm for the laser beams of the interferometers.

5.2.2 Tanks

The experiment tanks are constructed from stainless steel and contain the pendulums, suspension systems, optics and electrical/electronic equipment.

5.2.3 Vacuum system design

An outline of the proposed pumping system is shown in Figure 5.3, and a more detailed schematic of the pumping for the five centre tanks is presented in Figure 5.4.

It is necessary to gain access to the tanks frequently and hence it is important to pump the tanks down to operating pressure in as short a time as reasonable. The tube, on the

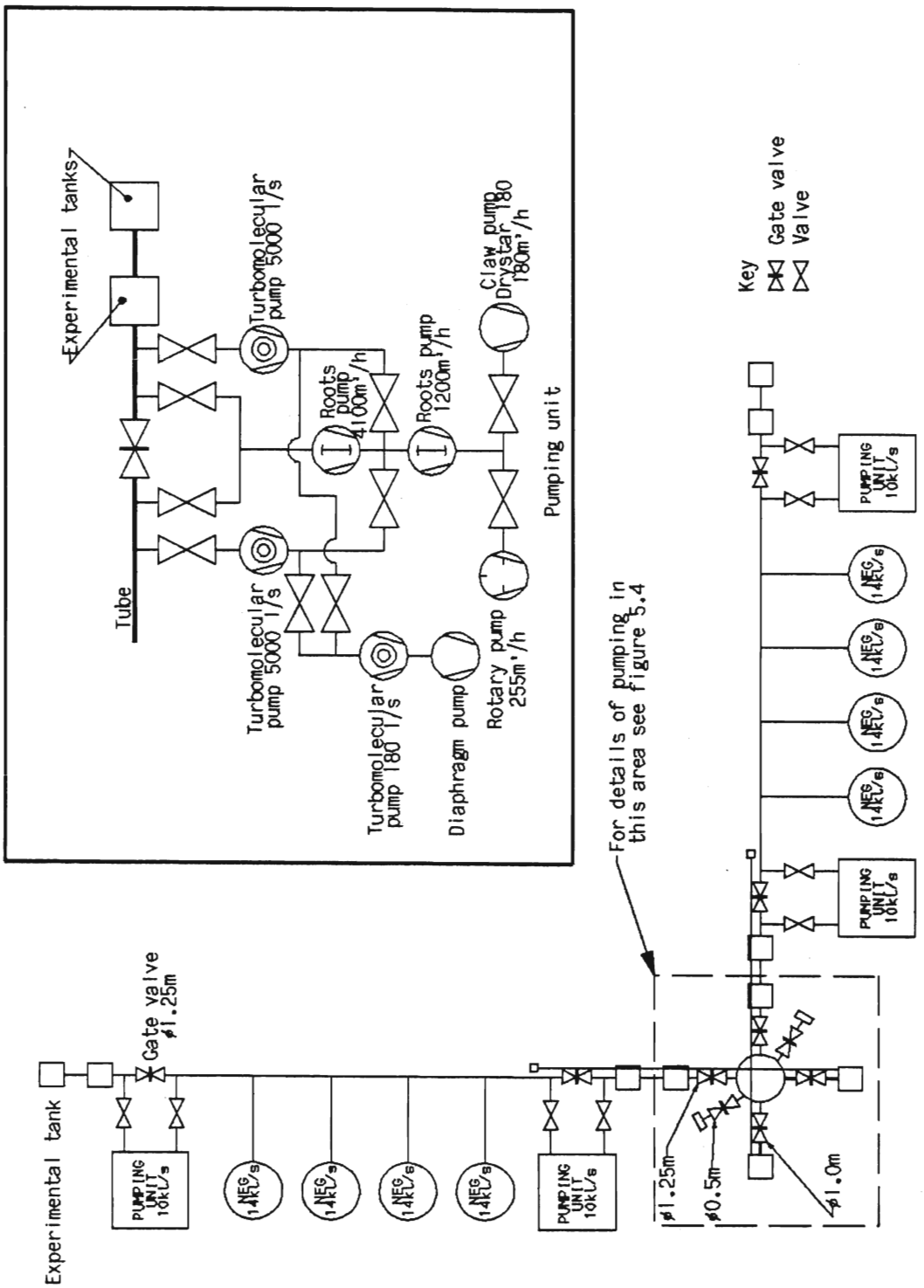

Figure 5.3: *Outline of the proposed pumping system.*

other hand, contains no equipment and should not need to be accessed. Therefore large gate valves of 125 cm bore are used to isolate the tanks from each 3 km length of tube. Other gate valves isolate the various tanks in the centre station, enabling modifications to be carried out whilst part of the detector is still operating.

The processing and pump down of the tube can take several weeks. The tanks should be down to pressure in several days.

To reduce the pumping requirements, the whole system is built to UHV standards using only metals and ceramics in the vacuum except for Viton seals in the large gate valves. The tube will be given a light bake, 150°C to 200°C, in air for 24 hours followed by a vacuum bake at the same temperature for 3 days. Experiments show that the benefits of the air bake are retained after letting the system up to air. The vacuum bake must be repeated after each let up. The specific surface outgassing rate has been measured to be $\sim 10^{-12}$ mbar l/s/cm^2 with this treatment after 3 days.

The tanks cannot be baked at this temperature when full of equipment. At best, a 80°C vacuum bake is assumed, to drive off most of the water. The surface areas of the tanks and equipment are not well known but are estimated at 10^6 cm^2 per tank. The specific surface outgassing rate is assumed to be 10^{-11} mbar l/s/cm^2.

With the above parameters the pumping system can be designed. The two tanks at the ends of the tubes are pumped by a 5000 l/s turbomolecular pump. Another 5000 l/s turbomolecular pump at each end of the two tubes contributes mainly to the tank pumping when the 125 cm diameter gate valves are open. A further 5000 l/s and four 2200 l/s turbomolecular pumps are used to pump the centrally located tanks.

In addition to the turbopumps at the ends of each 3 km arm there are four 14,000 l/s non-evaporable getter pumps spaced along each of the arms. The pumping system shown in Figure 5.3 should produce an average pressure below 10^{-8} mbar at the stated outgassing loads.

The turbomolecular pumps have gate or butterfly valves to isolate them from the vacuum tanks and tube. Like the tube gate valves, these are all-metal, except for the Viton gate seals.

The turbomolecular pumps are backed by a special high compression ratio turbomolecular pump which can be operated at high backing pressures. This latter feature enables the use of a dry (oil free) diaphragm-type backing pump.

The roughing pumps consist of a combination of roots, claw and rotary vane pumps, located at both ends of each tube arm. Roughing is expected to take 18 hours from atmosphere to 10^{-2} mbar for the tubes and 20 minutes for the two tanks on the ends of the arms. These pumps are also to be used to back the turbomolecular pumps at the higher throughputs.

The NEG pumps do not require backing pumps, but need activating at 800°C by electrical (ohmic) heating from a suitable power supply.

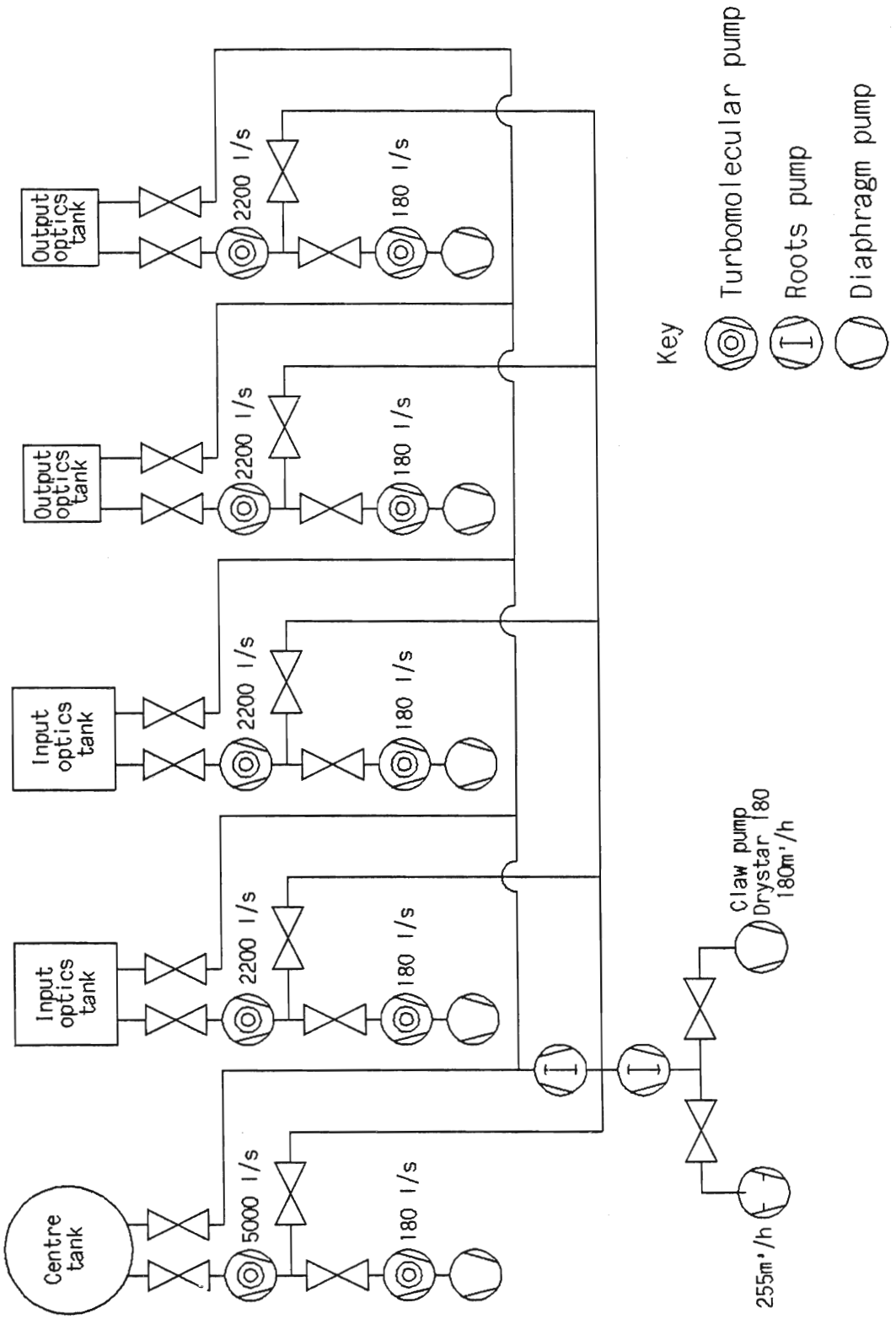

Figure 5.4: *Detail of the proposed pumping system at the centre station.*

5.2.4 Bake-out

The tubes are heated by passing a dc current down the entire 3 km length of each arm; see Figure 5.5 . The steady state power loss is reduced by thermally insulating the tube with 100 mm thick mineral wool blanket. The dc power supply, rated at 1800 V and 900 A, is located at the centre station.

The tanks are heated by commercial heater tapes.

5.2.5 Monitoring and control

Simple quadrupole mass analysers monitor the system and help to detect leaks. The heads are installed in the tanks and every 300 m along the tubes. In addition ion and wide range Pirani gauges are used to assess the total vacuum pressures in the appropriate ranges.

The roughing system is controlled 'manually'. The turbomolecular pumps and backing pumps are also manually operated but close down automatically in the event of a failure. The tube and pump gate valves are pneumatically operated and linked to the fail safe system.

The vacuum pressures are monitored through the facility computer system.

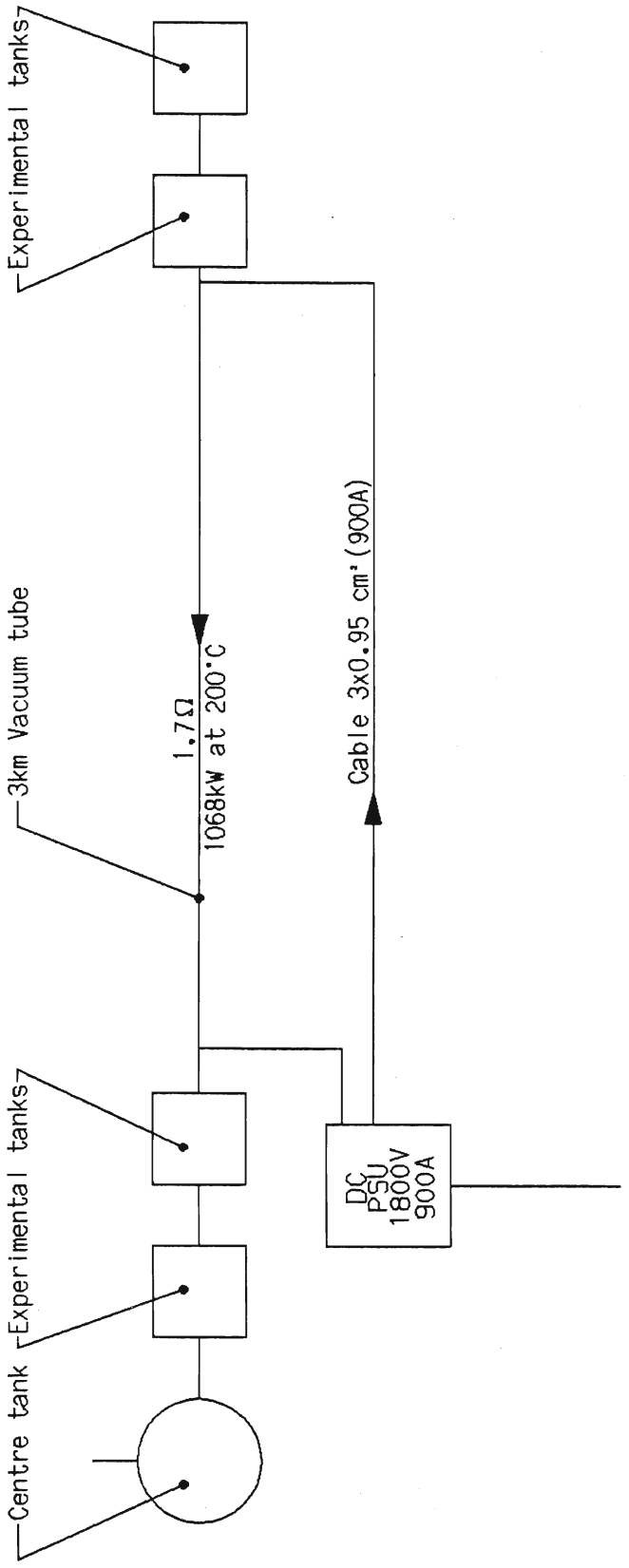

Figure 5.5: *Outline of the proposed system for baking the vacuum tubes.*

Chapter 6

Vibration Isolation

6.1 Introduction

The extent to which long baseline interferometric detectors can be operated with reasonable sensitivity at the lower end of the frequency spectrum will depend crucially on the level of seismic and mechanical isolation achievable [40]. The design of a vibration isolation system must allow for vibrations which may be ground borne, air borne, or structure borne, and which may arise either outside the detector (*i.e.* environmental noise including seismic noise) or associated with the detector (vacuum pumps *etc.*). The aim of the currently proposed isolation system is to reduce the effect of all such vibrations on the components of the detector (especially the test masses and other optical components) to allow the photon noise limited design sensitivity shown in Figure 3.3 for burst sources to be achieved. This implies that a limit to sensitivity due to seismic noise of $h \sim 10^{-23}$ or better for pulses at 100 Hz should be sought. A system designed to meet this criterion is expected to be more than adequate for frequencies above 100 Hz. Modifications may be added at a later date to extend the performance to frequencies below 100 Hz. For example a compact multiple pendulum system is under consideration at the Max-Planck-Institut for this purpose.

Once the levels of noise from the various sources and the acceptable level at each of the vulnerable components has been established, the necessary degree of isolation can be computed. Vibrations can of course be transmitted by several routes, and each route must be considered. Figure 6.1 shows schematically some of the possible vibration routes in the proposed design. The figure does not show the possibility of the conversion of low frequency noise to high frequency noise by non-linear components (an effect that we are confident can be kept small by suitable design), nor does it show any cross-coupling of vertical noise into the horizontal direction. This latter effect is very important and has the consequence that a high level of vertical isolation is required; the overall system designed to incorporate this vertical isolation is expected to have more than adequate direct horizontal isolation. Figure 6.2 shows a subset of the system, relating seismic motions to motions of the test mass by the most critical route.

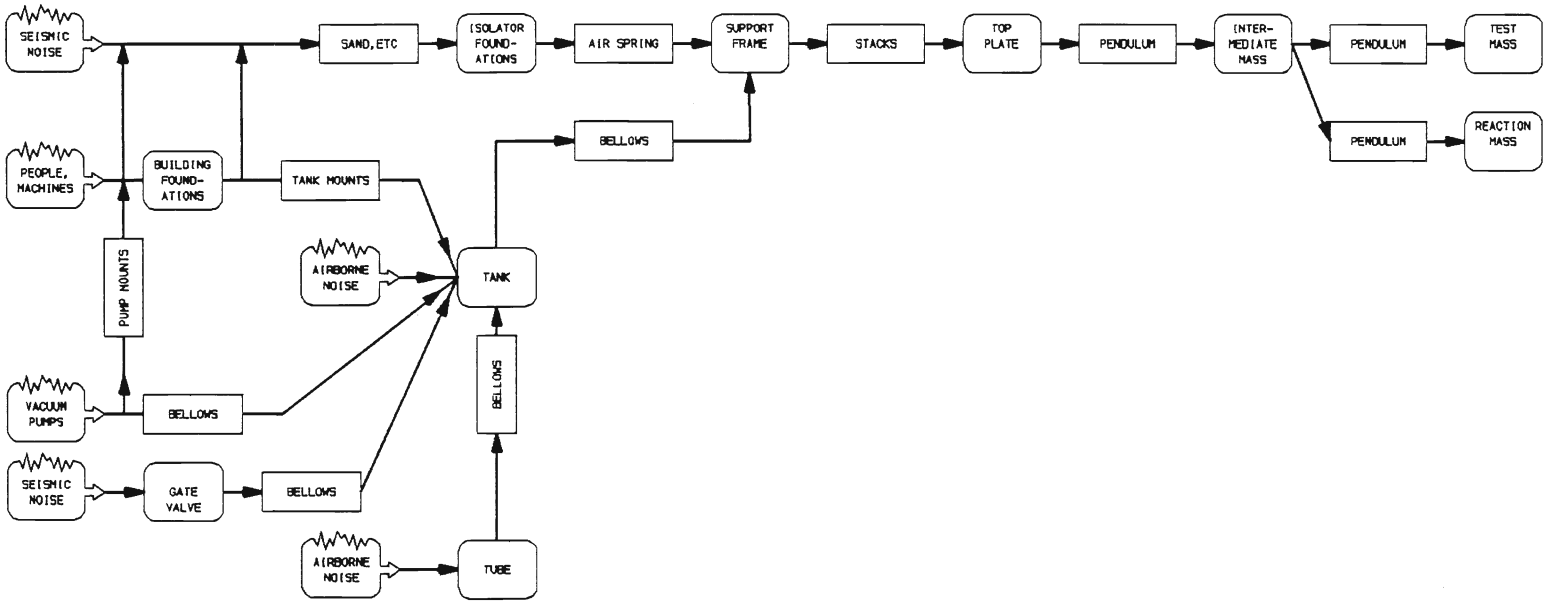

Figure 6.1: *Block diagram showing the possible routes by which vibrations may couple to the test masses.*

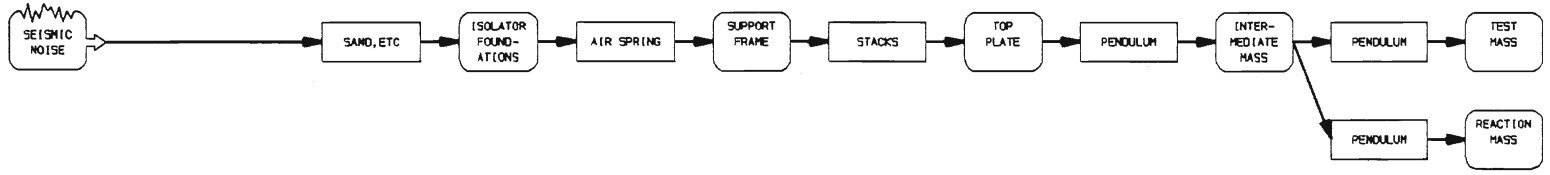

Figure 6.2: *Critical path by which vibrations can affect the test masses.*

6.2 Elements of the Vibration Isolation System

Figure 6.3 shows the configuration of our proposed design. The precise details are not at this stage finalised; for example, the lengths of the pendulum wires may differ from those illustrated. However the main components and the way they fit together can be seen.

Foundations

The foundations for the mass suspension system will be separate from those of the vacuum tank and the building. They will consist of massive reinforced concrete blocks surrounded by sand or another suitably absorbent material.

Air springs

These will be of a commercial type, incorporating active control to give a low effective natural frequency combined with compact design and low cost.

Isolation stack

This will be a 5 stage stack, each stage consisting of a layer of machined lead on silicone rubber, giving a very steep transmissibility curve beyond the highest natural frequencies in the vertical and horizontal directions. Further design work will be carried out to ensure that the presence of structural resonances in other parts of the system does not cause a significant degradation of the overall isolation. The mass in each stage will be 400 kg or greater. The stack will be fully encapsulated with thin foil to avoid outgassing problems for the main vacuum, and will be internally pumped.

Support frame and top plate

These will both be hollow structures, filled with a vibration damping compound to minimise the effects of internal vibration modes. The material will be non-magnetic stainless steel which will avoid any possible coupling to stray magnetic fields from nearby devices or to fluctuations in the Earth's magnetic field.

Pendulums

Two-stage pendulums will be used for the test masses, beamsplitters and other critical optical components. The pendulums will have natural frequencies of 1 Hz or less in the horizontal direction, and the wires will be made thin both to minimise the number of 'violin modes' in the frequency range of interest, and to reduce the natural resonant frequencies in the vertical. These suspensions, with their associated control systems, are discussed more fully in the section on suspension of masses.

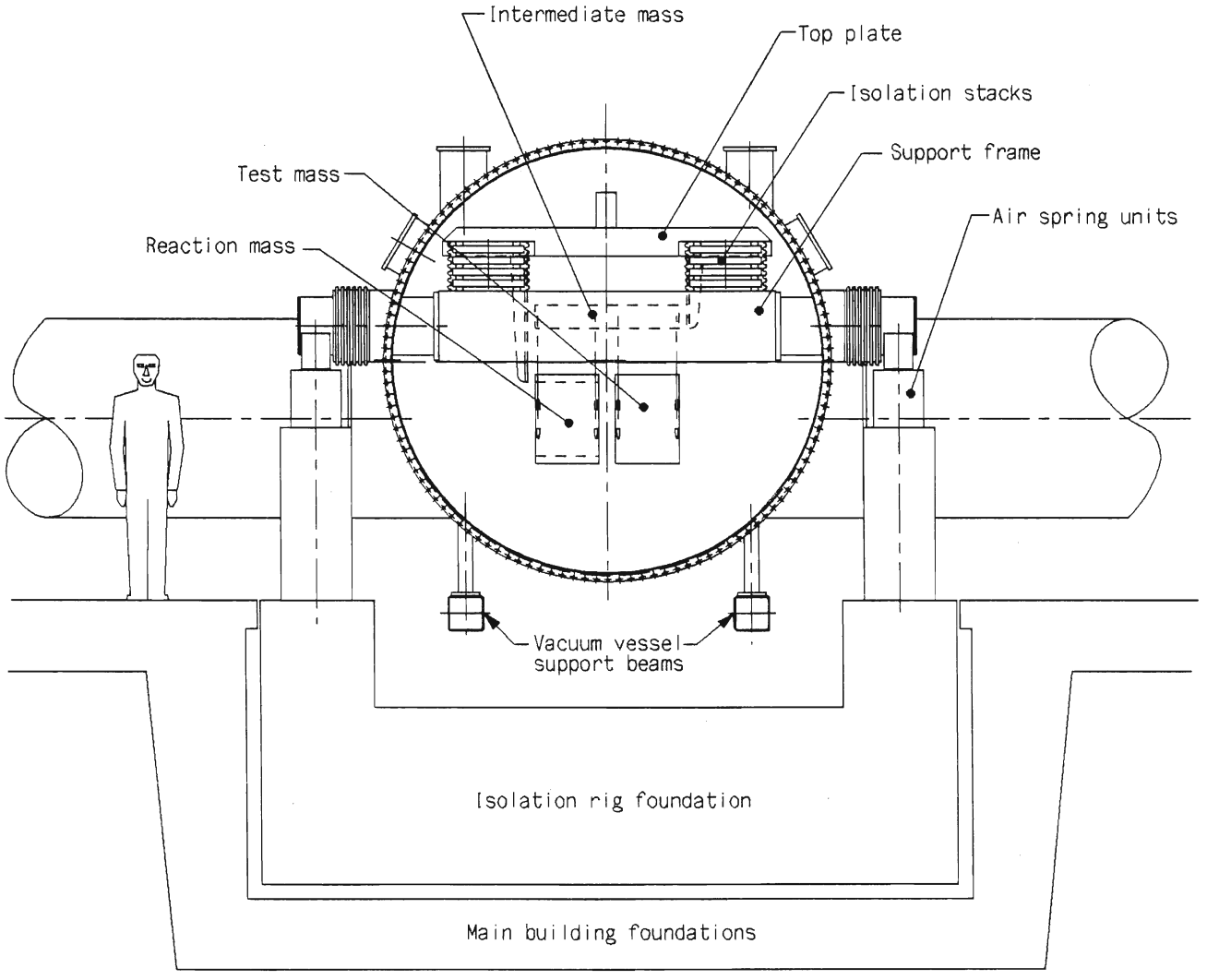

Figure 6.3: *Schematic diagram showing elements of the test mass suspension.*

6.3 Combined Performance

The performance of the overall system cannot be derived precisely by multiplying the performance of the individual parts. Furthermore, as mentioned above, one must consider both horizontal and vertical directions, since there will inevitably be some cross-coupling between the different directions. However an order of magnitude calculation can be made based on the following assumptions :–

Air springs transmissibility : (horizontal and vertical) at frequencies $\geq 50\,\mathrm{Hz} = 10^{-2}$

Isolation Stack transmissibility : horizontal – $(f_{\mathrm{sh}}/Q_{\mathrm{sh}}f)^5$, and vertical – $(f_{\mathrm{sv}}/Q_{\mathrm{sv}}f)^5$, where f_{sh} and f_{sv} are respectively the horizontal and vertical natural resonant frequencies of a single stage of the stack, Q_{sh} and Q_{sv} are the appropriate quality factors, and it is assumed in each case that we are considering frequencies $f > Q_{\mathrm{s}}f_{\mathrm{s}}$.

Double pendulum transmissibility : horizontal – $(1+(m_2/m_1)) \times (f_{\mathrm{ph}}/f)^4$, and vertical – $(f_{\mathrm{pv1}}/f)^2 \times (f_{\mathrm{pv2}}/f)^2$, where f_{ph} is the horizontal resonant frequency for each stage alone, f_{pv1} and f_{pv2} are the resonant frequencies in the vertical direction of each stage alone, and m_1 and m_2 are the upper and lower masses respectively.

Assuming a seismic noise spectrum of $(10^{-7}/f^2)\,\mathrm{m}/\sqrt{\mathrm{Hz}}$ in both the horizontal and vertical directions as the dominant source of noise, the resulting motion of each test mass in a bandwidth of $f/2$ around a frequency $f \geq 100\,\mathrm{Hz}$ is, in the horizontal direction

$$\sim 3 \times 10^{-26} \times \left[\frac{f_{\mathrm{sh}}}{10\,\mathrm{Hz}}\right]^5 \left[\frac{2}{Q_{\mathrm{sh}}}\right]^5 \left[\frac{f_{\mathrm{ph}}}{1\,\mathrm{Hz}}\right]^4 \left[1+\frac{m_2}{m_1}\right] \left[\frac{f}{100\,\mathrm{Hz}}\right]^{-11.5} \mathrm{m}\,,$$

and in the vertical direction

$$\sim 3 \times 10^{-19} \times \left[\frac{f_{\mathrm{sv}}}{30\,\mathrm{Hz}}\right]^5 \left[\frac{2}{Q_{\mathrm{sv}}}\right]^5 \left[\frac{f_{\mathrm{pv1}}}{15\,\mathrm{Hz}}\right]^2 \left[\frac{f_{\mathrm{pv2}}}{20\,\mathrm{Hz}}\right]^2 \left[\frac{f}{100\,\mathrm{Hz}}\right]^{-11.5} \mathrm{m}\,.$$

The values of f_{sh} and f_{sv} shown are conservative. Typical vertical frequencies for the double pendulum shown above are for the case of equal intermediate and test masses, and for each of the two pendulums being of horizontal frequency 1 Hz and suspended by steel piano wire loaded to a factor of 3 from breaking strain. The value of 2 chosen for the quality factors in the stacks is consistent with experimental results taken at Glasgow, where Q's of a few have been measured.

Thus assuming uncorrelated motions of the test masses, the limiting gravitational wave amplitude from the residual horizontal motion is

$$h \sim 2 \times 10^{-29} \times \left[\frac{f_{\mathrm{sh}}}{10\,\mathrm{Hz}}\right]^5 \left[\frac{2}{Q_{\mathrm{sh}}}\right]^5 \left[\frac{f_{\mathrm{ph}}}{1\,\mathrm{Hz}}\right]^4 \left[1+\frac{m_2}{m_1}\right] \left[\frac{f}{100\,\mathrm{Hz}}\right]^{-11.5} \left[\frac{3\,\mathrm{km}}{\ell}\right]$$

where ℓ is the arm length of the detector. Further, assuming the amount of cross-coupling of vertical to horizontal motion is $\sim 1\%$ (a figure which has been demonstrated

by the VIRGO group at Pisa for their multiple pendulum suspension system [41]), the residual vertical motion leads to a limiting amplitude of

$$h \sim 2 \times 10^{-24} \times \left[\frac{f_{\rm sv}}{30\,{\rm Hz}}\right]^5 \left[\frac{2}{Q_{\rm sv}}\right]^5 \left[\frac{f_{\rm pv1}}{15\,{\rm Hz}}\right]^2 \left[\frac{f_{\rm pv2}}{20\,{\rm Hz}}\right]^2 \left[\frac{f}{100\,{\rm Hz}}\right]^{-11.5} \left[\frac{3\,{\rm km}}{\ell}\right].$$

Thus we may conclude from these figures that the system should provide adequate isolation in the region of 100 Hz and above. However if more isolation were required in the vertical direction, this could be implemented by incorporating a spring of low natural resonant frequency as the first stage in the double pendulum, in the manner currently used in the prototype detector at Garching.

It should be noted that these simplified formulae will not apply above a few hundred Hz due to the presence of wire resonances and internal modes of the isolation system. However the isolation provided by the proposed system is in general increasing as a very steep function of frequency, and thus we expect that at these higher frequencies it will be more than adequate.

More accurate calculations based on the scheme outlined above have been done using the finite element method, and preliminary results suggest that the performance estimates given here are of the correct magnitude.

There are a number of possibilities for improving the seismic isolation at frequencies below 100 Hz. One approach is the use of active isolation systems of a number of types [42, 43, 44, 45, 46, 47]. Another approach is to increase the level of passive isolation. We note that there is some very promising work being done in this field by the VIRGO group using a multiple pendulum isolation system at Pisa [41, 48].

6.4 Suspension of Test Masses and Other Optical Elements

For the test masses which require axial displacement to allow arm length control, reaction masses of equal mass suspended from the same intermediate mass will be installed. (See Figure 6.3.) This feature is implemented for several reasons. Firstly, it implies that to first order no force is applied to the common point of suspension of the test mass, and reaction mass, thus minimising the likelihood of exciting any resonances of the top plate or its support frame. Secondly, it avoids the possibility of directly coupling in seismic and mechanical vibrations of any fixed backing plate used to support the feedback transducers. Thirdly, it avoids the possibility of resonances of such a plate limiting the bandwidth of the axial control systems. The intermediate mass will be approximately the same mass as the test mass/reaction mass combination in each case.

The axial control signals will be split, the low frequency part going to electromagnetic (coil/magnet) drive systems for the intermediate suspension masses and the higher frequency parts being applied between the test masses and reaction masses by electrostatic or electromagnetic drive systems. Orientation of the test masses in tilt and rotation will

be achieved by orientation of the intermediate suspension masses with respect to the top plate on the isolation stack by means of coil magnet drive systems. This reduces the amount of magnetic material directly on the test masses themselves. It also defines that the intermediate masses should be on single wire loop suspensions while the test masses should be on double wire loop suspensions. The intermediate masses and reaction masses should be damped electronically to the top plate of the stacks to damp out unwanted normal modes of the system.

A number of other optical items must be suspended. The beamsplitters and recycling mirrors in the central tank are to be hung as double pendulums, feedback to them being implemented with respect to a base plate hung and damped to the top plate of the antivibration stack in this tank. Other mirrors, Brewster angle splitters and external modulation units will be suspended in a similar way or mounted directly on the suspended plate.

The mirrors for the mode cleaners are to be suspended as single pendulums and damped and controlled with respect to suspended base plates as for the components in the central tank. Other optical components on the input beam line in the tank containing the input optics are to be mounted directly on a suspended base plate.

Chapter 7

Data Acquisition and Analysis

7.1 Data Acquisition

Various aspects of data acquisition and data analysis for gravitational wave detection have received great attention starting from the earliest days of Weber's *resonant bar* antennas, and the methods were continually refined in the subsequent two decades. In many respects one will be able to draw upon this experience.

One distinguishing feature of the data produced by the proposed *interferometric* gravitational wave detector is its broadband nature, resulting in storage requirements of the order of a few terabytes per year of operation (1 TB = 10^{12} Bytes). It is obvious that the acquisition, storage, exchange, and analysis of such large amounts of data need to be discussed in detail. But it will be shown that, even with today's commercially available equipment, the task is manageable, at a cost that is within reason. Developments in the next few years can be expected to improve the performance and at the same time reduce the prices of the electronic equipment considerably.

7.1.1 The interferometer signal and auxiliary data

In the mode in which the antenna is to be operated it is the compensating signal required to keep the interference of the recombined beams near minimum that is later to be analysed for gravitational wave signals. This signal requires sampling at a rate of $\sim 10\,\mathrm{kHz}$ as will be discussed later.

In addition to this signal proper, there are various operational data ("housekeeping data") that are necessary to characterise the operational status and the level of external noise contributions. The most important of these are such sources as seismic and acoustic noise and also fluctuations in the laser light (frequency, power, beam geometry). Particularly in the early experimental stages, such signals would also require sampling at kHz rates.

Furthermore, there will be slowly varying operational and environmental parameters such as vacuum pressure, meteorological or geomagnetic data; error point signals from

some of the detector's main servo loops also should be recorded. Flexibility for adding such parameters must be provided.

7.1.2 Data volume

Typically, for target frequencies up to several kHz (see Chapter 2) a sampling rate of not less than 10 kHz would be advisable. In order to provide sufficient dynamic range, an A/D conversion resolution of 16 bit (2 Bytes) seems a reasonable choice.

Together with the housekeeping information, data rates between 30 and 100 kB/s may have to be read out and stored. This data rate may vary, depending on the particular astrophysical goal, on the amount of narrowbanding, and on the desire to find correlations, or transfer functions, between external noise sources and the interferometer signal, particularly in the starting phases of the experiment.

At any rate one must envisage a data volume of the order of 1 to 3 TB (10^{12} Bytes) per year of operation. These data will have to be read out and stored (archived), but also copied and shipped for coincidence analysis with data of other installations.

7.1.3 Storage media

While the data rate of up to 100 kB/s could easily be handled by local area networks (LANs), transmission to a distant computing centre would be very expensive. Therefore, storage on site, *i.e.* at the location of the experiment, is required.

There are, at present, several well-established storage schemes, using either magnetic tape cassettes or optical discs. Very promising, both in storage density and in price, are the recently announced optical paper tapes [49].

In selecting the storage scheme, an important point is that a WORM system (write once – read many times) is sufficient. Most of the optical disk systems now on the market are of the WORM type. Tapes do not allow in-place changes, so in practice they can also be considered WORM media.

One distinction between tapes and optical disks is given by the access they allow. Optical disks allow some faster quasi-random access, while tapes are, even with fast forward- and re-wind, essentially sequential. But the main usages of the data, particularly in a first scan through them, will be sequential; only later will closer looks into the data require a more random access, but there the retrieval of the proper volume (disk or tape) can be expected to take more time than locating the interesting data inside this volume.

7.1.4 Hardware cost

Tape cassettes (video cassettes or digital audio cassettes) have now reached such a high data capacity (up to several GB) that exchange of the cassette will in general be required

only every 6 to 24 hours. Storage for a full year of data would currently cost about £10 k. Optical disks offer comparable storage capacities and densities, but currently are still a factor of 30 to 100 more expensive; this may change in time scales of a few years.

For data exchange with the collaborating laboratories some further expenditure for storage media will arise. But by using tape cassettes or erasable optical disks, only a one-off investment for about one year's worth of data is needed (assuming that each laboratory takes responsibility for archiving its own data).

The investment cost of the drives is in the order of several thousand pounds, both for magnetic and optical devices. A minimum of two drives is required, and an additional standby drive would be very desirable. Furthermore at least two drives are needed at the computing centre.

One further aspect is the space taken by archiving the data taken over many years. The magnetic tape cassettes from a full year's run would fill only a fraction of a cubic meter; and again optical disks would not be much different. Thus to have many years of data, together with copies from collaborating laboratories, would not present serious space problems.

The choice of the medium should not be made at the moment. The market is undergoing such rapid changes that by the time the large amounts of data need to be written, new developments may well have come up (such as "digital paper"), and prices for the media will certainly drop further.

Good coordination between the groups for maximum compatibility will be required to ensure an easy international exchange of data. This concerns the choice of the storage medium as well as the data format on these media. But again, it appears premature to make any decisions on that now.

7.1.5 Data integrity

High standards of reliability and integrity are required for all of the data that are to be read out from the detector system. An important aspect is to avoid all mutual interference (cross-talk) between individual signals, and in particular to avoid hum at the mains frequency and its harmonics. Ample use of isolating amplifiers (to avoid ground loops), and early A/D conversion (to avoid cross talk) are reasonable safety measures, and the expense of such measures is affordable (of order £10 k in all). For signals which have to be sent along the length of the arms, transmission via glass fibres is to be preferred.

The magnetic as well as the optical storage schemes provide ample error correction, a typical specification being, say, one unrecovered error in 10^{13} bits, *i.e.* of order one single bit error once a year.

7.1.6 Timing accuracy

Coincidence observations of short burst GW signals from distant antennas as well as the search for long term periodic GW signals require stable and synchronised clocks to be available at each receiving station. It is convenient to synchronise the sampling pulses with the clock pulses to avoid having to record high-accuracy time information.

Integration times of about a year, as may be used for the detection of periodic GW signals, require a long term clock stability of $< 10^{-11}$. Caesium atomic clocks, having a rate stability of $< 10^{-12}$ would provide adequate timing. More economically, however, accurate relative timing may be achieved by synchronising the respective local times with time signals broadcast by special radio transmitting stations.

The relative deviation between different local times should be only a very small fraction of the gravitational wave propagation time between the different antenna sites. One would want a relative accuracy of better than $50-100\,\mu$s for antenna separations of about 1000 km. The time signal of the German transmitter station DCF77 near Frankfurt, operated by the PTB, would yield this timing accuracy over distances of several hundred kilometers. At sites where continuous reception of a broadcast time signal is possible, local atomic clocks may not be required.

7.1.7 Data acquisition computer

A dedicated computer is required for each interferometer, equipped with sufficiently fast data access, with enough data handling speed to properly pack and edit the data, with enough internal storage (hard disk) to bridge tape exchange on one of the drives. A new generation PC, with a fast processor board, is bound to fulfill these requirements.

For reasons of data security, this data acquisition computer, running a relatively simple, well tested program, should be completely separate from a further computer on which various schemes of on-line data analysis or reduction will be tested. Programming of such an "intelligent" data processor will involve many trials and alterations, all of which would endanger the continuity of data storage. Moreover, it may be a more complex system than the acquisition computer, and one must not allow any failures in it to affect acquisition and storage.

7.2 Data Analysis

The large volume of data that an interferometric detector will acquire poses considerable difficulties for analysis. Since ideally the experiment will take data 24 hours a day, 365 days a year, and since interesting events (such as supernova explosions) must be reported to the astronomical community as quickly as possible, the data analysis system must be able to search the data in real time for at least the likely burst sources, particularly gravitational collapses and coalescing binaries. Moreover, it must be able to handle, with less immediacy, such tasks as pulsar searches and cross-correlation experiments.

These requirements seem best satisfied by having two separate computer installations for different phases of the analysis:

- two on-line systems (one per interferometer), each capable of searching for coalescing binaries and supernovae in real time in an interferometer output, and
- an off-line system capable of performing cross-correlations, pulsar searches, refinement of the analysis of events picked up by the on-line detector, the analysis of data from other detectors, and so on.

In addition, the international laser interferometric detector community may decide to pool resources to get a very fast computer to do all-sky, wide-bandwidth pulsar searches, which are beyond the capability of the off-line computer system we propose here. If this occurs, we will be expected to contribute, and we would bid to have this located in the German-British collaboration.

We shall consider the operational requirements for both the on-line and off-line systems in turn. We are guided by the extensive discussion of these points in a forthcoming book [23].

7.2.1 The on-line computer system

The most demanding job for the on-line system is to perform matched filtering for coalescing binary waveforms. Other tasks, such as calibrating the data, pre-whitening the noise (if necessary), checking vetoes and other housekeeping data, and searching the time-series data for gravitational collapse-type events, while not negligible, are much less demanding.

The set of filters for simple Newtonian point-mass coalescing binaries has a number of parameters: the mass parameter $\mathcal{M}$, the amplitude of the signal, its time of arrival (defined as the time when it reaches a certain fiducial frequency, say 100 Hz, in the detector), and the phase ϕ of the wave when it arrives. By correlating the data continuously with a template of the expected waveform from a particular binary system, one finds the signal's time-of arrival and amplitude from the time the correlation is a maximum and the value of that maximum. Thus, the stored templates form only a two-parameter set, depending on $\mathcal{M}$ and ϕ.

Despite the fact that there is some evidence that all known neutron stars have a mass of about $1.4\,M_\odot$, we cannot afford to make that assumption here; moreover, there should be some systems containing black holes of unknown mass. We must therefore be prepared to search for coalescing binary signals with mass parameters in a range something like 0.1–$20\,M_\odot$. Studies of the overlap between filters with slightly different mass parameters lead to the conclusion that we should provide for the ability to apply about 1000 filters to each stretch of data.

Given data sampled at 20 kHz, with two Bytes per datum, and given a typical filter duration of 2 seconds, then one can show that performing these correlations by fast Fourier transforms (FFTs) will require a processing speed of 60 Mflops and RAM storage for the filters of 16 MB. Each detector should have such a capability, for although the

low-frequency detector should see more coalescing binaries, the high-frequency detector will need to search for them too, especially black hole coalescences, whose ultimate gravitational wave frequency may reach 10 kHz if the black holes are of solar mass.

Computer technology develops so quickly that it would be unwise to try to specify the shape of such a system today, when it will not begin to be used for another five years or so. Repeated correlations on the same data set can be performed in a highly parallel fashion, so it is reasonable to expect that there will be a host computer running a parallel array of a number of computing elements. Such systems are easy to expand for any future developments.

Software for this analysis problem will not be trivial. While filtering is well understood, the on-line system has other elements that require more sophistication. In particular, it must have the ability to clean up or reject data under a variety of (possibly unforeseen) experimental conditions. It must also be able to make lists of possible events (threshold crossings) and to send such lists to the off-line computer system, which will forward them to other detector sites and search for coincidences. Such systems are under development at Cardiff, with the assistance of a group at the Inter-University Centre for Astronomy and Astrophysics (IUCAA) at Pune University, India. This work is also being coordinated with that in other detector groups through the international data analysis working party, chaired by Schutz.

The specification for each on-line system is thus:

- Computing speed: 60 Mflops,
- Memory: 16 MB,
- Communications: appropriate software and connections to electronic mail networks for the automatic transmission, perhaps hourly, of lists of candidate events to the off-line computer.

7.2.2 The off-line computer system

As we remarked in Chapter 2, certain kinds of off-line data analysis can absorb as much computing power as one can throw at them: a broadband all-sky search for unknown pulsars, using data taken by a single detector for 4 months, is beyond the capability of any foreseeable computer. The final size and speed of the off-line computer will be governed by computing technology at the time it is acquired.

The data that are taken at the detector will be stored on the archive medium (high-density digital tapes, optical discs, or optical paper) at the detector site, and then transported to the off-line site, where it will be processed and then stored along with data sets from other detectors around the world.

There are many tasks that the central off-line computer will have to perform:

- It must refine the estimates of filter parameters produced for candidate events by the first pass through the on-line system.

- It must accept event lists from the on-line system, forward them to computers at other detector sites around the world, and receive their lists in return. It must search these lists for coincidences within allowable time-delay windows, and then solve the "inverse problem" for real coincidences, *i.e.* infer the amplitude, polarisation, and direction of travel of the gravitational wave. It must then be able to notify cooperating astronomers, possibly by automatic electronic mail, of any events that might be observable, either from the ground or from satellites. There might be only an hour or so before a nearby coalescing binary might produce an optical display, and only a few hours for a supernova.
- It must be able to do cross-correlations between two detector outputs to search for a stochastic background. Narrow-band data will probably be used for maximum sensitivity.
- It must be able to process narrow-band data in an all-sky search for unknown pulsars in that frequency bandwidth, using FFTs to analyse the data from a single detector (*i.e.*, not cross-correlating with other detectors).
- It must be able to correlate wideband data from two detectors in order to search for any unpredicted signals that consist of wavetrains lasting 10 or more cycles, too weak to be seen in the time-series data of either detector.
- It must be able to search archived data in the light of subsequent information, such as looking for gravitational wave counterparts of events detected optically, or filtering old data for new predicted classes of sources for which theorists have developed waveform templates. These data must be accessible not only to project scientists and collaborators, but also – after a time to be agreed among the international laser interferometer community – to other scientists who wish to use it.

From this list, which is not necessarily exhaustive, the most demanding task is the processing of narrow-band data for an all-sky pulsar search. There is no simple criterion for the sensitivity one would like to achieve, but a computing speed of 300 Mflops is likely to be achieveable at reasonable cost in a few years, and as described in Chapter 2 it would permit a narrow-band observation lasting about 2 weeks, with quite interesting sensitivity. In order to perform the required FFTs, it would only need a memory of $2B\tau_{\rm int}$ Bytes, or about 5 MB for this operation. The original data set is of course much larger, but it is reduced to this by heterodyning the original frequency of observation down to zero, and then resampling at about 4 Hz, the Nyquist frequency for the 2 Hz band-limited data set produced by heterodyning. (See [23] for details.) For the data taken during a 100 hour test run (see Appendix A) a slightly different technique, reducing the amount of computing required, is being developed at the MPQ in Garching [50].

As with the on-line computer, this sort of computing speed would probably be achieved in a parallel array, but the software to achieve these sorts of speeds by coordinating all the computing elements to work on a *single* FFT will have to be carefully designed. Algorithms to do this are already available – one has been supplied with the N-Cube computer mentioned below – and we will test it and others. Another advantage of

having a parallel array is that when some of the other tasks are being performed it could in principle be subdivided to allow several of them to go on at once, for instance making two different searches on archived data.

The tasks required of the off-line computer demand a general-purpose computer with a sophisticated operating system, a multi-user machine that can communicate with many other computers simultaneously, and that can supervise the work of its attached parallel array to allow simultaneous use of different sections of it for smaller jobs when it is not doing an all-sky search. Such facilities are already available to some degree, and we are experimenting at present at Cardiff with a Sun 3/260 computer which hosts a 128-element N-Cube computer. The N-Cube can be subdivided among several users; when acting together the processors can reach a total rate of 40 Mflops on certain benchmark problems. It is also probably the ideal parallel architecture for performing FFTs, since its architecture minimises average communication times among processors. The fastest N-Cube available today can probably run FFTs at well above 1 Gflop, but at a considerable price. Given faster processors in a few years, a goal of 300 Mflops at a price of £200k does not seem unreasonable.

The choice of operating system and to some extent of the hardware will be made in coordination with the other international detectors, since the software for many aspects of the analysis should be as transportable as possible. Some of these choices will be made soon, and acquisition of equipment for the development of prototype analysis systems will need to be done soon after the project is approved. This can probably take the form of purchasing one of the workstations earlier than the rest of the equipment.

Associated with the off-line computer would be a number of peripherals, such as data archive equipment and suitable readers, a good-quality printer, a small number of workstations connected to the main computer by a fast network (which can access the parallel array and can also work independently to develop further software), and communication connections to international academic networks.

We can summarise the specification for the off-line system as follows:

- Computer: multiuser machine with a sophisticated operating system.
- Attached parallel processor: capable of 300 Mflops on a coordinated FFT across all elements. It must be able to be subdivided for independent work on different tasks, this reconfiguring being performed by software.
- Peripherals: workstations, archive data storage and reading equipment, communications to the academic networks, laser printer.

Chapter 8

Site, Buildings, and Services

8.1 Site

8.1.1 Choice of site

Both the UK and the German teams have been working on identifying suitable sites for the construction of an antenna.

In the UK, a search was carried out for suitable sites and one, at Tentsmuir Forest near St. Andrews, Scotland, has been selected. This site is large enough to allow the arms to be 2.6 km long.

Outline planning permission has been obtained to build such a detector. Full permission for an earlier proposal having arms only 1 km long is also held. Because all of the important issues have already been addressed, it is estimated that full permission for the larger detector will take about one year to obtain and this process has started. A seismic survey has been done at the site by the British Geological Survey, which shows that the displacement noise levels are typically given by

$$x = \frac{10^{-7}}{f^2} \mathrm{m}/\sqrt{\mathrm{Hz}}$$

which will be handled well by the proposed isolation system. Initial discussions with the Forestry Commission, which owns the land, have shown them to be supportive of the project, and an arrangement has been agreed whereby the land could be leased to Glasgow University at very low cost.

In Germany a survey has been done of potential sites in Bavaria. After aerial surveys, site surveys, seismic surveys and outline costings, four sites were found to be well suited to the present purpose. A similar search for the whole of the Federal Republic is nearly completed, and there are also suitable sites for the experiment in North Germany. Negotiations with landowners are soon to begin and initial planning enquiries have been made. The Ministerium für Wissenschaft und Kunst of Bavaria is actively investigating the site question.

8.1.2 Above or below ground

An antenna with arms partially or totally below ground is preferable to an above ground version, as mechanical disturbances such as seismic or acoustic noise are considerably reduced, and the environmental impacts are less, both visually and in terms of restricted access for people and wildlife.

For economic reasons, however, the UK team has asked for and obtained planning permission to build above ground at Tentsmuir. In Germany, work is underway towards obtaining planning permission.

In this proposal we present the costings for both the above ground and the partially below ground options.

8.1.3 Geometry of detector and possible future extension

The concept of the British/German proposal is such that it can later be extended to an observatory that is sensitive for gravitational waves of all polarisations and angles of incidence. To achieve this a total of three differently oriented interferometers are required and this can be realised with the addition of only *one* further 3 km arm to our proposed system.

The two configurations envisaged are indicated in Figure 8.1 .

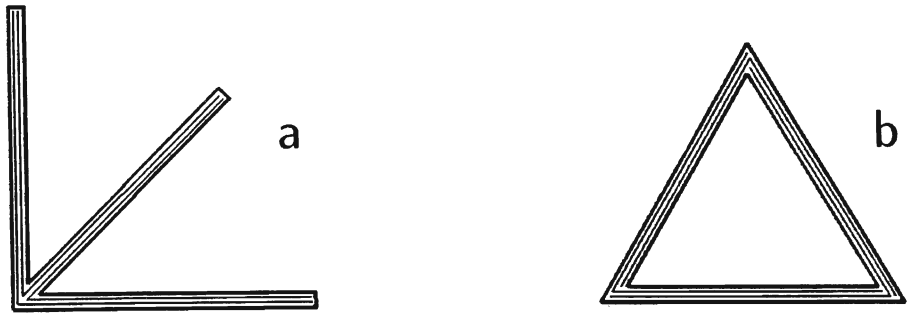

Figure 8.1: *Schematics of two configurations with three interferometers at one site:*
a. *rectangular, with bisector;*
b. *equilateral triangle.*

These extended configurations considered involve interferometers with opening angles ϕ other than 90°. Although these are less sensitive by a factor $\sin\phi$, performance *vs.* cost considerations make these configurations attractive compared with 2 separate and suitably oriented 90° detectors.

The overall sensitivities of the two configurations shown in Figure 8.1 are comparable. If we sum the signals from the three detectors in quadrature and average over all angles of incidence and polarisations, we find the triangular configuration only marginally better (by a factor 1.06) than the bisected rectangular one.

The triangular configuration has the advantage of having a more even response to polarisation and direction of propagation of the incoming radiation.

However, if our aim is to achieve the highest probability of successful detection at as early a stage as possible we believe it is best to aim for the geometrical arrangement that gives the highest sensitivity for the first detector built – *i.e.* to have the initially constructed arms at 90° to each other.

8.2 Buildings and Tube Housings

The Council Works Unit of SERC made a study of the civil engineering requirements of a Gravitational Wave Detector at the time of an earlier proposal to build a 1 km device. Outline plans were made of the buildings and the vacuum tube housings, and cost estimates were prepared. The CWU have since updated this work to allow for inflation, for the additional arm length, and for changes in the specifications of the buildings. These estimates are only accurate to within ±25% because of the unquantifiable nature of several factors pertaining to such work. The CWU have also prepared similar estimates of the cost of building partially below ground tunnels in the UK.

The proposed arrangement will require three buildings and approximately 6 km of housing (the Tentsmuir site requires only 5.2 km of housing because of limitations on the size of the site).

8.2.1 Buildings

Three main buildings are needed: the central building and the two end-stations. The buildings will be as simple as possible whilst still satisfying their functional requirements, minimising both construction and maintenance costs.

There will be a central building which houses the vacuum tanks for the central masses, the beamsplitters, and the input and output optics. There will also be space for a computer room, offices, a workshop, a mess, and toilets. The total area of the central building will be about 900 m^2.

The end stations each house two vacuum tanks for the end masses, and incorporate a small office and toilet. The floor area of each end station will be about 350 m^2.

8.2.2 Tube housings

Two options have been considered for the housings. For reasons explained above it is not possible at this stage to choose between the above ground housing shown in Figure 8.2 and the partially below ground housing shown in Figure 8.3. In any case the exact details of the housing will depend on the choice of site.

In the above-ground case, the enclosure would take the form of a 'tunnel' approximately 2 m wide by 2 m high with a steel skeleton, clad in profiled metal sheeting, built on a

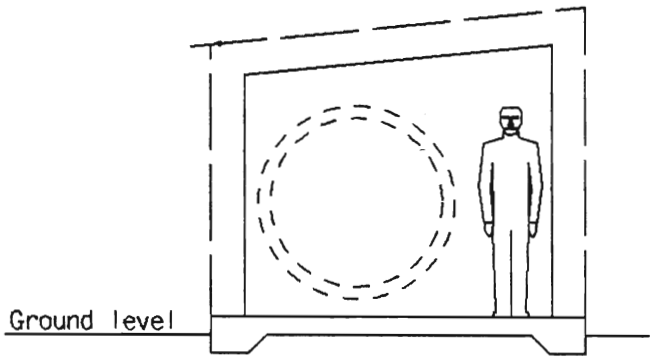

Figure 8.2: *Above-ground tube housing.*

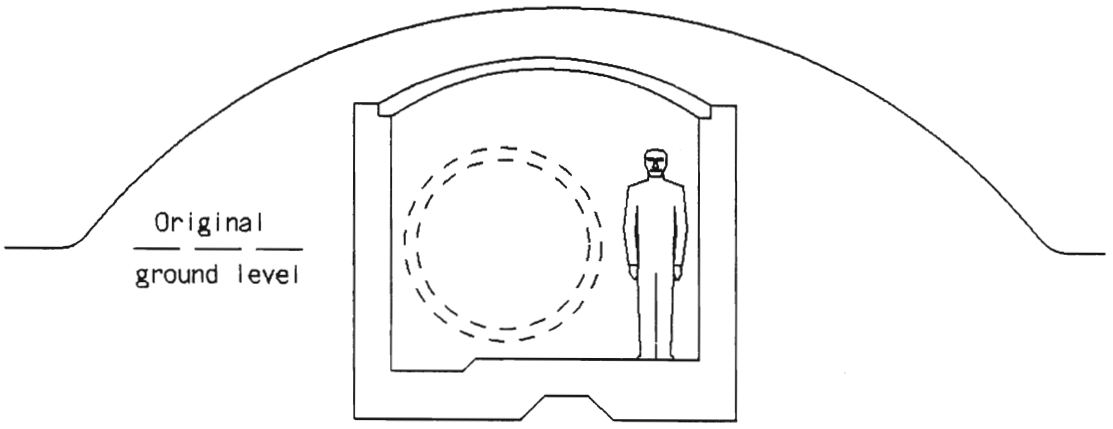

Figure 8.3: *Semi-submerged tube housing.*

continuous raft foundation. This would protect the vacuum tube from the weather and from vandalism.

If the arms were required to be partially below ground then a concrete structure would be built in a trench and the spoil heaped back over the top to form a mound. This would require drainage as well as ventilation, lighting, escape routes, and so on. The exact form would depend on the site conditions; that shown in the figure is derived from one of several options considered by Dorsch Consult in a feasibility study carried out for MPQ.

8.3 Services

8.3.1 Mechanical and electrical

All buildings will be provided with small power and lighting. All buildings except the garage and tube housing will be provided with heating; the computer room will be air conditioned; the buildings will have minimal external lighting; there will be fire extinguishers in all buildings and hydrants in the main building. A main electrical supply will be provided via a substation giving a total capacity of 2 MVA.

8.3.2 Water

The site will be provided with a mains water supply which will be distributed to all buildings. In addition there will be a closed system water cooling unit supplied to the main building with a cooling capacity of up to 100 kW. Waste water from all the buildings will go to septic tanks local to each building.

8.3.3 Other services

The intention would be to provide only basic unpaved tracks for the full length of each arm. At Tentsmuir this would involve grading and compacting the existing sand/gravel surface for new tracks; there is already a considerable length of track which could be used as it is. At other sites it may be necessary to import granular material to form a suitable track. No kerbs or drainage will be supplied.

Roof drainage will be to soakaways local to each building. It is not envisaged that a gas supply will be available. In the above-ground case footbridges will be provided over the tube housing every 1 km, and a single vehicle bridge will also be provided.

Chapter 9

Project Organisation and Costing

9.1 Management

It would be premature at this stage to attempt to put forward more than an outline of how the project might be managed, because the details will have to be agreed between all the participating institutions and the funding agencies. In addition, the legal structures and the mechanisms for financial control must take account of national practices and requirements appropriate to the actual site, which has yet to be selected.

Because the overall timescale and the total cost of the project could depend critically on the choice of site and construction method (*i.e.* above or partially below ground), it is suggested that an outline agreement, perhaps in the form of a Memorandum of Understanding between the interested parties, and in particular between the BMFT and SERC, is established as soon as possible. This will enable the limited infrastructure needed to support the initial phase of the project to be established and appropriately resourced, and in particular will provide an agreed mechanism whereby crucial early decisions can be taken with minimum delay.

It is suggested that a Project Leader, a Project Engineer and a Project Administrator are appointed as part of this initial agreement. Each might be expected to be an existing employee of one or other of the collaborating institutes, but could, if necessary, be a new appointment. These three would constitute the core of the project team, and would be responsible for the day to day management of the project, with the Project Leader carrying ultimate responsibility.

A Steering Committee, comprising independent nominees from the institutes and agencies plus the Project Leader, should also be set up without delay. Its meetings would normally be attended by representatives of all the research groups involved in the project. One of its first tasks would be to consider the input from the project team on the choice of site and the optimisation of the overall design, within such financial constraints as may be applied. The Steering Committee would be able to seek advice, if it wished, from independent experts, so that it would be able to recommend a particular design and site choice to the collaborating institutes and agencies and would be able to assist them in arriving at a final decision.

In the longer term, the steering committee would act as the interface between the project and the various sponsoring bodies, monitoring finances and the overall programme but primarily concerning itself with longer term strategy.

Once a site has been agreed, definitive costs must be prepared for approval and a full formal agreement can be made between the collaborating institutes and the funding agencies. Once established, the project will require a base. An institute in the country providing the site will act as 'host', furnishing the necessary infrastructure to run the project: financial services, contracts, accommodation *etc.* Glasgow University and MPQ are the obvious potential hosts. It may be advantageous for financial and legal reasons to make the detector formally part of the host institute, but that cannot be confirmed at this stage, and the situation may indeed be different between Germany and the UK.

At this point the detailed mechanisms for financial administration and control will need to be agreed and set up. The overall responsibility for running the project will clearly rest with the Project Leader, who will report to the Steering Committee and funding agencies at regular intervals.

9.2 Costs

Table 9.1 shows the estimated costs, at May 1989 prices, for two modes of construction (above or partially below ground) of a 3 km arm detector in both the UK and Germany. The main differences between the above and partially below ground options are obviously in the civil engineering costs, but the differences between the UK and Germany are more subtle. It should be noted that the VAT/MWSt situation is complex, and expert advice will need to be obtained when setting up operating procedures to ensure that liability for tax is minimised. The costs for the civil engineering work at a German site are assumed to be the same as those at a UK site (before tax). Discussions with staff at the Bauabteilung (Civil Engineering Department) of the Max-Planck-Gesellschaft confirm that this assumption is valid well within the accuracy of the estimates.

The uncertainty in these estimates is at least 10% overall, and somewhat larger in the civil engineering costs, which can be strongly site dependent.

Planning permission has already been obtained to build a 1 km arm detector on the Tentsmuir, Scotland, site, and outline planning permission has been given for a 2.6 km detector, the maximum the site can accommodate. This reduction in length from 3 km results in savings in civil engineering and vacuum system costs. The Tentsmuir costs are therefore shown separately in Table 9.2.

These cost estimates should be taken as upper bounds for the detectors proposed. The design allows the possibility of reducing the scope of the project in several different ways which could constrain the final total cost to lie between around £ 20 million and the estimates given. Any such reduction will affect either the sensitivity, or the flexibility, or both. This is a problem the project team will have to address once the total financial support from the funding agencies is known. A final detailed design which meets the financial constraints and is optimised for the particular site selected will have to be

Project built above ground

	MAY 1989 PRICES	UK Site		German Site	
		£ M	MDM	£ M	MDM
1.	Civil Engineering work	7.11	21.52	7.11	21.52
2.	CWU fees	0.98	2.95	0.05	0.15
3.	Other fees			0.98	2.95
4.	Vacuum system	7.13	21.57	7.13	21.57
5.	Experimental stations	5.59	16.92	5.59	16.92
6.	Control system	1.14	3.46	1.14	3.46
7.	Data acquisition	0.64	1.92	0.64	1.92
8.	Optics and lasers	3.75	11.36	3.75	11.36
9.	Travel and subsistence	0.34	1.03	0.44	1.33
10.	Tax	1.66	5.01	0.05	0.14
	Total excluding RAL effort	28.34	85.74	26.88	81.32
11.	RAL manpower costs	1.24	3.75	1.24	3.75
	Total cost	29.58	89.49	28.12	85.07

Project built partially below ground

	MAY 1989 PRICES	UK Site		German Site	
		£ M	MDM	£ M	MDM
1.	Civil Engineering work	11.92	36.06	11.92	36.06
2.	CWU fees	0.98	2.95	0.05	0.15
3.	Other fees			0.98	2.95
4.	Vacuum system	7.13	21.57	7.13	21.57
5.	Experimental stations	5.59	16.92	5.59	16.92
6.	Control system	1.14	3.46	1.14	3.46
7.	Data acquisition	0.64	1.92	0.64	1.92
8.	Optics and lasers	3.75	11.36	3.75	11.36
9.	Travel and subsistence	0.34	1.03	0.44	1.33
10.	Tax	2.38	7.19	0.05	0.14
	Total excluding RAL effort	33.87	102.46	31.69	95.68
11.	RAL manpower costs	1.24	3.75	1.24	3.75
	Total cost	35.11	106.21	32.93	99.61

Table 9.1: *Estimated costs for a typical UK site and a German site, May 1989 prices*

Project built above ground in Tentsmuir

	MAY 1989 PRICES	£ M	MDM
1.	Civil Engineering work	5.79	17.51
2.	CWU fees	0.98	2.96
3.	Other fees		
4.	Vacuum system	6.38	19.30
5.	Experimental stations	5.59	16.92
6.	Control system	1.14	3.46
7.	Data acquisition	0.64	1.92
8.	Optics and lasers	3.75	11.36
9.	Travel and subsistence	0.34	1.03
10.	Tax	1.53	4.63
	Total excluding RAL effort	26.14	79.09
11.	RAL manpower costs	1.24	3.75
	Total cost	27.38	82.84

Table 9.2: *Estimated costs for Tentsmuir site*

presented to the Steering Committee and the funding agencies before the project can be definitively approved.

The estimated spend profile for the shortest reasonable construction period of three years is given below for the case where the detector is built partially below ground in Germany. It covers a five year period, which allows for preparatory work and for bill payments carried over. The spend profiles for the other possibilities are broadly similar.

Typical spend profile for the construction phase

	£ M	~	MDM
Year 1	3.3		10
Year 2	8.2		25
Year 3	11.5		35
Year 4	6.6		20
Year 5	3.3		10

9.3 Running Costs

Estimates for the annual running costs, exclusive of staff salaries and overheads, are given below. These are very preliminary, and it is assumed that, on balance, costs will be much the same in either Germany or the UK.

Estimated annual running costs, May 1989 prices

	£k	~	kDM
Site Costs (rent, rates, etc)	50		150
Water, electricity & other services	220		650
Maintenance and consumables	400		1200
Continued work with prototypes	150		450
Subtotal	820		2450
Staff Costs (SERC only)	110		330
Travel and Subsistence	100		300
Total	1030		3080

These costs would have to be shared between the collaborating groups. How this should be done has yet to be discussed, and would clearly require the agreement of the funding agencies.

9.4 Timescale

This project can be seen as having seven discrete steps or phases, starting with the submission of this proposal and running through to the final operation of the detector. The lengths of time required to complete some of these phases cannot be estimated with any accuracy, because they depend on external factors outside the control of the proposers.

- **Step 1:** the funding agencies, on receipt of the proposal, evaluate its feasibility and desirability, and reach an agreement on supporting the project and on the level of support they are prepared to offer. This could take 6–12 months, starting from October 1989.
- **Step 2:** the project team is set up, resourced, and evaluates possible sites. One is selected and an optimised design which meets the financial constraints is prepared. This could take up to 12 months.
- **Step 3:** permission to build the proposed detector has to be obtained from the competent local authorities. For Tentsmuir, Scotland, this process is essentially complete, with outline planning permission for a 2.6 km detector needing to be converted into full planning permission. Planning permission for the North German sites can be obtained within a few months, but it could take a year or more for the Bavarian sites. During this period, detailed design and technical development would continue, so that the end of this step would see the production of a final design with definitive costings for ratification by the funding agencies.

- **Step 4:** the funding agencies would give final approval, allocate resources for construction, and the necessary structure to build the detector would be set up. This step could be quite short, say three months, if there were no unforeseen problems.
- **Step 5:** the construction phase. This has been studied in some detail and a chart showing a three year construction period is given in Figure 9.1. The actual construction period depends critically on the funding being available to match the optimal spend rate, and in practice construction may have to proceed more slowly to match available funds.
- **Step 6:** the commissioning phase. About three years will be required before the detector is sufficiently developed to be able to run for protracted periods at strain sensitivities approaching 10^{-21}.
- **Step 7:** the operational phase, during which regular extended operation will have priority over development. The design is such that continued development aimed at pushing the sensitivity towards the ultimate goal is compatible with operations.

On the assumption that Tentsmuir is selected, and that there are no unforeseen problems in obtaining final approval for the project, construction could start around mid 1991. The detector could be completed before the end of 1994 if the resources were available to meet an optimised construction programme. In practice, this may be a little optimistic, and these dates may be delayed by 6 or 12 months.

9.5 Exchange of Personnel between the British Group and MPQ

During the planning, construction and development phases of this experiment it is essential that there is significant interchange of personnel between the research groups involved. This is important for the coordination of the experimental and data analysis development work which has to carried out and should help the groups involve to operate as one team.

To this end Professor H. Walther of MPQ has recently suggested that J. Hough from Glasgow, and/or other members of the Glasgow group should spend two man months per year at MPQ, and that B.F. Schutz should spend one man month per year in MPQ. These visits would be funded by MPQ. The arrangements are welcomed by both the University of Glasgow and the University of Wales and organisational details are currently being worked out.

It is of course desirable that such interchanges should be bilateral. Following a short discussion with the chairman of SERC, it is proposed that SERC-funded visiting fellowships, to allow two members of the MPQ group to spend up to two months each per year in Britain, be made available.

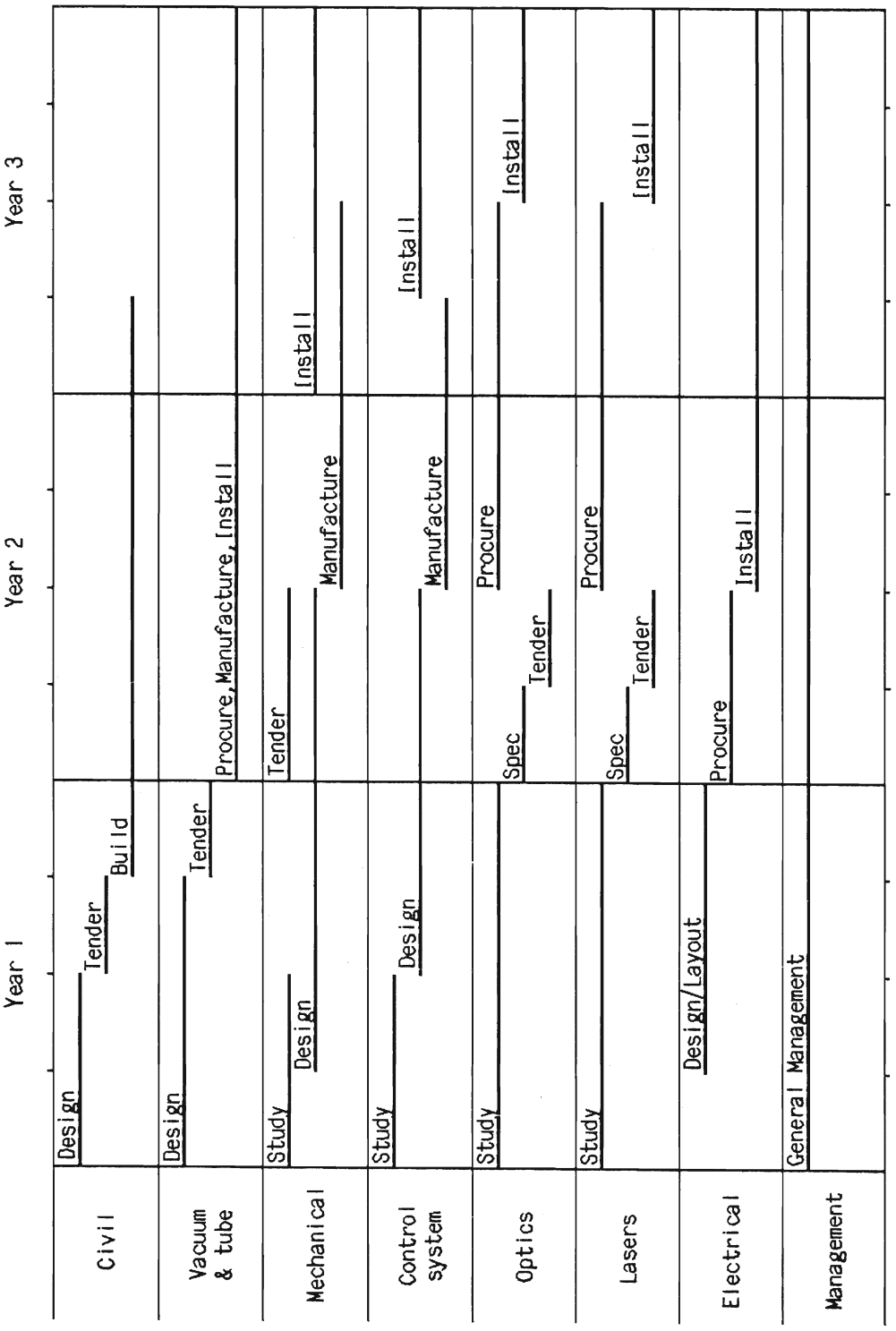

Figure 9.1: *Schedule for the construction phase.*

Appendix A

The Prototype Detectors at Garching and Glasgow

A.1 Introduction

Delay line detectors have been under development at the Max-Planck-Institut, Munich and later Garching, since 1974, initially on a 3 m baseline [51], and later on a baseline of 30 m [52].

The Fabry-Perot based prototype detector of 10 m arm length at the University of Glasgow has been under development for the last ten years [53] and followed earlier work that began around 1976 on a small scale delay line interferometer.

While most work on these instruments has been devoted to improving their sensitivities, periods of data taking have been undertaken, the most recent being a joint effort between Garching and Glasgow of 100 hours continuous duration. This run was carried out just after the reported optical observation of the pulsar in SN 1987a and demonstrated the high duty cycle possible with such instruments (89% and 99% for the Glasgow and Garching detectors, respectively).

A.2 The Prototype Detectors at Garching

A.2.1 The 3 m prototype

At the Max-Planck-Institut für Astrophysik, investigations of the laser interferometric scheme were begun in 1974. A prototype, using an argon ion laser, was built, with arms 3 m in length. After a brief pilot phase with a small rigid interferometer, it was then operated with optical delay lines (up to $N = 138$ beams). The set-up [51], even then, was quite similar to the current 30 m prototype that is shown in Figure A.1 .

The choice of the delay line scheme, with its ease of alignment and benign behaviour with respect to mirror motions may have played an important role in the rapid progress

achieved. Quite early, the prototype reached a respectable level of sensitivity and a high level of reliability and stability. These features made this prototype an ideal test bed for the study of various noise effects, some quite unforeseen [54].

The effects of various fluctuations in the laser illumination were studied, and remedies were proposed and implemented. In particular, the mechanisms by which scattered light introduces noise were studied in great detail [55]. A two-stage frequency stabilisation was conceived [56] and later implemented. Furthermore, schemes of additional phase modulations for "washing out" the scattered light echoes were developed and successfully tested [57, 58].

The effects due to fluctuations in the laser beam geometry (in lateral position, pointing, beam width) were studied, and a suitable remedy, the "mode cleaner", was found and implemented [35].

It was only through the combined application of all these measures that the sensitivity was further improved [59], eventually to reach the fundamental limit of shot noise, for steadily increasing levels of light power.

An important improvement also came from the study of the mechanical behaviour of the suspended optical components (mirrors, beamsplitter, Pockels cells). The mechanical resonances, typically in the kHz range (and mostly at relatively low Q values), were due to the way the optical components were attached to the "test masses". After trying out several schemes of mechanically fastening, or of glueing, the mirrors to their mounts, the radical solution of hanging the *bare* mirrors was found to be the most successful [59], not only for the far end mirrors, but also for the various components in the central tank [52].

A.2.2 The 30 m prototype

With the move of the Institut für Astrophysik to Garching, planning for a prototype of increased length, 30 m, was begun. This 30 m prototype was commissioned in 1983. The arms extend outside the building, the vacuum tubes are supported over a concrete bed later covered with concrete arches, thermal insulation, and finally soil. This housing provides reasonable protection from weather, temperature changes, and acoustic noise.

Most features of the general concept were taken over from the 3 m prototype, but larger tubes and tanks were chosen so as to accommodate larger mirrors and possibly a higher number of beams.

For seismic isolation a straightforward two-pendulum scheme is used. The four mirrors, the beamsplitter, the two Pockels cells, and a beam steering block are all suspended separately. Active damping ("local control") is provided via shadow-sensors incorporated into the coil-and-magnet systems by which the position of the components is controlled [52].

The laser beam is guided into the central vacuum tank via an optical fibre, the end of which is mounted to the (seismically isolated) beam steering block. The optical fibre is of the monomode type and thus also serves as a "mode cleaner".

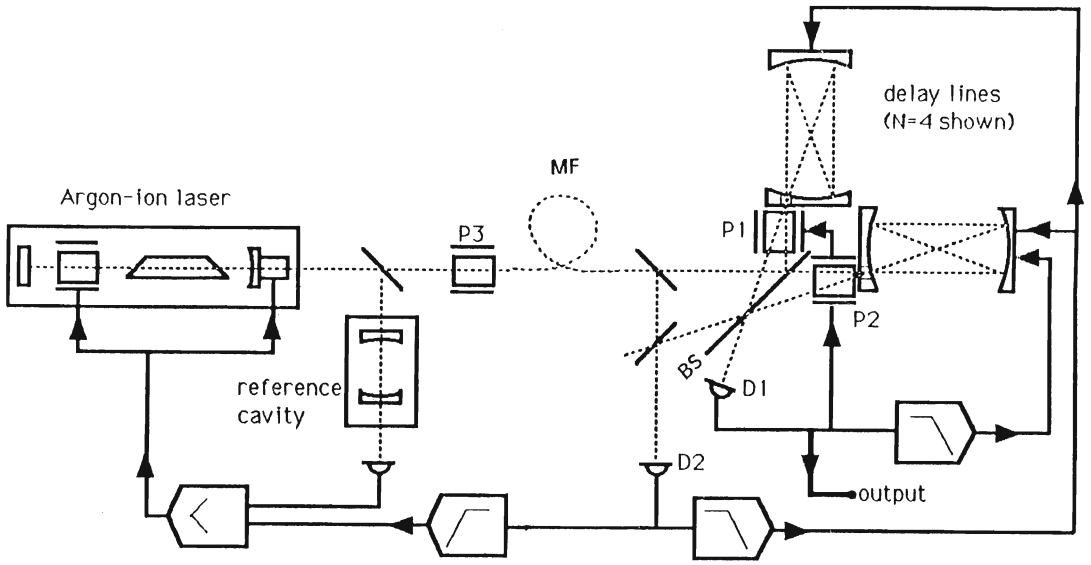

Figure A.1: *Schematic diagram of the Garching 30 metre prototype. The light from an argon ion laser is sent to the interferometer via a monomode glass fibre (MF). The Pockels cells P1, P2 serve for modulating the optical path as well as for maintaining the proper point of operation. The frequency of the light is stabilised in two stages: firstly with respect to a reference cavity, and then to the full path length of the interferometer, monitored by photodiode D2.*

A.2.3 Experiments with recycling and multiple mirror delay lines

As was pointed out in Chapter 3, recycling of laser light is an elegant means to achieve high light power in an interferometer. To test the feasibility of this scheme, a number of experiments have been performed. In a short interferometer, with armlengths of about 30 cm and separately suspended optical components, the best results were obtained with the beams reflected back on themselves at the interferometer mirrors. Power recycling could be obtained by inserting only one additional (again separately suspended) mirror between the laser and the interferometer. Due to wavefront distortion by the Pockels cells and due to losses at non ideal components the power enhancement was limited to a factor of slightly more than 10. The noise at the output of the interferometer was close to the shot noise limit for the enhanced power level [60].

Recycling experiments were also successfully carried out with 30 m armlengths in a three-mirror delay line, using two far mirrors and one near mirror. The additional mirror provides the missing degrees of freedom necessary to translate and point the output beam. In particular, it is possible to bring the output beam into coincidence with the input beam, for the purpose of recycling. This setup also allows smaller multiple beam patterns and finally smaller mirrors [4].

The experience gained with the multiple delay line was encouraging, particularly the stability of beam position and orientation, even without active control of the mirror orientations.

A.2.4 Sensitivity of the 30 m prototype

The sensitivity of an interferometer can be deduced from the (linear) noise spectral density $\tilde{h}(f)$ of the apparent strain $h(t)$ simulated by the noise. The strain h_1 that can be detected with unity signal-to-noise ratio in a given bandwidth Δf from f_ℓ to f_u would be

$$h_1 = \left(\int_{f_\ell}^{f_u} \left[\tilde{h}(f) \right]^2 \mathrm{d}f \right)^{1/2} .$$

In regions of flat ("white") noise this reduces to $h_1 \approx \tilde{h}(f) \cdot \sqrt{\Delta f}$. The fact that for a detection to be significant a much higher S/N ratio is required has been taken into account in Chapter 2 in setting up the sensitivity requirements.

The measured noise in the 30 m prototype is shown in Figure A.2 expressed as (linear) spectral density of equivalent mirror displacement $\tilde{\delta\ell}$ (left hand axis) or of strain $\tilde{\delta\ell}/\ell$ (right). Note that the frequency axis has a logarithmic scale. The data were taken in separate spans, each with several minutes of averaging. The number of passes in the delay line was set to $N = 90$, resulting in an optical path $L = N \cdot \ell$ of 2.7 km.

The noise at frequencies above 2 kHz is practically white, and it is very close to the theoretical shot-noise limit (horizontal line) for the light power in the interferometer (250 mW). The measured value in this frequency range corresponds to a mirror displacement $\tilde{\delta\ell}$ of $3.3 \times 10^{-18}\,\mathrm{m}/\sqrt{\mathrm{Hz}}$, or a strain $\tilde{h}$ of $1.1 \times 10^{-19}/\sqrt{\mathrm{Hz}}$.

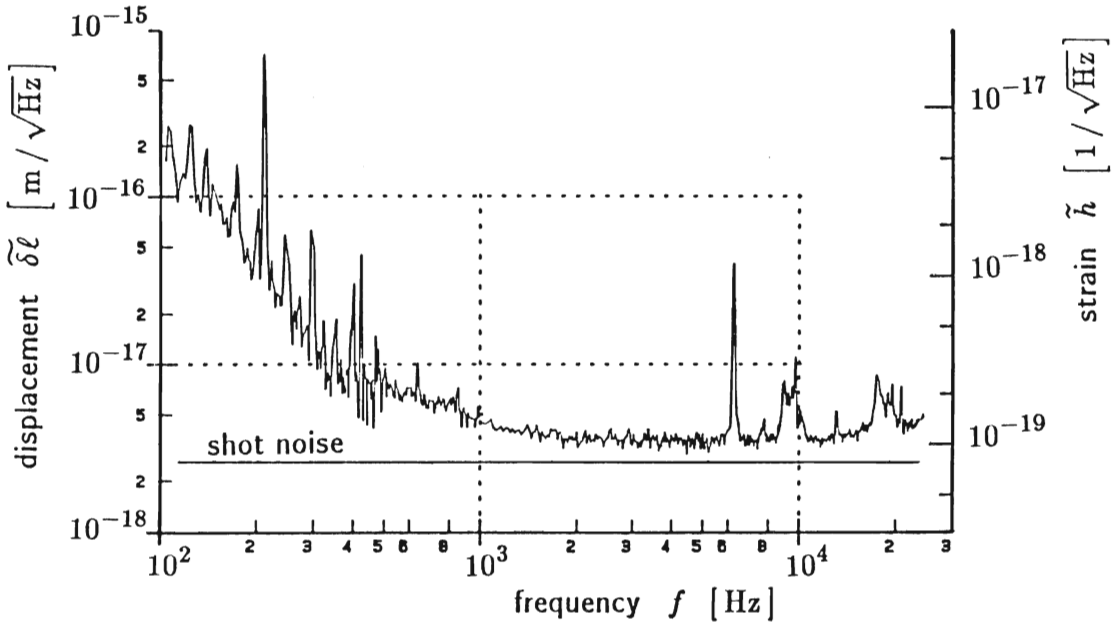

Figure A.2: *Noise spectral densities* ($\tilde{\delta\ell}$, $\tilde{h}$) *of the Garching prototype with optical path* $L = 90 \times 30\,\mathrm{m} = 2.7\,\mathrm{km}$

The lowest mechanical resonances of the mirrors (6.3 kHz), of the Pockels cells (9 to 10 kHz) and of the 'Zerodur' reference cavity (16 to 20 kHz) are all well above the measurement window envisaged (several hundred Hz up to a few kHz). The high noise contribution at low frequencies (< 500 Hz) is seen to be due to insufficient seismic isolation. A remedy here will require more elaborate, but straightforward, suspension systems, of the type discussed in Chapter 6.

A.3 The Prototype 10 m Detector at Glasgow

A.3.1 Introduction

The Fabry-Perot based prototype detector at the University of Glasgow has been under development for the last ten years and followed earlier work on a small scale delay line interferometer. While most work on the instrument has been devoted to improving its sensitivity, two periods of data taking have been undertaken, the more recent being in conjunction with the detector at the Max-Planck-Institut, Garching.

A.3.2 General description

The prototype detector has two perpendicular arms each of 10 m length formed between fused silica test masses which are hung as pendulums. A schematic diagram of the layout is shown in Figure A.3. Ultra low loss dielectric mirrors are optically contacted on to the four test masses in the arms to form very high finesse cavities in each arm. Finesses of approximately 4000 are achieved for illuminating light of wavelength 514 nm from an argon laser, and this number is equivalent to having more than 1000 passes up and down each cavity. The argon laser light enters the system through a single mode optical fibre. Optical isolation of the cavities, fibre and laser is provided by Faraday effect isolators. The light from the fibre reaches a beamsplitter mounted on a fifth mass suspended as a pendulum and the cavities are illuminated through polarisers and quarter wave plates by the beams from this splitter. The polariser / quarter-wave-plate combinations act so that the light impinging on the cavities is of circular polarisation which allows isolation of the cavities from each other and separation of the light reflected from each cavity. The beamsplitter and cavities are all contained in a vacuum system at a pressure of $\sim 5 \times 10^{-4}$ mbar. All the test masses in the system and the beamsplitter mass have their orientations (tilt and rotation) damped and controlled by servo systems. Most of these use light from a helium neon laser reflected from a mirror on the mass on to a position sensing diode as an angular displacement sensor, and control is by electromagnetic drive to the tops of the four wires which suspend each mass. However one mass uses a system of combined shadow detectors / coil magnet feedback elements, sensing the orientation of the mass and feeding back on it directly. This last arrangement was developed by the group in the Max-Planck-Institut, Garching. The orientation controls are such that the mirrors on the masses may be turned very finely to allow the resonances of the cavities to be optimised.

A.3.3 Operation of the detector

The laser has to be frequency locked to one of the cavities – the primary cavity – to keep this cavity resonating. In more detail the laser is locked to the cavity at frequencies above a few Hz but at lower frequencies the distance between the masses is damped and locked to the frequency of the laser. (Until recently the feedback element in the laser was an electro-optic modulator). The other cavity – the secondary cavity – then has its length locked so that it resonates with the light from the laser. The length is adjusted by means of coils which can push on magnets mounted on one of the test masses. Presently the signal to be recorded from the detector is taken early in this second loop.

Note the use of electronic subtraction of the error point signal in the primary loop from the detected signal in the secondary loop. This cancels the effect of any residual frequency fluctuations of the laser.

The laser and cavity servo loops use the *rf* sideband reflection locking technique. Phase modulation at 12 MHz is put on to the input laser beam by a phase modulator. The light directly reflected from the front mirror of each cavity retains the sidebands of this modulation but the light which enters a cavity and then leaks back out has the sidebands removed. The effect of this is that the total reflected light from each cavity becomes amplitude modulated at the original modulation frequency, with the amount of amplitude modulation being proportional to the phase difference between the incident laser light and the light stored in the cavity. The levels of modulation can be sensed by synchronous detection and provide the basic signals for the two main feedback loops.

Two other stabilisation systems are also used. The laser amplitude is controlled and stabilised by means of a diode sensing / Pockels cell feedback arrangement. To ease the acquisition of lock, the initial swinging of the masses in the secondary cavity is damped down by means of illuminating the cavity with helium neon light, sensing the moving Fabry-Perot fringes and feeding back a derived damping signal to the suspension points of the masses. (This system is not shown in Figure A.3.)

A.3.4 Sensitivity of the 10 m detector

The detector sensitivity has been steadily improving over the ten years that it has been under development. To a great extent this improvement has been due to the work carried out on stabilising the frequency, power and geometry of the light from the illuminating laser. However, the most important (and surprising) noise source discovered has been associated with the bonding of the mirrors to the test masses. Different types of bond were tried ranging from apiezon grease through cyanoacrylate glue to optical contacting, with the best performance being obtained with optical contacting. Displacement noise levels of $\sim 1.7 \times 10^{-18}\,\mathrm{m}/\sqrt{\mathrm{Hz}}$ over a range of frequency between 1500 Hz and 2500 Hz are typically observed. (See Figure A.4.)

The performance is still not at the level set by shot noise in the photocurrent from the light detected ($\sim$ 30 mW from each cavity) and the detector also exhibits occasional excess noise pulses. Recently work has been focussed on reducing slight fluctuations in

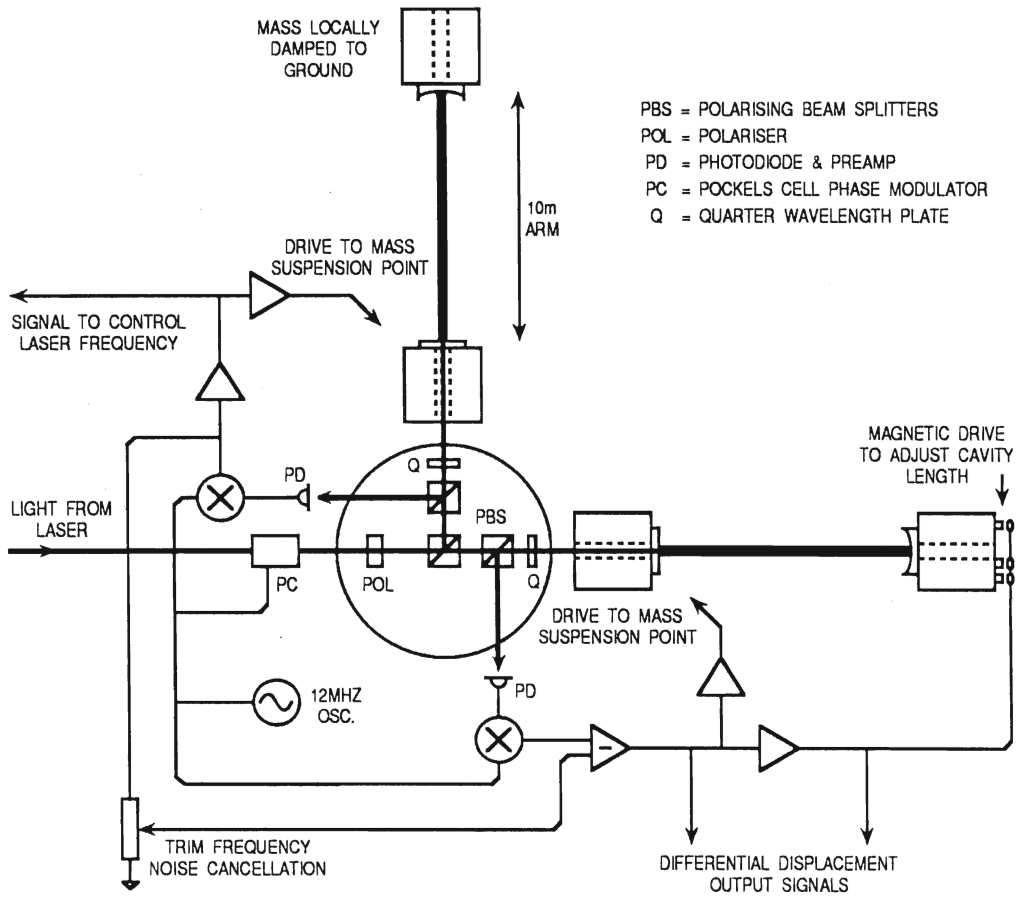

Figure A.3: *Diagram showing the main optical components of the Glasgow prototype detector.*

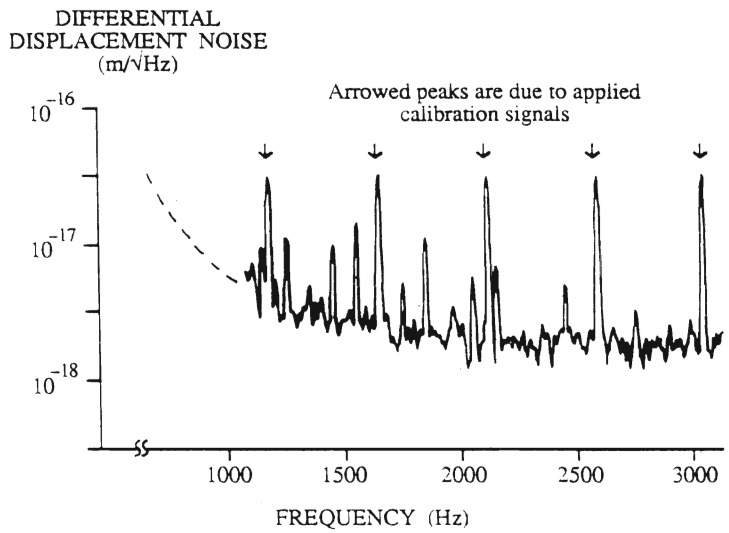

Figure A.4: *Displacement sensitivity of the Glasgow prototype interferometer.*

the mode structure of the light from the laser which appear to cause some of the impulsive signals in the interferometer output. Elimination of the optical contacts between the mirrors and the test masses is also planned to avoid noise due to imperfections in these joints; large solid fused silica mirrors (5 inches diameter, 4 inches long) are being specially fabricated and coated for this purpose.

A.4 The 100 Hour Data Run

In early March 1989 a coincident 100 hour test run of the Garching and Glasgow prototypes was carried out. Its aim was

- to prove that continuous operation of interferometric antennas is possible;
- to provide long term data which can be analyzed for (non-gaussian) noise contributions; and to histogram their frequency of occurrence versus strength;
- to rehearse the logistics of data acquisition, archiving, and data exchange;
- and, only as a faint possibility, to find some gravitational waves, or some other hidden correlations between the data of distant antennas.

In particular the first objective, to verify and quantify the reliability of interferometric antennas, has gained in importance as the planning for a large antenna has progressed.

A very accurate and reliable (glitch-free) timing is of importance for all coincidence measurements between two detectors, but added significance came from the news of possible pulsar activity [14] of the supernova remnant of SN 1987a, with pulse rates of 1.969 kHz. To search for gravitational wave signals (at twice this frequency) required a timing accuracy of better than 50 μs.

A first publication on the MPQ part of the 100 hour data run is being prepared, partly to document (in full detail) the apparatus used, the mode of operation adopted, and the format of the data recorded, and partly to describe the general behaviour of the overall set-up, composed of the detector proper and the data acquisition system.

The 100 hour test run verified the high degree of reliability and relock capability of the prototypes. At Garching the duty cycle of the *detector proper* was found to be a very remarkable 99 %: when the data acquisition hardware was ready to take data, the interferometer was out of lock for only 1 % of the time [50]. At Glasgow, the duty cycle was also very high – 89 %.

A closer investigation of the recorded data is under way. One first goal of the data analysis was to collect information on the data quality, and on the noise level, as a function of time. This analysis helped to detect and interpret some correlations between the operating parameters of the interferometers and the noise levels observed.

Furthermore a search for signals at the reported pulsar frequency, 1969 Hz, of the SN 1987a remnant, and its second harmonic, has been started at MPQ [50]. By first transposing the signal, with numerical heterodyning, to very low frequencies, the amount of data to be scanned has been reduced by three powers of ten.

Appendix B

International Collaborations

The German and British groups play a strong part in a number of international collaborations aimed at the development and operation of gravitational wave detectors using laser interferometry.

B.1 European Collaborations

In particular a strong European collaboration was set up about four years ago between the groups in Britain, France, Italy and Germany with the general aim of coordinating the development of gravitational wave detectors in Europe. This collaboration has been strongly underpinned by the existence of EC-sponsored twinning contracts between the research groups in the four countries. These contracts provided funding for some collaborative experimental developments relevant to high power laser interferometry for gravitational wave detectors. Work on high power lasers, on the testing of ultra high quality mirrors, and on the development of seismic isolation systems was carried out between the groups. Several meetings were also held for the exchange of results and ideas. A new application for further EC funding for such work is currently in preparation.

One aim of the European collaboration has been to encourage funding of at least two detectors in Europe [61]. It is planned that these detectors would operate together, and with the detectors in the USA as a worldwide network.

B.2 Australian Collaboration

A further collaboration has been formed between the British/German group and two research groups in Australia, one at the University of Western Australia and one at the Australian National University, who are proposing to build a similar long baseline detector [7]. In return for making available the engineering designs and plans for the German/British detector, our group will be given first access, if desired, to a second interferometer planned for the Australian system.

B.3 Worldwide Collaboration

During the last year a worldwide collaboration involving Britain, France, Germany, Italy and the USA has been formed. Eight working groups – an extension of groups originally set up in Europe – have been created, covering lasers, optics, simulation, vacuum, control systems, isolation systems, data acquisition and data analysis, with representation from the research groups of the participating countries. The aim of these is to encourage full collaboration on experimental design and development and to coordinate experiments to be carried out with the large detectors.

B.4 Specialised Collaborations

One other collaboration of a smaller scale and more specialised nature is being set up. This entails a data analysis group at the Inter-University Centre for Astrophysics and Astronomy, Pune, India having an agreement to work with the relevant part of our group led by Bernard Schutz at the University of Wales.

References

[1] R.L. Forward: *Wideband laser interferometer gravitational radiation experiment*, Phys. Rev. D **17** (1978) 379–390

[2] R. Weiss: *Electromagnetically coupled broadband gravitational antenna*, Quarterly Progress Report, Research Laboratory of Electronics, MIT **105** (1972) 54–76

[3] J. Hough, B.J. Meers, G.P. Newton, N.A. Robertson, H. Ward, B.F. Schutz, R.W.P. Drever: *A British Long Baseline Gravitational Wave Observatory*, Design Study Report GWD/RAL/86–001 (1986)

[4] K. Maischberger, A. Rüdiger, R. Schilling, L. Schnupp, D. H. Shoemaker, W. Winkler: *Vorschlag für den Bau eines großen Laser-Interferometers zur Messung von Gravitationswellen*, June 1985, MPQ Report 96,
— updated version, June 1987, MPQ Report 129,
— English translations of *chapter summaries*: MPQ Report 131

[5] R. Vogt: *The LIGO project – a progress report*, talk given at the Twelfth Intern. Conf. on General Relativity and Gravitation (GR12), Boulder 1989, to be reported in the Conference Proceedings, Cambridge University Press, New York (in press)

[6] A. Giazotto, A. Brillet, *et al.*: *The VIRGO Project*, (1989)

[7] D. Blair, J. Ferreirinho, P. Veitch, R.J. Sandeman, H.A. Bachor, D. McClelland, A. Wrightson: *Proposal for the Australian International Gravitational Observatory*, (1989)

[8] K.S. Thorne: *Gravitational Radiation* in: *300 Years of Gravitation*, Eds. S.W. Hawking, W. Israel, Cambridge University Press (1987)

[9] B.F. Schutz, Ed.: *Gravitational Wave Data Analysis*, Kluwer, Dordrecht (1989)

[10] C.M. Will: *Theory and Experiment in Gravitational Physics*, Cambridge University Press, Cambridge, England (1981)

[11] B.F. Schutz: *Data analysis requirements of networks of detectors*, in: *Gravitational Wave Data Analysis*, Ed. B.F. Schutz, Kluwer, Dordrecht (1989) 315–326

[12] T. Piran, R.F. Stark: *Numerical relativity, rotating gravitational collapse, and gravitational radiation*, in: *Dynamical Spacetimes and Numerical Relativity*, Ed. J.M. Centrella, Cambridge University Press, Cambridge, England (1986) 40–73

[13] B.F. Schutz: *Gravitational wave sources and their detectability*, Class. Quant. Grav. (1989) (in press)

[14] J. Kristian *et al.*: *Submillisecond optical pulsar in supernova 1987A*, Nature **338** (1989) 234–236

[15] S. Anderson, P. Gorham, S. Kulkarni, T. Prince, and A. Wolszczan: *PSR 2127+11C*, I.A.U. Circ. **4772** (1989),
— and also private communication

[16] J.G. Ables, C.E. Jacka, D. McConnell, P.A. Hamilton, P.M. McCulloch, and P.J. Hall: *PSR 0021-72A and 0021-72B*, I.A.U. Circ. **4602** (1988)

[17] A. Krolak: *Coalescing binaries to post-Newtonian order*, in: *Gravitational Wave Data Analysis*, Ed. B.F. Schutz, Kluwer, Dordrecht (1989) 59–69

[18] M. Tinto: *Coincidence probabilities for networks of laser interferometric detectors observing coalescing compact binaries*, in: *Gravitational Wave Data Analysis*, Ed. B.F. Schutz, Kluwer, Dordrecht (1989) 299–313

[19] J.P.A. Clark, E.P.J. van den Heuvel, W. Sutantyo: *Formation of neutron star binaries and their importance for gravitational radiation*, Astron. & Astrophys. **72** (1979) 120–128

[20] R.W.P. Drever: *Interferometric detectors of gravitational radiation*, in: *Gravitational Radiation*, Les Houches 1982, Eds. N. Deruelle, T. Piran, North-Holland Publ. Co. (1983) 321–338

[21] J.-Y. Vinet, B.J. Meers, C. Nary Man, A. Brillet: *Optimization of long-baseline optical interferometers for gravitational-wave detection*, Phys. Rev. D **38** (1988) 433–447

[22] B.J. Meers: *Recycling in laser interferometric gravitational wave detectors*, Phys. Rev. D **38** (1988) 2317–2326

[23] B.F. Schutz: *Data processing analysis and storage for interfermetric antennas*, in: *The Detection of Gravitational Radiation*, Ed. D. Blair, Cambridge University Press, Cambridge, England, (in press)

[24] B.F. Schutz: *Determining the Hubble constant from gravitational wave observations*, Nature **323** (1986) 310–311

[25] D. Herriot, H. Kogelnik, R. Kompfner: *Off-axis paths in spherical mirror interferometers*, Appl. Opt. **3** (1964) 523–526

[26] R.W.P. Drever and Colleagues: *Gravitational wave detectors using laser interferometers and optical cavities: Ideas, principles and prospects*, in: *Quantum Optics, Experimental Gravitation, and Measurement Theory*, Eds. P. Meystre, M.O. Scully, Plenum Press New York (1983) 503–514

[27] C.M. Caves: *Quantum-mechanical radiation-pressure fluctuations in an interferometer*, Phys. Rev. Lett. **45** (1980) 75–79

[28] R. Loudon: *Quantum limit on the Michelson interferometer used for gravitational-wave detection*, Phys. Rev. Lett. **47** (1981) 815–818

[29] L.A. Wu, M. Xiao, and H.J. Kimble: *Squeezed states of light from an optical parametric oscillator*, J. Opt. Soc. Am. B **4** (1987) 1465

[30] M. Xiao, L.A. Wu and H.J. Kimble: *Precision measurement beyond the shot-noise limit*, Phys. Rev. Lett. **59**, (1987) 278–281; P. Grangier, R. E. Slusher, B. Yurke and A. LaPorta: *Squeezed-light–enhanced polarization interferometer*, Phys. Rev. Lett. **59** (1987) 2153–2156

[31] C.M. Caves: *Quantum-mechanical noise in an interferometer*, Phys. Rev. D **23** (1981) 1693–1708

[32] J. Gea-Banacloche and G. Leuchs: *Squeezed states for interferometric gravitational wave detectors*, J. Modern Opt. **34** (1987) 793; for imperfect interferometers see: J. Gea-Banacloche and G. Leuchs, J. Opt. Soc. Am. B **4**, (1987) 1667; J. Gea-Banacloche and G. Leuchs, J. Modern Opt. in print (1989)

[33] J. Gea-Banacloche and G. Leuchs: *Use of squeezed states in interferometric gravitational wave detectors*, in: *The Detection of Gravitational Radiation*, Ed. D. Blair, Cambridge University Press, Cambridge, England (1989)

[34] R.W.P. Drever, J.L. Hall, F.V. Kowalski, J. Hough, G.M. Ford, A.J. Munley, H. Ward: *Laser phase and frequency stabilization using an optical resonator* Appl. Phys. B **31** (1983) 97–105

[35] A. Rüdiger, R. Schilling, L. Schnupp, W. Winkler, H. Billing, K. Maischberger: *A mode selector to suppress fluctuations in laser beam geometry*, Optica Acta **28** (1981) 641–658

[36] N.A. Robertson, S. Hoggan, J.B. Mangan, J. Hough: *Intensity stabilisation of an argon laser using an electro-optic modulator – Performance and limitations* Appl. Phys. B **39** (1986) 149–153

[37] C.N. Man, A. Brillet: *Injection locking of argon-ion lasers*, Opt. Lett. **9** (1984) 333–334

[38] G.A. Kerr, J. Hough: *Coherent Addition of Laser Oscillators for Use in Gravitational Wave Antennas*, to appear in Appl. Phys. B (accepted for publication)

[39] D. Shoemaker, A. Brillet, C.N. Man, O. Crégut, G. Kerr: *Frequency-stabilized laser-diode-pumped Nd:YAG laser*, Opt. Lett. **14** (1989) 609–611

[40] N.A. Robertson: *Seismic Isolation*, in: *The Detection of Gravitational Radiation*, Ed. D. Blair, Cambridge University Press, Cambridge, England (in press)

[41] R. Del Fabbro, A. Di Virgilio, A. Giazotto, H. Kautzky, V. Montelatici, D. Passuello: *Low Frequency Behaviour of the Pisa Seismic Noise Super-Attenuator for Gravitational Wave Detection*, Phys. Lett. A (Netherlands) **133** (1988) 471–475

[42] N.A. Robertson, R.W.P. Drever, I. Kerr, J. Hough: *Passive and active seismic isolation for gravitational radiation detectors and other instruments*, J. Phys. E: Sci. Instrum. **15** (1982) 1101–1105

[43] R.L. Rinker, J.E. Faller: *'Super spring' - A long period vibration isolation*, in: *Precision Instruments and Fundamental Constants II*, Eds. B.N. Taylor, W.D. Phillips, National Bureau of Standards (USA), Spec. Pub. **617** (1984) 411–417

[44] P.R. Saulson: *Vibration isolation for broadband gravitational wave antennas*, Rev. Sci. Instrum. **55** (1984) 1315–1320

[45] A. Giazotto, D. Passuello, A. Stefanini: *One-mile equivalent length interferometric pendulum for seismic noise reduction* Rev. Sci. Instrum. **57** (1986) 1145–1151

[46] E. Campani, A. Giazotto, D. Passuello: *Performance of an analogue phase follower* Rev. Sci. Instrum. **57** (1986) 79–81

[47] Y.T. Chen, R.W.P Drever, talk given at the *International Conference on Experimental Gravitational Physics*, Guangzhou 1987 (unpublished)

[48] R. Del Fabbro, A. Di Virgilio, A. Giazotto, H. Kautzky, V. Montelatici, D. Passuello: *First Results from the Pisa Seismic Noise Super-Attenuator for Low Frequency Gravitational Wave Detection*, Phys. Lett. A (Netherlands) **132** (1988) 237–240

[49] D. Pountain: *Digital Paper*, Byte **14** (1989) 274–280

[50] T.M. Niebauer, A. Rüdiger, R. Schilling, L. Schnupp, W. Winkler, G. Leuchs: *Some results from a 100 hour data run with the Garching 30 m prototype*, talk given at the Twelfth Intern. Conf. on General Relativity and Gravitation (GR12), Boulder 1989, to be reported in the Conference Proceedings, Cambridge University Press, New York (in press)

[51] H. Billing, K. Maischberger, A. Rüdiger, R. Schilling, L. Schnupp, W. Winkler: *An argon laser interferometer for the detection of gravitational radiation*, J. Phys. E: Sci. Instrum. **12** (1979) 1043–1050

[52] D. Shoemaker, R. Schilling, L. Schnupp, W. Winkler, K. Maischberger, A. Rüdiger: *Noise behavior of the Garching 30 meter prototype gravitational wave detector*, Phys. Rev. D **38** (1988) 423–432

[53] H. Ward *et al.*: *The Glasgow gravitational wave detector - present progress and future plans*, in: *Experimental Gravitational Physics*, (Proc. Guangzhou 1987), Eds. P.F. Michelson, Hu En-ke, G. Pizzella, World Scientific (1988) 322–327

[54] K. Maischberger, A. Rüdiger, R. Schilling, L. Schnupp, W. Winkler, H. Billing: *Noise investigations in a laser interferometer for the detection of gravitational radiation*, Proc. Second Marcel Grossmann Meeting on General Relativity, Trieste 1979, Ed. R. Ruffini, North-Holland Publ. Co. (1982) 1083–1100

[55] W. Winkler: *Eine optische Verzögerungsleitung für ein Breitband-Gravitationswellenexperiment*, Ph.D. Thesis, München 1983, Internal Report MPQ 74

[56] H. Billing, W. Winkler, R. Schilling, A. Rüdiger, K. Maischberger, L. Schnupp: *The Munich gravitational wave detector using laser interferometry*, in: *Quantum Optics, Experimental Gravitation, and Measurement Theory*, Eds. P. Meystre, M.O. Scully, Plenum Press New York (1983) 525–566

[57] R. Schilling, L. Schnupp, W. Winkler, H. Billing, K. Maischberger, A. Rüdiger: *A method to blot out scattered light effects and its application to a gravitational wave detector*, J. Phys. E: Sci. Instrum. **14** (1981) 65–70

[58] L. Schnupp, W. Winkler, K. Maischberger, A. Rüdiger, R. Schilling: *Reduction of noise due to scattered light in gravitational wave antennas by modulating the phase of the laser light*, J. Phys. E: Sci. Instrum. **18** (1985) 482–485

[59] R. Schilling, L. Schnupp, D.H. Shoemaker, W. Winkler, K. Maischberger, A. Rüdiger: *Improved sensitivities in laser interferometers for the detection of gravitational waves*, Journées Relativistes, Aussois 1984; Proceedings in: *Gravitation, Geometry, and Relativistic Physics*, Lecture Notes in Physics **212** (1984) 213–221

[60] K. Maischberger, A. Rüdiger, R. Schilling, L. Schnupp, W. Winkler and G. Leuchs: *Status of the Garching 30 meter prototype for a large gravitational wave detector*, in: *Experimental Gravitational Physics*, (Proc. Guangzhou 1987), Eds. P.F. Michelson, Hu En-ke, G. Pizzella, World Scientific (1988) 316–321

[61] Report of an *Ad-hoc working group on the future of interferometric gravitational wave antennas in Europe*, March 1988 – copies submitted to SERC and BMFT in 1988